DEVELOPMENT OF THERAPEUTICS TARGETING THE HEPATOCYTE GROWTH FACTOR (HGF)/MET SYSTEM

By

LEEN H. KAWAS

A dissertation submitted in partial fulfillment of
the requirements for the degree of

DOCTOR OF PHILOSOPHY

WASHINGTON STATE UNIVERSITY
Division of Pharmacology and Toxicology

DECEMBER 2011

To the Faculty of Washington State University:

The members of the Committee appointed to examine the dissertation of LEEN H. KAWAS find it satisfactory and recommend that it be accepted.

_____

Joseph W. Harding, Ph.D., Chair

_____

John W. Wright, Ph.D.

_____

Kathryn E. Meier, Ph.D.

_____

Michael D. Varnum, Ph.D.

_____

Michael F. Sardinia, Ph.D.

ACKNOWLEDGMENTS

There are many people who I wish to thank for their help and support throughout my experience at Washington State. First, and foremost I would like to thank my mentor, and friend, Dr. Joe Harding for his motivation, support, enthusiasm, and immense knowledge. His guidance helped me in all the time of research and writing of this thesis. I will never forget your kindness and wisdom. Thank you for everything.

Besides my advisor, I would like to thank the rest of my committee Dr. John Wright, Dr. Michael Varnum, Dr. Michael Sardinia, and Dr. Kathryn Meier, for their encouragement, insightful comments, and for always being available. My sincere thanks go to my friend Dr. Kathryn Meier for the great help and professional guidance.

I would also like to thank the members of the Harding and Wayman labs, past and present for the help and cooperation on my research experiments. Special thanks to Dr. Gary Wayman and Dr. Talley Lambert for your generous help with all my questions and requests. I am also thankful for the Abu-Lail group in the Bioengineering Department for the help and support they provided with the last part of my project.

I would also like to thank my friends here in Pullman Ahmad Shalan, Amer Hamdan, Salma, Yesenia, Pinar, Nehal, and Mona Younis. Ahmad and Amer thank you for putting up with me in my good and bad days.

I would like to thank my Father, sisters and brother for their love and support through all my endeavors. Last, but not least I would like to thank my late Mother Khadeejeh Qutishat for showing us the way to achieve our goals, for believing in us, and for supporting us in our ups and downs. Thank you for your invaluable love. May your soul rest in peace.

DEVELOPMENT OF THERAPEUTICS TARGETING THE HEPATOCYTE GROWTH FACTOR (HGF)/MET SYSTEM

Abstract

By Leen H. Kawas, Ph.D.
Washington State University
December 2011

Chair: Joseph W. Harding

In this dissertation I will describe the development of prototype small molecule therapeutics directed at the HGF/Met system. In addition I will introduce a new approach for quantitatively localizing Met at the sub-cellular level, which should aid in identifying physiological and pathophysiological processes that may be impacted by these new therapeutic agents.

According to the National Institute of Health; cancer is responsible for nearly 25% of all deaths in United States, making it the second leading cause of death in the nation. Despite the enormity of the problem and the massive expenditures that have been made to improve treatment, only modest progress has been made. Clearly there is a need for novel and effective treatment options focused on new molecular targets. One particularly attractive anti-cancer target is the HGF/ Met system, which is hyperactive in many human cancers. Not-surprisingly, the development of HGF/Met blockers is currently a major focus of the pharmaceutical industry.

Here I present a new therapeutic approach to block the HGF/Met system, which has intrinsic specificity, low cost, and exploits a semi-unique property of this system: the need for HGF to pre-dimerize before it can activate Met. Previous efforts by the Harding laboratory demonstrated that Norleual (an AngIV analog) exhibits anti-Met and anti-cancer activities.

Homology between Norleual and the dimerization domain (Hinge region) of HGF led to the hypothesis that Norleual acts by interfering with HGF dimerization/multimerization and functions as a dominant negative Hinge-region mimic. To further validate the idea the that Norleual was acting as a Hinge region mimic, we synthesized a hexapeptide representing the Hinge sequence and established its capacity to similarly block HGF-dependent activation of Met and HGF-dependent cellular functions. Despite their impressive anti-cancer profiles, Norleual and the Hinge peptide are highly unstable, making their direct transition to clinical use problematic. Thus another family of AngIV analogs (6AH family) has been developed with improved metabolic stability and pharmacokinetic properties; these agents have a 6-amniohexanoic amide substituted at the C-terminal position. Here I show that the 6AH family members demonstrate a range of biological and therapeutic activities against the HGF/Met system, and that this activity is correlated to their ability to bind HGF and block its dimerization.

In last part of these dissertation studies I use atomic force microscopy (AFM) to ascertain the sub-cellular localization of Met on hippocampal neurons and to distinguish between activated and non-activated receptors. I show that aggregated/active Met is localized to the dendrites, where it exerts its role as a determinant of synaptic connectivity by regulating the density and structure of dendritic spines.

TABLE OF CONTENT

LIST OF TABLES

LIST OF FIGURES

Dedication

To My Mom, Khadeejeh.

CHAPTER ONE

INTRODUCTION

Hepatocyte growth factor/scatter factor (HGF/SF) and its tyrosine kinase (TK) receptor Met arose late in development and are unique to vertebrates. The binding of HGF/SF to its cell surface receptor Met stimulates mitogenesis, motogenesis, and morphogenesis in a wide range of cellular targets. Dysregulation of these signals often leads to neoplastic alterations and to cancer. The HGF/Met system is also recognized to be involved in cognition, induction of LTP (long-term potentiation), and has significant cerebroprotective effects. Because of the close linkage between the HGF/Met system and cancer and cognition, development of molecules to target HGF/Met is being vigorously pursued.

1.1 Met basic domain organization

The MET receptor tyrosine kinase, which is a prototypical member of the insulin receptor subfamily of growth factor receptors (Furge et al., 2000), was first recognized as an oncogene in a human osteogenic sarcoma cell line. A mutant gain-of-function form that resulted from DNA rearrangement contained the translocated promoter region (TPR) locus on chromosome 1 linked to sequences from the MET locus on chromosome 7. Subsequent elucidation of the full length coding sequence of Met revealed it to be a membrane-spanning tyrosine kinase receptor. The Met receptor was found to interact with a single protein ligand, HGF, resulting in a multitude of cellular activities, including motility, proliferation, survival, and morphogenesis (Birchmeier et al., 2003; Peruzzi and Bottaro, 2006).

Both HGF/SF and Met are expressed as single-chain precursors, which are proteolytically processed into mature heterodimers (Peruzzi and Bottaro, 2006). The Met precursor is processed at a furin site that is located between residues 307 and 308 to generate a 50-KDa highly glycosylated extracellular α-subunit and a 140-KDa transmembrane β-subunit, which are linked together by a disulfide bridge to form the mature 185-Kda complex (Stella and Comoglio, 1999; Birchmeier et al., 2003; Gao and Vande Woude, 2005). The α-subunit is entirely extracellular while the β chain consists of an ectodomain, the transmembrane helix and a cytoplasmic portion that contains several functional domains.

Novel insights into the detailed domain structure of Met ectodomain have recently been obtained through structural and biochemical studies, which have shown that the α chain and the first 212 residues of the β chain form a high affinity binding site for HGF. This region of Met is homologous to the sema domain of semaphorins, which play a critical role in axon guidance, and may fold into a β-propeller structure (Gherardi et al., 2003; Stamos et al., 2004). A comparable propeller is present at the amino terminus of integrin α-chains and is also essential for protein-protein interactions (Xiong et al., 2002; Gherardi et al., 2003; Sheth et al., 2008). The remainder of the extracellular region consists of a small cysteine rich PSI domain similar to that found in plexins, semaphorins and integrins; and a four IgG-like repeats reminiscent of those found in plexins and transcription factors (Bork et al., 1999; Gherardi et al., 2003; Sheth et al., 2008).

The cytoplasmic tail of Met, which is highly conserved in all receptor tyrosine kinases, consists of a juxtamembrane region (just after the transmembrane helix), followed by the tyrosine kinase catalytic domain, and a carboxy-terminal docking region (Hubbard and Till, 2000; Sheth et al., 2008). The juxtamembrane region, which is a major site of negative-feedback control of Met, contains a c-Cbl-binding domain that includes a critical tyrosine (Tyr 1003), the

phosphorylation of which mediates the interaction of c-Cbl with Met. C-Cbl, a ubiquitin ligase, is responsible for Met polyubiqination and ultimately its endocytosis and degradation (Peschard et al., 2004). This region also includes a stretch of 47 highly conserved amino acid residues that surround Ser^{985}, which is a substrate for both protein kinase-C and protein phosphatase-2A.Ser^{985} phosphorylation results in the inhibition of Met kinase activity (Matsumoto et al., 2008).

Contiguous to the juxtamembrane domain is the kinase domain, which includes an auto-phosphorylation site within the activation loop that encompasses tyrosine residues Tyr^{1234} and Tyr^{1235}; phosphorylation of these residues activates the intrinsic kinase activity of the receptor (Longati et al., 1994; Furge et al., 2000; Eder et al., 2009). Phosphorylation of other tyrosine residues (Tyr^{1349} Tyr^{1356}) near the C-terminus of Met activates a multi-substrate docking site that is conserved among Met family members. Consensus sequences that include tyrosines 1349 and 1356 (Y ^{1349}VHVNATY ^{1356}VNV) form docking sites that bind signal transducers containing Src homology-2 (SH2) domain, phosphotyrosine binding domain (PTB), and Met binding domain (MBD) containing signal transducers (Ponzetto et al., 1994; Pelicci et al., 1995; Weidner et al., 1996).

1.2 HGF/SF structure, activation, dimerization, and binding to the Met receptor

Hepatocyte growth factor/Scatter factor (HGF/SF) is a vertebrate heteromeric polypeptide growth factor. Sequence analysis demonstrates that HGF/SF has an unusual domain structure, which closely resembles the proteinases of the plasminogen family. The plasminogens are typically circulating pro-enzymes, which upon activation are responsible for the degradation of many blood plasma proteins (Gherardi et al., 2006; Basilico et al., 2008). The HGF gene is located on chromosome 7q21.1, across 70 Kb, and is composed of 18 exons and 17 introns (Seki

et al., 1991). The translation of the single 6 Kb transcript gives rise to a pre-pro-polypeptide of 728 amino acids that is stored in the extracellular matrix in association with proteoglycans that it binds with high affinity (Stella and Comoglio, 1999; Basilico et al., 2008).

HGF/SF consists of seven domains: an amino terminal domain, a linker-dimerization domain, four kringle domains (K1-K4), and a serine proteinase homology (SPH) domain (Lokker et al., 1992). The single chain pro-polypeptide is proteolytically processed by convertases that cleave at a trypsin-like site just after K4, between R^{494} and V^{495}, to yield a mature αβ heterodimer bound by a disulfide link (Stella and Comoglio, 1999; Birchmeier et al., 2003; Gherardi et al., 2006). This conversion to the mature form is effected by several serine proteinases, including the plasminogen activator uPA (urokinase plasminogen activator), coagulation factors X, XI and XII, and a close homologue of factor XII. Both the pro-pre-HGF and the active disulfide-linked heterodimer appear to bind Met with high affinity; however, Met can only be activated by the processed dimerized form of the ligand (Lokker et al., 1992; Sheth et al., 2008).

The α subunit (60 KDa) contains the N-terminal domain that includes the hairpin, homolgous to the plasminogen activation peptide, and four kringle domains that form a triple-looped cysteine rich motif that is involved in protein-protein interactions. The β chain is similarly related to the catalytic domain of serine proteases but includes two mutations at the active site (H to Q and S to Y) that render it enzymatically inactive. This same heteromeric structure is also found in macrophage stimulating protein (MSP) and other members of the HGF family (Holmes et al., 2007; Basilico et al., 2008).

Mutagenesis and crystallographic studies have shown that the high affinity binding site for HGF consist of the two sites or half sites in the α chain that are located in the N-terminal

domain and the first kringle domain. Additionally, binding sites with lower affinities have been found in the second and fourth kringle domain of the α chain. These sites do not appear to be important for Met activation. The third kringle domain displays no ability to bind or activate Met. The SP domain of the β chain has also been revealed to have a role in the binding of the full- length HGF to Met but with low affinity (Stamos et al., 2004; Holmes et al., 2007). In addition to Met, HGF/SF can also bind heparin sulphate (HS) (Lyon et al., 1994) and dermatan sulphate (DS) (Lyon et al., 1998; bechard et al., 2001). These glycosaminoglycans (GAGs) function as co-receptors and potentiate the activation of Met on target cells (Lyon et al., 2002; Birchmeier et al., 2003; Holmes et al., 2007). Both heparin and heparin sulphate, which appear to have important roles in HGF dimerization, possess a high affinity binding site that interacts with the NK1 (see below) region of the protein (Lietha et al., 2001; Lyon et al., 2004). It is postulated that the binding of HGF/SF to the GAGs is important for limiting the diffusion of HGF/SF *in vivo*. Unlike fibroblast growth factor (FGF), the binding of HGF/SF to the GAGs does not seem to be critical for receptor activation (Lokker et al., 1992; Schwall et al., 1996; DiGabriele et al., 1998; Hartmann et al., 1998).

In addition to full length HGF/SF, naturally occurring truncated variants of the factor have been identified (e.g., NK1 and NK2) that have aided in understanding the role of key domains in mediating different biological responses (Ultsch et al., 1998; Chirgadze et al., 1999b; Lietha et al., 2001; Gherardi et al., 2006). The fragment containing the amino terminal and K1 (NK1) has been shown to contain the main receptor binding site; studies of its structure have shed light on the mechanism of ligand-receptor interaction. The crystal structure of the NK1-heparin complex demonstrated a tightly packed head to tail dimer (Tolbert et al., 2007). A central area encompassing the interdomain linker amino acids (K122, D123, Y124, I125, R126, and

N127) has been found at the dimer interface (Lokker et al., 1992; Stella and Comoglio, 1999; Youles et al., 2008). The consistent presence of HGF dimer in a head-to-tail orientation in different crystallographic environments suggest that the dimer is the biologically active form of HGF. The formation of the dimer, which contains two Met binding domains that are located on opposing faces, leads to the engagement of two Met molecules to form the active dimerized receptor (Lokker et al., 1992).

1.3 Met signaling

The binding of active HGF ligand to functionally mature Met results in receptor dimerization or multimerization, and trans-phosphorylation of multiple selected tyrosines in the intracellular region, creating docking sites for downstream signaling pathways. Different signal transducers are recruited and activated depending on the amino acid sequence flanking the phosphorylated tyrosine (Comoglio, 2001; Birchmeier et al., 2003; Holmes et al., 2007; Youles et al., 2008). Met has a unique bidentate docking site at the C-terminal, which consist of Y^{1349} and Y^{1356}. Upon phosphorylation this docking site binds Src-homology-2 (SH2) containing proteins, which are important for the activation of several downstream effectors pathways including RAS/ERK, PI3K/AKT, STATs, PLCγ, and c-Src.

The interaction of the effectors with the receptor can either be direct, in which proteins like Grb2 and the p85 subunit of the PI3K bind directly to phosphotyrosines on Met, or indirect through binding to phosphotyrosines on the scaffolding protein GAB1 (Grb2-associated binding protein 1). Thus, GAB1 is a key participant in much of the downstream signaling that is initiated by Met.

Because of steric reasons, the bididentate site found on one Met molecule restricts the simultaneous binding of additional substrates. However, the binding of Gab1 to the phosphorylated (p) Y^{1349} on one Met molecule, and Grb2 binding to (p)Y^{1356} to the second Met may enable an interaction between Gab1 and Grb2 on the Met dimer or multimer (Ponzetto et al., 1994; Weidner et al., 1996; Lock et al., 2000; Liu et al., 2008; Youles et al., 2008). Moreover, signaling through the HGF/Met system can be modulated depending on the identity and location of associated proteins. For example, the α6β4 integrin can potentiate the HGF activation of the RAS and PI3K (Trusolino et al., 2001), plexin B1 (Giordano et al., 2002) and the v6 splice variant of CD44, which links Met to the cytoskeleton (Orian-Rousseau et al., 2002). The death receptor Fas can be sequestered by Met, thus preventing Fas ligand binding results in blockade of Fas receptor aggregation and inhibition of apoptosis (Wang et al., 2002). Furthermore, the interaction of Met with the epidermal growth factor receptor (EGFR) or HER-2 enhances the invasion and proliferation of mammalian epithelial cells, thus promoting malignancies (Khoury et al., 2005; Bonine-Summers et al., 2007). A similar synergism has been observed between Met and the IGF-I receptor , which induces migration and invasion of pancreatic carcinomas (Bauer et al., 2006). Even more interesting is the induction of Met expression by Ras, protein which normally acts downstream of Met, resulting in a positive feedback loop (Webb et al., 1998). Together this network of interactions can adjust and ultimately establish the extent and duration of Met signaling.

1.4 HGF/Met in development

A number of studies have shown that the HGF/Met system plays an important role in vertebrate development. The HGF/SF effect is diverse, cannot be assigned to a single developmental stage or developmental event, and does not involve the same cellular responses on all occasions (Boccaccio and Comoglio, 2006).

During embryogenesis, transformation of the one-plane two-layered germinal disc into a three-dimensional body relies on the transition of some cells from an epithelial phenotype to multi-potent stem cells that can differentiate into cells with a mesenchymal phenotype that exhibit increased cell motility. This process is referred to as the epithelial-mesenchymal transition (EMT). Throughout embryogenesis, HGF/Met is a critical participant in many complex developmental processes like gastrulation (when the embryonic epithelium originates the mesoderm), epithelial morphogenesis, angiogenesis, myoblast migration, bone remodeling and nerve sprouting (Birchmeier and Gherardi, 1998; Boccaccio and Comoglio, 2006; Gentile et al., 2008). Without a doubt, cell proliferation, migration, escape from apoptosis, invasion of surrounding tissues and reorganization into new structures are required during those events.

The pivotal role of HGF/Met during embryogenesis is emphasized by the observation that mice with a homozygous mutation of either *hgf* or *met* die *in utero* owing to severe defects in placental development. This results in a suboptimal supply of oxygen and nutrients to the embryo, thus compromising survival (Uehara et al., 1995; Birchmeier and Gherardi, 1998; Gentile et al., 2008). These embryos are characterized by small livers (Schmidt et al., 1995), missing muscles due to defects in the migration of myoblasts from the somites to the limbs (Bladt et al., 1995), and compromised nerve outgrowth (Maina et al., 2001).

1.5 HGF/Met signaling in the adults

Both HGF and its receptor are widely expressed in adult tissue, and play multiple roles in postnatal physiological and pathophysiological events. An increase in HGF/SF and Met expression is prominent in a number of injured tissues. This has been observed with liver, kidney, or heart injury, in which plasma levels of HGF/SF rise, and HGF/SF expression is increased in both damaged and intact organs (Nakamura et al., 2000; Matsumoto and Nakamura, 2001; Rabkin et al., 2001; Michalopoulos, 2007). This broad HGF/Met response is part of the general defensive physiological reaction to damaging insults (Michalopoulos, 2007).

HGF/SF also exhibits cyto-protective activities in vivo. Administration of HGF before or immediately after an insult guards against tissue damage (Roos et al., 1995; Nakamura et al., 2000; Jin et al., 2003). Multiple experiments have identified HGF/SF as a powerful hepatic-mitogen. Introduction of HGF either ectopically or through transgenic expression of HGF/SF potentiates proliferation of hepatocytes and increases liver size, facilitating liver regeneration (Michalopoulos, 2007). Current interest into the therapeutic application of the HGF/Met system in liver, renal, heart disease, wound healing, and degenerative diseases is extensive and is expected to grow in the next few years.

1.6 HGF/Met and their therapeutic potentials

1.6.1 HGF therapeutics in the liver

HGF is known to protect the liver against external insults. In addition, HGF generation has also been associated with several liver and extra-hepatic diseases. Experimental and clinical evidence indicates that HGF plays a crucial role in liver regeneration. Liver cirrhosis is the irreversible end result of fibrous scarring and hepatocellular regeneration and is a major cause of morbidity and mortality worldwide with no effective therapy. Although there is no specific etiology for this disease, cirrhosis has been defined as a chronic disease of the liver in which dispersed damage and regeneration of hepatic parenchymal cells have taken place and in which dissemination of connective tissue has resulted in inadequate organization of the lobular and vascular structures (Fujimoto and Kaneda, 1999; Kaibori et al., 2002). Ideally, approaches for the treatment of liver cirrhosis should include attenuation of fibrogenesis, encouragement of hepatocyte mitosis, and reformation of tissue architecture.

Studies have shown that exogenous administration of recombinant HGF increases the potential for liver regeneration after hepatoctomy, especially in the case of cirrhotic liver (Boros and Miller, 1995; Kaibori et al., 2002; Borowiak et al., 2004). Conversely, studies have shown that the clofibrate-related compounds, which increase HGF/SF levels, can induce hepatomegaly, proliferation of hepatic peroxisomes, and hepatic carcinoma (Xu and Wu, 1999). The linkage of HGF/SF both positively and negatively to hepatic diseases has made HGF-related therapeutics a hot area for pharmaceutical development.

1.6.2 HGF therapeutics in the renal system

HGF exhibits a remarkably powerful anti-fibrotic effect that ameliorates tissue fibrosis in a wide range of animal models and tissues (Liu and Yang, 2006). Evidence has documented the

therapeutic effect of exogenous HGF in chronic allograft nephropathic rats, a model of chronic inflammation and progressive tissue scarring. The intramuscular administration of the human HGF gene reduced the rate of mortality, restrained inflammation and infiltration, and reduced renal fibrosis (Liu and Yang, 2006).

1.6.3 HGF in the eye

The ability of HGF to induce mitogenesis, motogenesis, morphogenesis, tubulogenesis, and angiogenesis has been implicated in various retinal diseases, as described below.

1.6.3.1 Macular degeneration

Age-related macular degeneration (ARMD) is the most common cause of irreversible vision loss in Americans over the age of 60. It is predicted that 10 million Americans will suffer from some level of this age-related visual damage during their retirement years. In normal healthy eyes, retinal pigment epithelial (RPE) cells form a polarized monolayer adjacent to the photoreceptors and are involved in various activities that are essential to retinal homeostasis and visual function. In the case of macular degeneration, unfortunately, adhesions and communication between RPE cells are lost because of inflammation. When inflammation occurs, RPE cells secrete many growth factors including HGF/SF, which stimulates the division and migration of RPE and the formation of new vasculature from existing blood vessels (angiogenesis). HGF also stimulates the production of other growth factors (e.g. VEGF), which further promote the formation of new blood vessels that invade neighboring matrix (Jun et al.,

2007). Hence the use of HGF blockers could be used either prophylactically, or as a treatment to slow down the progression of the disease and subsequent loss of vision.

1.6.3.2 Diabetic retinopathy

Proliferative diabetic retinopathy (PDR), which entails a distinctive neovascularization of the retina that is characterized by invasion of vessels into the vitreous cavity, is coupled with bleeding and scarring around the proliferative channel (Katsura et al., 1998). There is substantial evidence that multiple growth factors are involved in the onset and progression of the neovascularization process in general and in the PDR specifically. These include basic fibroblast growth factor (bFGF), Insulin-like growth factors (IGF-I), vascular endothelial growth factor (VEGF), and HGF. Of these, HGF has the most pronounced effects on endothelial growth and mitogenic activity (Boulton, 1999). Studies have found that levels of HGF in the vitreous fluid of PDR patients are considerably higher than in non-diabetic patients, and that the levels of HGF are especially high in the active stage of PDR (Katsura et al., 1998). This suggests that HGF stimulates or perpetuates neovascularization in PDR. Therefore, it is plausible to think that an HGF antagonist would be a promising option as a prophylactic treatment, or to ameliorate the progression of PDR.

1.6.4 HGF and the cardiovascular system

Coronary artery disease (CAD) ischemic events and myocardial infarction are the major causes of cardiac failure in the Western world. The only option for severe coronary blockage and

atherosclerosis is bypass surgery. Two pathological events in CAD play major roles in the loss of cardiac function observed: 1) blockage of the coronary arteries resulting in decreased blood perfusion to the heart; and 2) the formation of fibrotic tissue after cardiac insult resulting in ventricle remodeling and decreased compliance. Increased levels of HGF in the circulation have been reported after acute myocardial infarction (Zhu et al., 2000; Jin et al., 2003). This increase in circulating HGF can be used as biological marker for heart injury and gives a clue regarding its protective role (Ueda et al., 2001). Pharmaceuticals that enhance HGF/Met signaling could potentially be used in the treatment of myocardial infarction, providing protection against oxidative stress and cell death due to apoptosis as well as reducing the formation of fibrotic tissue (Ahmet et al., 2002; Kondo et al., 2004; Pietronave et al., 2010). Moreover, another beneficial effect of HGF following myocardial infarction could lie in its ability to induce neovascularization, which could support formation of new cardiac vasculature that would improve reperfusion of the myocardium.

1.6.5 HGF and Wound healing

Excessive scarring is typified by unnecessary accumulation of ECM components in the wound, due to an inappropriate balance between ECM synthesis and degradation. Therapy for pathologic scarring may be directed at inhibiting the synthesis and promoting the degradation of the ECM. HGF in the skin promotes wound healing effectively in several ways: enhancing the proliferation and motility of dermal vascular endothelial cells; stimulating the motility of epidermal keratinocytes; enhancing local blood supply; and accelerating the re-epithelialization of the wound (Nakanishi et al., 2002). Re-epithelialization inhibits the formation of scars.

Studies have shown that HGF gene transfer accelerates dermal wound healing by stimulating angiogenesis and reepithelialization (Nakanishi et al., 2002). Therapeutic approaches that augment HGF/SF would be expected to promote wound healing and prevent scar formation.

1.6.6 HGF in adipose tissue

Obesity is a health problem of epidemic magnitude, and is a major risk factor for cardiovascular disease, type 2 diabetes mellitus, and various types of cancer. Obesity is linked to several alterations in the physiological functions of adipose tissue. These changes lead to insulin resistance, chronic inflammation, and altered secretion of numerous cytokines and growth factors. Recent work have shown that both that HGF/SF and vascular endothelial growth factor (VEGF) are synthesized in human adipose tissue, and that the level of serum HGF/SF is elevated more than three fold in obese individuals (Bell et al., 2006).

HGF that is secreted from adipocytes is suggested to act in a paracrine fashion to promote tumorigenesis in breast tissue (Tuck et al., 1996; Bell et al., 2006). Moreover, studies have indicated that high circulating levels of HGF in patients with coronary artery disease predispose them to a greater long-term risk of atherothrombotic events following percutaneous coronary revascularization (Susen et al., 2005; Bell et al., 2006).Taken together, these observations and others implicate high circulating HGF derived from adipose tissue in the development of cardiovascular disease and cancer.

1.7 HGF/Met in cancer

Cancer is a heterogeneous group of diseases that result from the accumulation of genetic mutations. These mutations cause altered function in proto-oncogenes leading to dysregulation of DNA repair, proliferation, and apoptotic signaling (Tannock, 2005). The dysregulation in the signals within a group of cells leads to the uncontrolled growth, and invasion that either directly intrudes upon and destroys adjacent tissue or metastasizes and spreads to other locations in the body through the lymphatic system or the bloodstream.

A dysfunctioning Met and HGF/SF system appears to be a critical trait of numerous human malignancies. Ectopic overexpression of HGF/SF and/or Met in mouse and human cell lines leads them to develop tumorigenic and metastatic phenotypes in athymic nude mice (Rong et al., 1994). A large number of studies have shown that the HGF/Met pathway is one of the most dysregulated pathways in human malignancies, which include, but are not limited to: bladder, breast, cervical, colorectal, endometrial, esophageal, gastric, head and neck, kidney, liver, lung, nasopharyngeal, ovarian, pancreatic, prostate, and thyroid cancers. Lastly, activating mutations of Met have been discovered in sporadic and inherited forms of human renal papillary carcinomas (Danilkovitch-Miagkova and Zbar, 2002). These mutations which alter sequences within the kinase domain have also been found in other types of solid tumors and metastatic lesions. At this point it is worth mentioning that HGF/SF over- or miss-expression often correlates with poor prognosis, and that the down-regulation of MET or HGF/SF expression in human tumor cells reduces their tumorigenicity (Abounader et al., 2002) .

Activation of Met in cancer occurs most often through ligand autocrine or paracrine activation. Osteosarcomas and globlastoma mutliforme, which express both MET and HGF/SF

are examples of dysfunctional autocrine control. In other instances where paracrine control is paramount, MET over-expression has been reported in human primary tumors while HGF/SF is provided by stromal cells and not by the tumor itself (Houldsworth et al., 1990; Kuniyasu et al., 1992; Hara et al., 1998; Tong et al., 2004; Miller et al., 2006; Bean et al., 2007).

The list of neoplasms in which Met overexpression has been detected is growing relentlessly. In the case of carcinomas, excessive levels of Met expression have been found in virtually every malignancy (Danilkovitch-Miagkova and Zbar, 2002). Receptor over-expression can lead to local receptor oligomerization generating cells reactive to sub-threshold ligand concentrations. HGF itself is able to trigger the transcription of Met (Boccaccio et al., 1994), and it is thus HGF, which is universally expressed by stromal cells throughout the body, that typically drives over expression of Met in tumors (Aguirre Ghiso et al., 1999; Parr et al., 2004). This unique quality of HGF permits it to play a critical role, which engages paracrine positive feedback loops that supports the growth and metastasis of cancer cells. Interestingly, this notion is in agreement with the observation that Met activating mutations require HGF to enhance their catalytic effectiveness (Michieli et al., 1999).

HGF can also abnormally stimulate Met in an autocrine manner, as exemplified by glioblastomas (Weidner et al., 1990), breast carcinomas (Potempa and Ridley, 1998), rhabdomyosarcomas (Hartmann et al., 1994) and osteosarcomas (Ridley et al., 1995). With multiple mechanisms of activation, it is clear that both Met and HGF/SF are major contributors to the progression of most human cancers. Additionally, the demonstrated activities of Met and HGF/SF in proliferation, invasion, angiogenesis and anti-apoptosis (Weidner et al., 1990; Rong et al., 1994; Kitamura et al., 2000; Xiao et al., 2001; Wang et al., 2002; Derksen et al., 2003) demarcate the different stages at which these molecules can participate in tumor development.

Although Met is used as a general marker for cancer, it is also an indicator of biological significance with respect to malignancy and patient prognosis, with high levels correlated with a poor prognosis. Molecules that inhibit Met and HGF/SF can therefore be expected to interfere with the molecular causes of many cancers, and should significantly help in attenuating malignant and metastatic transformations.

1.8 Met pathway inhibitors for cancer therapy progress and challenges

The specificity advantage of target-based treatments has drastically changed the way cancer is treated. Among the many possible therapeutic targets, Met and its ligand HGF/SF have recently gained extensive attention. As indicated above, the Met pathway is dysregulated in most human malignancies. With its characterized pro-neoplastic activities, it is not surprising that numerous Met pathway inhibitors are currently being evaluated in the clinic. Keeping in mind the complexity of cancer as a disease, combination treatments which include a Met antagonist might ultimately provide maximal clinical benefit.

Methods for targeting Met activity: Multiple approaches have been employed to inhibit Met activation with each method targeting one of the serial steps involved in Met activation and regulation. These range from the earliest step of the communication between Met with its ligand HGF/SF, to the downstream dissemination of the Met pathway by Met-associated transducers. Below is a description for some of the methods being used to target the HGF/Met system.

1.8.1 HGF and Met biological variants

HGF/SF variants have been investigated as competitive antagonists of HGF binding to Met. Many experimental results have shown that the entire disulfide bound mature form of HGF/SF is needed for receptor dimerization and activation. Various truncated forms of HGF/SF have been developed; their powerful antagonistic activity has been experimentally confirmed in a range of *in vitro* and *in vivo* models.

Pre-clinical studies have demonstrated that the biological fragments of HGF: NK2, NK4, and a non-uncleavable form of HGF, competitively antagonize HGF effects. NK2, a naturally occurring fragment of HGF consisting of the N-terminal hairpin loop (N domain) and the first two kringle domains (K2), is able to inhibit HGF-induced epithelial mitogenesis and morphogenesis *in vitro* (Chan et al., 1991; Comoglio et al., 2008). NK4 is a fragment of HGF including the entire α-chain but lacking the β-chain. The inhibitory activity of NK4 has been studied extensively and has been demonstrated in multiple *in vitro* and *in vivo* models. These models have utilized various methods for compound delivery, ranging from direct administration of the purified protein to gene therapy techniques (Kuba et al., 2000; Matsumoto and Nakamura, 2003; Matsumoto et al., 2008). A non-processable form of HGF concomitantly blocks Met catalytic activation and HGF proteolytic maturation, by binding to both Met directly and by competing for pro-HGF convertases, respectively (Mazzone et al., 2004).

A decoy Met variant, which is a recombinant inactive molecule made up of the entire Met extracellular domain, acts a competitive antagonist. The decoy Met works by interacting with both HGF and full-length Met, impounding the ligand and interfering with receptor dimerization, respectively (Michieli et al., 2004). Finally, a peptide comprising the Sema domain, which is

essential for normal HGF/Met binding, is capable of blocking ligand binding and receptor dimerization, resulting in the inhibition of Met dependent signaling pathways and blocking HGF induced cellular migration (Kong-Beltran et al., 2004). Although this approach seems promising, obstacles related to molecule size, proteolytic degradation, and drug delivery need to be addressed.

1.8.2 Antibodies against HGF and MET

Numerous therapeutic mAbs that specifically block Met activation are being developed. A number of these have reached clinical development. Amgen has reported the generation of some fully humanized monoclonal antibodies against HGF that exhibit therapeutic potential in mice with subcutaneous xenografts of human glioma cell lines featuring an HGF-dependent autocrine loop (Burgess et al., 2006).

Several initial efforts at the development of anti-Met antibodies with anti-cancer activity failed because the antibodies tended to have agonistic rather than antagonistic effects. These unwanted effects are due to the bivalent structure of the immunoglobulins that resulted in potentiation of Met dimerization. The structural constraint of those agents has been overcome by generating a one-armed antibody (OA-5D5), which is composed of a monovalent Fab fragment with murine variable domains for the heavy and light chains fused to human IgG1 constant domains. In preclinical studies, OA-5D5 can almost completely inhibit intracerebral growth of HGF-expressing glioblastoma cells when delivered locally, directly into the brain (Martens et al., 2006). The antibody is reported to be in the early stages of clinical development (Comoglio et al., 2008).

DN30, an additional monoclonal antibody against the Met extracellular domain, is capable of reducing anchorage-independent growth and xenograft development of gastric carcinoma cells. DN30 also inhibits melanoma metastasis (Petrelli et al., 2006). Remarkably, the mechanism of action of this antibody depends on its ability to induce proteolytic cleavage of Met extracellular domains, generating a 'decoy effect' that prevents HGF/SF binding and subsequent Met dimerization.

This approach, while promising, it is prohibitively expensive. Extrapolation from other anti-cancer biologics currently on the market suggests that the costs of this treatment regime will exceed $50,000 per patient thus limiting its widespread use. Moreover, a variety of factors can weaken antibody efficacy (Reilly et al., 1995). These include the following: (1) restricted diffusion of the antibody into a large solid tumor or into vital regions such as the brain; (2) reduced extravasation of antibodies into target sites owing to reduced vascular permeability; (3) cross-reactivity and nonspecific binding of antibody to normal tissues, reducing the targeting effect; (4) heterogeneous tumor uptake resulting in untreated zones; (5) increased metabolism of injected antibodies, reducing therapeutic effects; and (6) rapid formation of human anti-human antibodies, inactivating the therapeutic antibody. Toxic effects have also been a major obstacle in the development of therapeutic antibodies for cancer.

1.8.3 Small molecule Tyrosine Kinase inhibitors (TKIs)/Met inhibitors

TKIs, which block the intracellular consequences of Met activation, are the most extensively studied family of drugs that target the Met pathway. They are divided into selective or nonselective TKIs according to their selectivity toward Met. Of the many strategies that have

been suggested as a mean to neutralize the Met system, the pharmaceutical industry has focused on the use of "kinase inhibitors" that act at the catalytic site of the kinase. Unfortunately even the best of these drugs have specificity issues in that they affect the action of other kinases unrelated to Met resulting in unwanted side-effects. Some members of this group of drugs have already dropped out of clinical trials because of toxicity concerns.

1.9 HGF/Met a neurotrophic system

HGF and Met are actively expressed in both the developing and adult brains and nerves. The Met system is essential for both the central and peripheral nervous systems to function properly. A large number of studies have shown that HGF and Met are expressed in multiple areas of the brain including the frontal cortex, subependyma, thalamus, cerebellar cortex, deep gray matter, and the hippocampus, an important area for cognition.

The biological activities described above also characterize Met functions in the brain where HGF/Met signaling is neurotrophic (Honda et al., 1995) and protective (Zhang et al., 2000; Takeo et al., 2007; Tyndall and Walikonis, 2007; Takeuchi et al., 2008).Similar to its activities in other tissues, Met in the brain is involved in development, acting as a guidance factor during differentiation, motogenesis and neuritogenesis (Ebens et al., 1996; Sun et al., 2002; Tyndall and Walikonis, 2007). HGF/ Met signaling has also been shown to promote healing following brain injury (Trapp et al., 2008) and especially after ischemic brain injury (Takeo et al., 2007). HGF also displayed neuroprotective effects in animal models for neurodegenerative diseases including amyotrophic lateral sclerosis (ALS). The general pro-survival, pro-proliferative, and pro-migratory functions of HGF, plus its prominant neurotrophic

activities, support the use of HGF as a potential therapeutic agent for the treatment of various diseases of the nervous system.

1.10 Project overview

Currently the pharmaceutical industry is employing two general approaches to block Met dependent cellular activities. The first utilizes single armed humanized antibodies to HGF or Met. This approach, while extremely promising due to its high specificity, is exorbitantly expensive. The second line of development currently being advanced is the use of kinase inhibitors. Although these drugs are able to block Met intracellular signaling, they possess an inherent lack of specificity because they interact with the ATP binding site, which is similar among multiple tyrosine kinases, increasing the risk of serious side effects.

Here I introduce a third approach, which has intrinsic specificity, low cost, and exploits a semi-unique property of this system; namely, the need for HGF to dimerize or multimerize prior to interacting with Met. Several reports have shown that HGF forms dimers and/or multimers, which are arranged in a head-to-tail orientation, prior to its interaction with Met (Youles et al., 2008). The dimer interface encompasses an inter-domain linker amino acids (K122, D123, Y124, I125, R126, and N127), referred to as the Hinge region (Abbate et al., 2011).

Recent work in our laboratory (Yamamoto et al., 2010) has shown that Norleual, an angiotensin IV analog, is a potent anti-HGF/Met antagonist displaying strong anti-cancer activity. Until recently the mechanism responsible for the biological activity of AngIV analogs was unknown. A homologous sequence-conservation screen against all possible transcripts revealed a partial match between AngIV and the Hinge region of HGF (Yamamoto et al., 2010).

This realization initiated the hypothesis that these AngIV analogs are modifying Met activity by interfering with HGF dimerization/multimerization and acting as dominant negative Hinge region mimetics. The demonstration that inhibition of Met activation by AngIV-related peptides appears to be dependent upon their ability to block HGF dimerization led us to speculate whether a peptide representing the Hinge region would have similar activities. The work presented in Chapter 2 demonstrates that not only can a Hinge peptide block HGF dimerization and HGF-dependent cellular activity, but that it also exhibits profound anti-cancer activity. These data have spawned the hypothesis that superior HGF/Met antagonists can be rationally designed, based on the actual structure of the Hinge region.

Despite Norleual's impressive anti-cancer profile, it is metabolically unstable, making its transition to clinical use problematic. Thus a new family of AngIV- related peptidomimetics has been developed, which has been referred to as the 6AH family because 6-amniohexanoic amide is substituted at the C-terminal position. This substitution, along with D-norleucine at the N-terminal, enhances the metabolic resistance of family members. The lead compound in this family, D-Nle-Tyr-Ile-6AH, as well as other members of the family, have shown a range of biological and therapeutic activities. This work is presented in Chapter 3.

As described above HGF is a neurotrophic protein works through its tyrosine kinase receptor, Met, to facilitate learning, long-term potentiation, induction of neurite outgrowth, and cerebroprotection against toxicants. These functions predict that the HGF/Met system should be localized to functional synapses and regulate synaptic reorganization. Recent work in our laboratory showed that Met activation results in an increase in dendritic spine density and functional synapses, and that Met is concentrated in brain regions like the hippocampus, which is of special importance for cognitive functions (Benoist unpublished data). In Chapter 4, using

atomic force microscopy (AFM), I determined the differential localization of Met on hippocampal pyramidal neurons. Understanding the pattern of Met distribution and association on cell surfaces can provide a fingerprint useful for a diagnostic comparison with alterations underlying ligand–receptor dysfunction seen in various neurological diseases. To this end, an AFM tip modified with a specific Met antibody was used to map the differential localization of Met to the cell body or dendrites of pyramidal cells by specific ligand-receptor force spectroscopy.

1.11 References

Abbate V, Bassindale AR, Brandstadt KF and Taylor PG (2011) A large scale enzyme screen in the search for new methods of silicon-oxygen bond formation. *J Inorg Biochem* **105**:268-275.

Abounader R, Lal B, Luddy C, Koe G, Davidson B, Rosen EM and Laterra J (2002) In vivo targeting of SF/HGF and Met expression via U1snRNA/ribozymes inhibits glioma growth and angiogenesis and promotes apoptosis. *FASEB JOURNAL* **16**:108-110.

Aguirre Ghiso JA, Alonso DF, Farías EF, Gomez DE and de Kier Joffé (1999) Deregulation of the signaling pathways controlling urokinase production. Its relationship with the invasive phenotype. *European journal of biochemistry / FEBS* **263**:295-304.

Ahmet I, Sawa Y, Iwata K and Matsuda H (2002) Gene transfection of hepatocyte growth factor attenuates cardiac remodeling in the canine heart: A novel gene therapy for cardiomyopathy. *Journal of Thoracic and Cardiovascular Surgery* **124**:957-963.

Basilico C, Arnesano A, Galluzzo M, Comoglio PM and Michieli P (2008) A High Affinity Hepatocyte Growth Factor-binding Site in the Immunoglobulin-like Region of Met, in *Journal of Biological Chemistry* pp 21267-21277.

Bauer TW, Somcio RJ, Fan F, Liu W, Johnson M, Lesslie DP, Evans DB, Gallick GE and Ellis LM (2006) Regulatory role of Met in insulin-like growth factor-I receptor-mediated migration and invasion of human pancreatic carcinoma cells. *Molecular cancer therapeutics* **5**:1676-1682.

Bean J, Brennan C, Shih J-Y, Riely G, Viale A, Wang L, Chitale D, Motoi N, Szoke J, Broderick S, Balak M, Chang W-C, Yu C-J, Gazdar A, Pass H, Rusch V, Gerald W, Huang S-F,

Yang P-C, Miller V, Ladanyi M, Yang C-H and Pao W (2007) MET amplification occurs with or without T790M mutations in EGFR mutant lung tumors with acquired resistance to gefitinib or erlotinib. *Proceedings of the National Academy of Sciences of the United States of America.* **104**:20932.

Bechard D, Gentina T, Delehedde M, Scherpereel A, Lyon M, Aumercier M, Vazeux R, Richet C, Degand P, Jude B, Janin A, Fernig DG, Tonnel AB and Lassalle P (2001) Endocan is a novel chondroitin sulfate/dermatan sulfate proteoglycan that promotes hepatocyte growth factor/scatter factor mitogenic activity. *The Journal of biological chemistry* **276**:48341-48349.

Bell LN, Ward JL, Degawa-Yamauchi M, Bovenkerk JE, Jones R, Cacucci BM, Gupta CE, Sheridan C, Sheridan K, Shankar SS, Steinberg HO, March KL and Considine RV (2006) Adipose tissue production of hepatocyte growth factor contributes to elevated serum HGF in obesity. *American journal of physiology. Endocrinology and metabolism* **291**:843-848.

Birchmeier C, Birchmeier W, Gherardi E and Vande Woude GF (2003) MET, METASTASIS, MOTILITY AND MORE, in *Nature Reviews Molecular Cell Biology* pp 915-925, Nature Publishing Group.

Birchmeier C and Gherardi E (1998) Developmental Roles of HGF/SF and Its Receptor, The Met Tyrosine Kinase. *Trends in cell biology* **8**:404-409.

Bladt F, Riethmacher D, Isenmann S, Aguzzi A and Birchmeier C (1995) Essential role for the Met receptor in the migration of myogenic precursor cells into the limb bud. *Nature* **376**:768-771.

Boccaccio C and Comoglio PM (2006) Invasive growth: a MET-driven genetic programme for cancer and stem cells. *Nature reviews. Cancer* **6**:637-645.

Boccaccio C, Gaudino G, Gambarotta G, Galimi F and Comoglio PM (1994) Hepatocyte growth factor (HGF) receptor expression is inducible and is part of the delayed-early response to HGF. *The Journal of biological chemistry* **269**:12846-12851.

Bonine-Summers AR, Aakre ME, Brown KA, Arteaga CL, Pietenpol JA, Moses HL and Cheng N (2007) Epidermal growth factor receptor plays a significant role in hepatocyte growth factor mediated biological responses in mammary epithelial cells. *Cancer biology & therapy* **6**:561-570.

Bork P, Doerks T, Springer TA and Snel B (1999) Domains in plexins: links to integrins and transcription factors. *Trends in biochemical sciences* **24**:261-263.

Boros P and Miller CM (1995) Hepatocyte growth factor: A multifunctional cytokine. *Lancet* **345**:293.

Borowiak M, Garratt AN, Wüstefeld T, Strehle M, Trautwein C, Birchmeier C and Wigler MH (2004) Met Provides Essential Signals for Liver Regeneration. *Proceedings of the National Academy of Sciences of the United States of America* **101**:10608-10613.

Boulton M (1999) A role for hepatocyte growth factor in diabetic retinopathy? *British journal of ophthalmology.* **83**:763.

Burgess T, Coxon A, Meyer S, Sun J, Rex K, Tsuruda T, Chen Q, Ho SY, Li L, Kaufman S, McDorman K, Cattley RC, Elliott G, Zhang K, Feng X, Jia XC, Green L, Radinsky R and Kendall R (2006) Fully human monoclonal antibodies to hepatocyte growth factor with therapeutic potential against hepatocyte growth factor/Met-dependent human tumors. *Cancer research* **66**:1721-1729.

Chan AM, Rubin JS, Bottaro DP, Hirschfield DW, Chedid M and Aaronson SA (1991) Identification of a competitive HGF antagonist encoded by an alternative transcript. *Science (New York, N.Y.)* **254**:1382-1385.

Chirgadze DY, Hepple JP, Zhou H, Byrd RA, Blundell TL and Gherardi E (1999) Crystal structure of the NK1 fragment of HGF/SF suggests a novel mode for growth factor dimerization and receptor binding. *Nature structural biology* **6**:72-79.

Comoglio PM (2001) Pathway specificity for Met signalling, in *Nature Cell Biology* p E161, Nature Publishing Group.

Comoglio PM, Giordano S and Trusolino L (2008) Drug development of MET inhibitors: targeting oncogene addiction and expedience. *Nature reviews. Drug discovery* **7**:504-516.

Danilkovitch-Miagkova A and Zbar B (2002) Dysregulation of Met receptor tyrosine kinase activity in invasive tumors. *The Journal of clinical investigation* **109**:863-867.

Derksen PW, de Gorter DJ, Meijer HP, Bende RJ, van Dijk M, Lokhorst HM, Bloem AC, Spaargaren M and Pals ST (2003) The hepatocyte growth factor/Met pathway controls proliferation and apoptosis in multiple myeloma. *Leukemia : official journal of the Leukemia Society of America, Leukemia Research Fund, U.K* **17**:764-774.

DiGabriele AD, Lax I, Chen DI, Svahn CM, Jaye M, Schlessinger J and Hendrickson WA (1998) Structure of a heparin-linked biologically active dimer of fibroblast growth factor. *Nature* **393**:812-817.

Ebens A, Brose K, Leonardo ED, Hanson MG, Jr., Bladt F, Birchmeier C, Barres BA and Tessier-Lavigne M (1996) Hepatocyte growth factor/scatter factor is an axonal chemoattractant and a neurotrophic factor for spinal motor neurons. *Neuron* **17**:1157-1172.

Eder JP, Vande Woude GF, Boerner SA and LoRusso PM (2009) Novel therapeutic inhibitors of the Met signaling pathway in cancer. *Clinical cancer research : an official journal of the American Association for Cancer Research* **15**:2207-2214.

Fujimoto J and Kaneda Y (1999) Reversing liver cirrhosis: impact of gene therapy for liver cirrhosis. *Gene therapy-Basingstoke* **6**:305-306.

Furge KA, Zhang Y-W and Vande Woude GF (2000) Met receptor tyrosine kinase: enhanced signaling through adapter proteins, in *Oncogene* p 5582, Nature Publishing Group.

Gao CF and Vande Woude GF (2005) HGF/SF-Met signaling in tumor progression. *Cell research-English edition-* **15**:49-51.

Gentile A, Trusolino L and Comoglio P (2008) The Met tyrosine kinase receptor in development and cancer. *Cancer and Metastasis Reviews* **27**:85-94.

Gherardi E, Sandin S, Petoukhov MV, Finch J, Youles ME, Ã"Fverstedt L-Gr, Miguel RN, Biundell TL, Vande Woude GF, Skoglund U and Svergun DI (2006) Structural basis of hepatocyte growth factor/scatter factor and MET signalling, in *Proceedings of the National Academy of Sciences of the United States of America* pp 4046-4051.

Gherardi E, Youles ME, Miguel RN, Blundell TL, Lamele L, Gough J, Bandyopadhyay A, Hartmann G and Butler PJG (2003) Functional map and domain structure of MET, the product of the Met protooncogene and receptor for hepatocyte growth factor/scatter factor, in *Proceedings of the National Academy of Sciences of the United States of America* pp 12039-12044.

Giordano S, Corso S, Conrotto P, Artigiani S, Gilestro G, Barberis D, Tamagnone L and Comoglio PM (2002) The semaphorin 4D receptor controls invasive growth by coupling with Met. *Nature cell biology* **4**:720-724.

Hara T, Ooi A, Kobayashi M, Mai M, Yanagihara K and Nakanishi I (1998) Amplification of c-myc, K-sam, and Met in Gastric Cancers: Detection by Fluorescence In Situ Hybridization. *Laboratory investigation.* **78**:1143.

Hartmann G, Prospero T, Brinkmann V, Ozcelik O, Winter G, Hepple J, Batley S, Bladt F, Sachs M, Birchmeier C, Birchmeier W and Gherardi E (1998) Engineered mutants of HGF/SF with reduced binding to heparan sulphate proteoglycans, decreased clearance and enhanced activity in vivo. *Current Biology* **8**.

Hartmann G, Weidner KM, Schwarz H and Birchmeier W (1994) The motility signal of scatter factor/hepatocyte growth factor mediated through the receptor tyrosine kinase met requires intracellular action of Ras. *The Journal of biological chemistry* **269**:21936-21939.

Holmes O, Pillozzi S, Deakin JA, Carafoli F, Kemp L, Butler PJG, Lyon M and Gherardi E (2007) Insights into the Structure/Function of Hepatocyte Growth Factor/Scatter Factor from Studies with Individual Domains, in *Journal of Molecular Biology* **367:** 395-408.

Honda S, Kagoshima M, Wanaka A, Tohyama M, Matsumoto K and Nakamura T (1995) Localization and functional coupling of HGF and Met/HGF receptor in rat brain: implication as neurotrophic factor. *Brain research. Molecular brain research* **32**:197-210.

Houldsworth J, Cordon-Cardo C, Ladanyi M, Kelsen DP and Chaganti RS (1990) Gene amplification in gastric and esophageal adenocarcinomas. *Cancer research* **50**:6417-6422.

Hubbard SR and Till JH (2000) Protein tyrosine kinase structure and function. *Annual review of biochemistry.* **69**:373-398.

Jin H, Yang R, Li W, Ogasawara AK, Schwall R, Eberhard DA, Zheng Z, Kahn D and Paoni NF (2003) Early Treatment with Hepatocyte Growth Factor Improves Cardiac Function in Experimental Heart Failure Induced by Myocardial Infarction. *Jornal of pharmacology and experimental therapeutics* **304**:654-705.

Jun EJ, Kim HS and Kim YH (2007) Role of HGF/Met in serum-starved ARPE-19 cells. *Korean journal of ophthalmology : KJO* **21**:244-250.

Kaibori M, Inoue T, Oda M, Naka D, Kawaguchi T, Kitamura N, Miyazawa K, Kwon AH, Kamiyama Y and Okumura T (2002) Exogenously Administered HGF Activator Augments Liver Regeneration through the Production of Biologically Active HGF. *Biochemical and Biophysical Research Communications* **290**:475-481.

Katsura Y, Okano T, Noritake M, Kosano H, Nishigori H, Kado S and Matsuoka T (1998) Hepatocyte growth factor in vitreous fluid of patients with proliferative diabetic retinopathy and other retinal disorders. *Diabetes care* **21**:1759-1763.

Khoury H, Naujokas MA, Zuo D, Sangwan V, Frigault MM, Petkiewicz S, Dankort DL, Muller WJ and Park M (2005) HGF Converts ErbB2/Neu Epithelial Morphogenesis to Cell Invasion. *Molecular biology of the cell /* **16**:550.

Kitamura S, Kondo S, Shinomura Y, Kanayama S, Miyazaki Y, Kiyohara T, Hiraoka S and Matsuzawa Y (2000) Met/HGF receptor modulates bcl-w expression and inhibits apoptosis in human colorectal cancers. *British Journal of Cancer* **83**:668-673.

Kondo I, Ohmori K, Oshita A, Takeuchi H, Fuke S, Shinomiya K, Noma T, Namba T and Kohno M (2004) Treatment of acute myocardial infarction by hepatocyte growth factor gene transfer: the first demonstration of myocardial transfer of a "functional" gene using

ultrasonic microbubble destruction. *Journal of the American College of Cardiology* **44**:644-653.

Kong-Beltran M, Stamos J and Wickramasinghe D (2004) The Sema domain of Met is necessary for receptor dimerization and activation. *Cancer cell.* **6**:75-84.

Kuba K, Matsumoto K, Date K, Shimura H, Tanaka M and Nakamura T (2000) HGF/NK4, a four-kringle antagonist of hepatocyte growth factor, is an angiogenesis inhibitor that suppresses tumor growth and metastasis in mice. *Cancer research* **60**:6737-6743.

Kuniyasu H, Yasui W, Kitadai Y, Yokozaki H, Ito H and Tahara E (1992) Frequent amplification of the Met gene in scirrhous type stomach cancer. *Biochemical and Biophysical Research Communications* **189**:227-232.

Lietha D, Chirgadze DY, Mulloy B, Blundell TL and Gherardi E (2001) Crystal structures of NK1-heparin complexes reveal the basis for NK1 activity and enable engineering of potent agonists of the MET receptor. *EMBO* **20**:5543.

Liu X, Newton RC and Scherle PA (2009) Developing Met pathway inhibitors for cancer therapy: progress and challenges. *Trends in molecular medicine* **16**:37-45.

Liu X, Yao W, Newton RC and Scherle PA (2008) Targeting the Met signaling pathway for cancer therapy. *Expert opinion on investigational drugs* **17**:997-1011.

Liu Y and Yang J (2006) Hepatocyte growth factor: New arsenal in the fights against renal fibrosis? *Kidney International* **70**:238-240.

Lock LS, Royal I, Naujokas MA and Park M (2000) Identification of an atypical Grb2 carboxyl-terminal SH3 domain binding site in Gab docking proteins reveals Grb2-dependent and -independent recruitment of Gab1 to receptor tyrosine kinases. *The Journal of biological chemistry* **275**:31536-31545.

Lokker NA, Mark MR, Luis EA, Bennett GL, Robbins KA, Baker JB and Godowski PJ (1992) Structure-function analysis of hepatocyte growth factor: identification of variants that lack mitogenic activity yet retain high affinity receptor binding. *The EMBO journal* **11**:2503-2510.

Longati P, Bardelli A, Ponzetto C, Naldini L and Comoglio PM (1994) Tyrosines1234-1235 are critical for activation of the tyrosine kinase encoded by the MET proto-oncogene (HGF receptor). *Oncogene* **9**:49-57.

Lyon M, Deakin JA and Gallagher JT (2002) The mode of action of heparan and dermatan sulfates in the regulation of hepatocyte growth factor/scatter factor. *The Journal of biological chemistry* **277**:1040-1046.

Lyon M, Deakin JA, Lietha D, Gherardi E and Gallagher JT (2004) The interactions of hepatocyte growth factor/scatter factor and its NK1 and NK2 variants with glycosaminoglycans using a modified gel mobility shift assay. Elucidation of the minimal size of binding and activatory oligosaccharides. *The Journal of biological chemistry* **279**:43560-43567.

Lyon M, Deakin JA, Mizuno K, Nakamura T and Gallagher JT (1994) Interaction of hepatocyte growth factor with heparan sulfate. Elucidation of the major heparan sulfate structural determinants. *The Journal of biological chemistry* **269**:11216-11223.

Lyon M, Deakin JA, Rahmoune H, Fernig DG, Nakamura T and Gallagher JT (1998) Hepatocyte growth factor/scatter factor binds with high affinity to dermatan sulfate. *The Journal of biological chemistry* **273**:271-278.

Maina F, Panté G, Helmbacher F, Andres R, Porthin A, Davies AM, Ponzetto C and Klein R (2001) Coupling Met to specific pathways results in distinct developmental outcomes. *Molecular cell* **7**:1293-1306.

Martens T, Schmidt N-O, Eckerich C, Fillbrandt R, Merchant M, Schwall R, Westphal M and Lamszus K (2006) A Novel One-Armed Anti-Met Antibody Inhibits Glioblastoma Growth In vivo. *Clinical cancer research : an official journal of the American Association for Cancer Research.* **12**:6144.

Matsumoto K and Nakamura T (2001) Hepatocyte growth factor: Renotropic role and potential therapeutics for renal diseases. *Kidney International* **59**:2023-2038.

Matsumoto K and Nakamura T (2003) NK4 (HGF-antagonist/angiogenesis inhibitor) in cancer biology and therapeutics. *CANCER SCIENCE* **94**:321-327.

Matsumoto K, Nakamura T, Sakai K and Nakamura T (2008) Hepatocyte growth factor and Met in tumor biology and therapeutic approach with NK4. *Proteomics.*:3360.

Mazzone M, Basilico C, Cavassa S, Pennacchietti S, Risio M, Naldini L, Comoglio PM and Michieli P (2004) An uncleavable form of pro-scatter factor suppresses tumor growth and dissemination in mice. *The Journal of clinical investigation* **114**:1418-1432.

Michalopoulos GK (2007) Liver regeneration. *Journal of cellular physiology* **213**:286-300.

Michieli P, Basilico C, Pennacchietti S, Maffe A, Tamagnone L, Giordano S, Bardelli A and Comoglio PM (1999) Mutant Met-mediated transformation is ligand-dependent and can be inhibited by HGF antagonists. *Oncogene* **18**.

Michieli P, Mazzone M, Basilico C, Cavassa S, Sottile A, Naldini L and Comoglio PM (2004) Targeting the tumor and its microenvironment by a dual-function decoy Met receptor. *Cancer cell.* **6**:61-73.

Miller CT, Lin L, Casper AM, Lim J, Thomas DG, Orringer MB, Chang AC, Chambers AF, Giordano TJ and Glover TW (2006) Genomic amplification of MET with boundaries within fragile site FRA7G and upregulation of MET pathways in esophageal adenocarcinoma. *ONCOGENE -BASINGSTOKE-* **25**:409-418.

Nakamura T, Mizuno S, Matsumoto K, Sawa Y and Matsuda H (2000) Myocardial protection from ischemia/reperfusion injury by endogenous and exogenous HGF. *The Journal of clinical investigation* **106**:1511-1519.

Nakanishi K, Uenoyama M, Tomita N, Morishita R, Kaneda Y, Ogihara T, Matsumoto K, Nakamura T, Maruta A, Matsuyama S, Kawai T, Aurues T, Hayashi T and Ikeda T (2002) Gene Transfer of Human Hepatocyte Growth Factor into Rat Skin Wounds Mediated by Liposomes Coated with the Sendai Virus (Hemagglutinating Virus of Japan). *The American journal of pathology.* **161**:1761.

Orian-Rousseau V, Chen L, Sleeman JP, Herrlich P and Ponta H (2002) CD44 is required for two consecutive steps in HGF/Met signaling. *Genes & development* **16**:3074-3086.

Parr C, Watkins G, Mansel RE and Jiang WG (2004) The hepatocyte growth factor regulatory factors in human breast cancer. *Clinical cancer research : an official journal of the American Association for Cancer Research* **10**:202-211.

Pelicci G, Giordano S, Zhen Z and Salcini AE (1995) The motogenic and mitogenic responses to HGF are amplified by the Shc adaptor protein. *Oncogene.* **10**:1631.

Peruzzi B and Bottaro DP (2006) Targeting the Met signaling pathway in cancer. *Clinical cancer research : an official journal of the American Association for Cancer Research* **12**:3657-3660.

Peschard P, Ishiyama N, Lin T, Lipkowitz S and Park M (2004) A conserved DpYR motif in the juxtamembrane domain of the Met receptor family forms an atypical c-Cbl/Cbl-b tyrosine kinase binding domain binding site required for suppression of oncogenic activation. *The Journal of biological chemistry* **279**:29565-29571.

Petrelli A, Circosta P, Granziero L, Mazzone M, Pisacane A, Fenoglio S, Comoglio PM and Giordano S (2006) Ab-Induced Ectodomain Shedding Mediates Hepatocyte Growth Factor Receptor down-Regulation and Hampers Biological Activity. *Proceedings of the National Academy of Sciences of the United States of America* **103**:5090-5095.

Pietronave S, Forte G, Locarno D, Merlin S, Zamperone A, Nicotra G, Isidoro C, Di Nardo P and Prat M (2010) Agonist monoclonal antibodies against HGF receptor protect cardiac muscle cells from apoptosis. *American journal of physiology.* **298**:H1155-65.

Ponzetto C, Bardelli A, Zhen Z, Maina F, dalla Zonca P, Giordano S, Graziani A, Panayotou G and Comoglio PM (1994) A multifunctional docking site mediates signaling and transformation by the hepatocyte growth factor/scatter factor receptor family. *Cell* **77**:261-271.

Potempa S and Ridley AJ (1998) Activation of Both MAP Kinase and Phosphatidylinositide 3-Kinase by Ras Is Required for Hepatocyte Growth Factor/Scatter Factor-induced Adherens Junction Disassembly. *Molecular biology of the cell* **9**:2185-2200.

Rabkin R, Fervenza F, Tsao T, Sibley R, Friedlaender M, Hsu F, Lassman C, Hausmann M, Huie P and Schwall RH (2001) Hepatocyte growth factor receptor in acute tubular necrosis. *Journal of the American Society of Nephrology : JASN* **12**:531-540.

Reilly RM, Sandhu J, Alvarez-Diez TM, Gallinger S, Kirsh J and Stern H (1995) Problems of delivery of monoclonal antibodies. Pharmaceutical and pharmacokinetic solutions. *Clinical pharmacokinetics* **28**:126-142.

Ridley AJ, Comoglio PM and Hall A (1995) Regulation of scatter factor/hepatocyte growth factor responses by Ras, Rac, and Rho in MDCK cells. *Molecular and cellular biology* **15**:1110-1122.

Rong S, Segal S, Anver M, Resau JH and Woude GFV (1994) Invasiveness and Metastasis of NIH 3T3 Cells Induced by Met-Hepatocyte Growth Factor/Scatter Factor Autocrine Stimulation. *Proceedings of the National Academy of Sciences of the United States of America* **91**:4731-4735.

Roos F, Ryan AM, Chamow SM, Bennett GL and Schwall RH (1995) Induction of liver growth in normal mice by infusion of hepatocyte growth factor/scatter factor. *The American journal of physiology* **268**:380-386.

Schmidt C, Bladt F, Goedecke S, Brinkmann V, Zschiesche W, Sharpe M, Gherardi E and Birchmeier C (1995) Scatter factor/hepatocyte growth factor is essential for liver development. *Nature* **373**:699-702.

Schwall RH, Chang LY, Godowski PJ, Kahn DW, Hillan KJ, Bauer KD and Zioncheck TF (1996) Heparin Induces Dimerization and Confers Proliferative Activity onto the Hepatocyte Growth Factor Antagonists NK1 and NK2. *The Journal of Cell Biology* **133**:709-718.

Seki T, Hagiya M, Shimonishi M, Nakamura T and Shimizu S (1991) Organization of the human hepatocyte growth factor-encoding gene. *Gene* **102**:213-219.

Sheth PR, Hays JL, Elferink LA and Watowich SJ (2008) Biochemical Basis for the Functional Switch That Regulates Hepatocyte Growth Factor Receptor Tyrosine Kinase Activation, in *Biochemistry* pp 4028-4038.

Stamos J, Lazarus RA, Yao X, Kirchhofer D and Wiesmann C (2004) Crystal structure of the HGF beta-chain in complex with the Sema domain of the Met receptor. *EMBO JOURNAL* **23**:2325-2335.

Stella MC and Comoglio PM (1999) HGF: a multifunctional growth factor controlling cell scattering. *The international journal of biochemistry & cell biology.* **31**:1357-1362.

Sun W, Funakoshi H and Nakamura T (2002) Localization and functional role of hepatocyte growth factor (HGF) and its receptor Met in the rat developing cerebral cortex. *Molecular Brain Research* **103**.

Susen S, Sautière K, Mouquet Fdr, Cuilleret Fo, Chmaït A, McFadden EnP, Hennache B, Richard F, de Groote P, Lablanche J-M, Dallongeville J, Bauters C, Jude B and Van Belle E (2005) Serum hepatocyte growth factor levels predict long-term clinical outcome after percutaneous coronary revascularization. *European Heart Journal* **26**:2387-2395.

Takeo S, Takagi N and Takagi K (2007) [Ischemic brain injury and hepatocyte growth factor]. *Yakugaku zasshi : Journal of the Pharmaceutical Society of Japan* **127**:1813-1823.

Takeuchi D, Sato N, Shimamura M, Kurinami H, Takeda S, Shinohara M, Suzuki S, Kojima M, Ogihara T and Morishita R (2008) Alleviation of Abeta-induced cognitive impairment by ultrasound-mediated gene transfer of HGF in a mouse model. *Gene therapy* **15**:561-571.

Tannock I (2005) *The basic science of oncology*. McGraw-Hill, Medical Pub. Division, New York.

Tolbert WD, Daugherty J, Gao C, Xie Q, Miranti C, Gherardi E, Woude GV and Xu HE (2007) A mechanistic basis for converting a receptor tyrosine kinase agonist to an antagonist. *Proceedings of the National Academy of Sciences of the United States of America* **104**:14592-14597.

Tong CY, Hui AB, Yin XL, Pang JC, Zhu XL, Poon WS and Ng HK (2004) Detection of oncogene amplifications in medulloblastomas by comparative genomic hybridization and array-based comparative genomic hybridization. *Journal of neurosurgery* **100**:187-193.

Trapp T, Kögler G, El-Khattouti A, Sorg RV, Besselmann M, Föcking M, Bührle CP, Trompeter I, Fischer JC and Wernet P (2008) Hepatocyte Growth Factor/Met Axis-mediated Tropism of Cord Blood-derived Unrestricted Somatic Stem Cells for Neuronal Injury. *Journal of Biological Chemistry* **283**.

Trusolino L, Bertotti A and Comoglio PM (2001) A signaling adapter function for alpha6beta4 integrin in the control of HGF-dependent invasive growth. *Cell* **107**:643-654.

Tuck AB, Park M, Sterns EE, Boag A and Elliott BE (1996) Coexpression of Hepatocyte Growth Factor and Receptor (Met) in Human Breast Carcinoma. *American Journal of Pathology* **148**:225-232.

Tyndall SJ and Walikonis RS (2007) Signaling by hepatocyte growth factor in neurons is induced by pharmacological stimulation of synaptic activity. *Synapse (New York, N.Y.)* **61**:199-204.

Ueda H, Nakamura T, Matsumoto K, Sawa Y and Matsuda H (2001) A potential cardioprotective role of hepatocyte growth factor in myocardial infarction in rats. *Cardiovascular research* **51**:41-50.

Uehara Y, Minowa O, Mori C, Shiota K, Kuno J, Noda T and Kitamura N (1995) Placental defect and embryonic lethality in mice lacking hepatocyte growth factor/scatter factor. *Nature* **373**:702-705.

Ultsch M, Lokker NA, Godowski PJ and de Vos AM (1998) Crystal structure of the NK1 fragment of human hepatocyte growth factor at 2.0 A resolution. *Structure (London, England : 1993)* **6**:1383-1393.

Wang X, DeFrances MC, Dai Y, Pediaditakis P, Johnson C, Bell A, Michalopoulos GK and Zarnegar R (2002) A mechanism of cell survival: sequestration of Fas by the HGF receptor Met. *Molecular cell* **9**:411-421.

Webb CP, Taylor GA, Jeffers M, Fiscella M, Oskarsson M, Resau JH and Vande Woude GF (1998) Evidence for a role of Met-HGF/SF during Ras-mediated tumorigenesis/metastasis. *Oncogene* **17**:2019-2025.

Weidner KM, Behrens Jr, Vandekerckhove J and Birchmeier W (1990) Scatter Factor: Molecular Characteristics and Effect on the Invasiveness of Epithelial Cells. *The Journal of Cell Biology* **111**:2097-2108.

Weidner KM, Di Cesare S, Sachs M, Brinkmann V, Behrens J and Birchmeier W (1996) Interaction between Gab1 and the Met receptor tyrosine kinase is responsible for epithelial morphogenesis. *Nature* **384**:173-176.

Xiao G-H, Jeffers M, Bellacosa A, Mitsuuchi Y, Woude GFV and Testa JR (2001) Anti-Apoptotic Signaling by Hepatocyte Growth Factor/Met via the Phosphatidylinositol 3-Kinase/Akt and Mitogen-Activated Protein Kinase Pathways. *Proceedings of the National Academy of Sciences of the United States of America* **98**:247-252.

Xiong JP, Stehle T, Zhang R, Joachimiak A, Frech M, Goodman SL and Arnaout MA (2002) Crystal structure of the extracellular segment of integrin alpha Vbeta3 in complex with an Arg-Gly-Asp ligand. *Science (New York, N.Y.)* **296**:151-155.

Xu W and Wu SG (1999) The possible relationship between hepatomegaly and release of HGF into plasma induced by clofibrate in rats. World Journal of Gastroenterology. **5**: 440-442.

Yamamoto BJ, Elias PD, Masino JA, Hudson BD, McCoy AT, Anderson ZJ, Varnum MD, Sardinia MF, Wright JW and Harding JW (2010) The Angiotensin IV Analog Nle-Tyr-Leu-ψ-(CH2-NH2)3-4-His-Pro-Phe (Norleual) Can Act as a Hepatocyte Growth Factor/Met Inhibitor. *The Journal of pharmacology and experimental therapeutics.* **333**:161.

Youles M, Holmes O, Petoukhov MV, Nessen MA, Stivala S, Svergun DI and Gherardi E (2008) Engineering the NK1 Fragment of Hepatocyte Growth Factor/Scatter Factor as a MET Receptor Antagonist, in *Journal of Molecular Biology* **3**: 616-622.

Zhang L, Himi T, Morita I and Murota S (2000) Hepatocyte growth factor protects cultured rat cerebellar granule neurons from apoptosis via the phosphatidylinositol-3 kinase/Akt pathway. *Journal of neuroscience research* **59**:489-496.

Zhu Y, Hojo Y, Ikeda U and Shimada K (2000) Production of hepatocyte growth factor during acute myocardial infarction. *Heart (British Cardiac Society)* **83**:450-455.

CHAPTER TWO

MIMICS OF THE DIMERIZATION DOMAIN OF HEPATOCYTE GROWTH FACTOR EXHIBIT ANTI-MET AND ANTI-CANCER ACTIVITY

2.1 Abstract

The angiotensin IV analog Norleual [Nle-Tyr-Leu-ψ-(CH_2-NH_2)-Leu-His-Pro-Phe] has been shown recently to act as an HGF/Met antagonist capable of blocking the binding of HGF to the Met receptor, inhibiting HGF-dependent activation of Met, and attenuating HGF-dependent cellular activities. Additionally, Norleual exhibited marked anti-cancer activity. Homology between Norleual and the dimerization domain (Hinge region) of HGF led to the hypothesis that Norleual acts by interfering with HGF dimerization/multimerization and functions as a dominant negative Hinge-region mimic. To test this hypothesis we investigated the ability of Norleual to bind to and inhibit the dimerization of HGF. To further evaluate the idea that Norleual was acting as a Hinge region mimic, we synthesized a hexapeptide representing the HGF Hinge sequence and established its capacity to similarly block HGF-dependent activation of Met and HGF-dependent cellular functions. The Hinge peptide not only bound with high affinity directly to HGF and blocked its dimerization, but it also inhibited HGF-dependent Met activation, suppressed HGF-dependent cellular functions, and exhibited anti-cancer activity. The major implication of this study is that molecules targeting the dimerization domain of HGF may represent novel and viable anti-cancer therapeutics; the development of such molecules should be feasible using Norleual and the Hinge peptide as synthetic templates.

2.2 Introduction

The binding of HGF to its cell surface receptor, Met, stimulates mitogenesis, motogenesis, and morphogenesis in a wide range of cellular targets (Birchmeier et al., 2003), including: epithelial cells (Kakazu et al., 2004), endothelial cells (Kanda et al., 2006), hematopoetic cells (Ratajczak et al., 1997), neurons (Maina and Klein, 1999; Thompson et al., 2004), melanocytes (Halaban et al., 1992), and hepatocytes (Cramer et al., 2004). Together these actions are responsible for HGF's impact on development, homeostasis, and tissue regeneration (Kopp, 1998). Dysregulation of the HGF/Met system often leads to neoplastic changes and to cancer (Danilkovitch-Miagkova and Zbar, 2002; Gentile et al., 2008); the HGF/Met system is one of the most commonly dysregulated systems in cancer (both human and animal) (Takayama et al., 1997; Liu et al., 2008). In addition to direct effects on the behavior of cancer cells, the HGF/Met system is a critical regulator of angiogenesis, a process that is essential for tumor growth and an enabler of metastasis (Sengupta et al., 2003; Zhang et al., 2003). Because of the close linkage between the HGF/Met system and cancer, the development of molecules that block HGF/Met has become a focus of the pharmaceutical industry (Liu et al., 2010).

One potential therapeutic approach to inhibit the HGF/Met system, which has yet to be actively pursued, is blockade of the HGF dimerization process. Ligand dimerization is an essential step in the course of HGF and ultimately Met activation (Gherardi et al., 2006; Youles et al., 2008). A critical participant in the dimerization process is an HGF domain that lies between its N-terminal and first kringle domains, referred to as the Hinge region (Youles et al., 2008; Yamamoto et al., 2010). Our laboratory has developed a family of small peptoid-like molecules based on angiotensin IV (AngIV), which are hypothesized here to act as mimics of the

HGF dimerization domain. The anti-cancer activity of one these molecules, Norleual, appears to depend on its ability to potently inhibit HGF/Met signaling (Yamamoto et al., 2010). Despite this apparent link between the AngIV and HGF/Met systems, the exact molecular mechanism underlying the action of analogs like Norleual has remained unclear. Homology between Norleual and the Hinge region of HGF led us to hypothesize that Norleual acts to block HGF dimerization and thus Met activation (Yamamoto et al, 2010).

In support of this hypothesis, we have determined that Norleual binds with high affinity to HGF and, as predicted, potently inhibits HGF dimerization. These observations led to the corollary hypothesis that a peptide encompassing the Hinge region should exhibit biological and chemical properties similar to Norleual. Like Norleual the hexapeptide representing the Hinge region (KDYIRN) was found to bind to HGF with high affinity and inhibit HGF dimerization. Further functional analysis demonstrated the capacity of the Hinge peptide to block HGF-dependent Met phosphorylation, cell proliferation, and scattering at concentrations in the picomolar range. Not only was the Hinge peptide capable of inhibiting HGF-dependent cellular actions *in-vitro,* but like Norleual (Yamamoto et al., 2010), it significantly suppressed pulmonary colonization by B16-F10 murine melanoma cells in C57BL/6 mice, which are characterized by an overactive HGF/Met system (Takayama et al., 1997; Ferraro et al., 2006). These data lead us to propose that Norleual and the Hinge peptide exert their anti-Met and anti-cancer activities by blocking HGF dimerization, thus interfering with HGF-dependent activation of Met. Furthermore, these findings suggest that effective anti-cancer therapeutics can be developed using the Hinge region sequence as the parent synthetic template.

2.3 Materials & Methods

Animals. Male C57BL/6 mice, 6-8 months old, from Taconic Farms were used for *in vivo* studies. Mice with free access to Purina rat chow were housed individually in an American Accreditation for Laboratory Animal Care-approved vivarium maintained at 22±1°C on a 12-h alternating light/dark cycle initiated at 06:00 h.

Compounds. Nle-Tyr-Leu-ψ-$(CH_2\text{-}NH_2)^{3\text{-}4}$-His-Pro-Phe (Norleual) and the Hinge peptide (KDYIRN) were synthesized using Fmoc-based solid-phase peptide synthesis methods and purified by reverse phase HPLC in the Harding laboratory. Purity and structure were verified by LC-MS. Hepatocyte growth factor (HGF) was purchased from R&D Systems (Minneapolis, MN). ^{3}H- Hinge peptide (KDYIRN, [tyrosine-2, 6-^{3}H) with a specific activity=43.4Ci/mmol and an HPLC purity >99% was custom synthesized by ViTrax (Placentia, CA).

Antibodies. Anti-Met and anti-phospho-Gab1 antibodies were purchased from Cell Signaling Technology (Beverly, MA). Anti-Gab1 was purchased from Upstate Biologicals (Lake Placid, NY) and the phospho-Met antibody was purchased from AbCam, Inc (Cambridge,MA).

Cell culture. Human embryonic kidney cells 293 (HEK293), Madin Darby canine kidney cells (MDCK), and B16F10 murine melanoma cells were grown in DMEM, 10% fetal bovine serum (FBS). Cells were grown to 90-100% confluency before use. For most but not all studies HEK and MDCK cells were serum starved for 24 hours prior to the initiation of drug treatment.

HGF Binding. The binding of ^{3}H-Hinge to HGF was assessed using a soluble binding assay. Saturation isotherms were developed for the interaction of ^{3}H-Hinge with HGF. 250µl of PBS containing human HGF (1.25ng) were incubated with multiple concentrations of ^{3}H-Hinge

ranging from 10^{-13} M to 10^{-8} for 40 minutes at 37^0C. Preliminary kinetic studies indicated that equilibrium binding was reached by 40 minutes of incubation at 37^0C. The incubates were then spun through Bio-Gel P6 spin columns (400 µl packed volume) for 1 minute to separate free and bound ^{3}H-Hinge and the eluent collected. Five milliliters of scintillation fluid was added to the eluent, which contained the HGF bound ^{3}H-Hinge, and then counted using a scintillation counter. Total disintegrations per minute of bound ^{3}H-Hinge were calculated based on machine counting efficiency. Using the soluble binding assay Norleual binding to HGF was assessed by competition in which ^{3}H-Hinge was allowed to bind to HGF in the presence of varying concentrations of Norleual between 10^{-13} M to 10^{-8}M (half-log dilutions). Saturation Isotherms and competition binding curves were performed in quadruplicate. The affinity of ^{3}H-Hinge for HGF (Kd) and total binding (Bmax) along with the Ki values for the binding of Norleual were determined using the Prism 5 and InStat v.3.05 graphical/statistical programs (GraphPad, San Diego).

Dimerization. HGF dimerization was assessed using PAGE followed by silver staining. Human HGF at a concentration of 0.08ng/µl with or without drugs was incubated with heparin at a final concentration of 5µg/ml. 25 mM BS3 cross linker (Pierce Chemical; Rockford, IL) was then added to the reaction for 30 min at 37^0C. Subsequently the reaction was quenched with 20mM Tris buffer. Qualitatively identical results were also obtained in the absence of BS3 attesting to the high affinity of the HGF/HGF dimer. Loading buffer was then added to each sample and the mixture separated by native PAGE using gradient Criterion XT precast gels (4-12% Bis-Tris; Biorad Laboratories, Hercules, CA). Similar results were obtained in the presence of SDS. Next the gel was silver stained for the detection of the HGF monomers and dimers. Bands were quantitated from digital images using a UVP phosphoimager (Upland, CA).

Western blotting. HEK293 cells were seeded in 6 well tissue culture plates and grown to 95% confluency in DMEM containing 10% FBS. The cells were serum deprived for 24 hours prior to the treatment to reduce the basal levels of phospho-Met and phospho-Gab1. Following serum starvation, cocktails comprised of vehicle and HGF with/without Norleual or the Hinge peptide were prepared and pre-incubated for 30 minutes at room temperature. The cocktail was then added to the cells for 10 minutes to stimulate the Met receptor and downstream proteins. Cells were harvested using RIPA lysis buffer (Upstate) fortified with phosphatase inhibitor cocktails 1 and 2 (Sigma-Aldrich; St. Louis, MO). The lysate was clarified by centrifugation at 15,000 g for 15 minutes, protein concentrations were determined using the BCA total protein assay, and then appropriate volumes of the lysates were diluted with 2x reducing Laemmli buffer and heated for ten minutes at 95° C. Samples containing identical amounts of protein were resolved using SDS-PAGE (Criterion, BioRad Laboratories), transferred to nitrocellulose, and blocked in Tris-buffered saline (TBS) containing 5% milk for one hour at room temperature. The phospho-Met antibody, Met antibody, phospho-Gab1 antibody, or Gab-1 antibody were added to the blocking buffer at a final concentration of 1:1000 and incubated at 4° C overnight with gentle agitation. The membranes were then washed several times with water and TBS (PBS, 0.05% Tween-20), a 1:5000 dilution of horseradish-peroxidase conjugated goat anti-rabbit antiserum was added, and the membranes further incubated for one hour at room temperature. Proteins were visualized using the Supersignal West Pico Chemiluminescent Substrate system (Pierce, Fenton, MO) and molecular weights determined by comparison to protein ladders (BenchMark, Invitrogen; and Kaleidoscope, BioRad). Images were digitized and analyzed using a UVP phosphoimager.

Cell proliferation. 5000 MDCK cells were seeded into the wells of a 96 well plates in

10% FBS DMEM to induce cellular quiescence. Serum levels were reduced to 2% for twenty-four hours prior to initiating the treatments. Following serum reduction, 10 ng/ml HGF alone and with various concentrations of Norleual, Hinge peptide, or PBS vehicle were added to the media. The cells were allowed to grow under these conditions for four days with a daily addition of Norleual or Hinge peptide. On the fourth day, 1 mg/ml of 1-(4, 5-Dimethylthiazol-2-yl) 3, 5-diphenylformazan reagent (MTT, Sigma-Aldrich) prepared in PBS was added to the cells and incubated for four hours. Dimethyl sulfoxide diluted in a .01M glycine buffer was added to solubilize the cell membranes and the absorbance of reduced MTT in the buffer was quantitated at 590 nm using a plate reader (Biotek Synergy 2, Winooski, VT). HGF-dependent proliferation was determined by subtracting the basal proliferation (in the absence of HGF) from total proliferation rates in groups containing HGF.

Scattering assay. MDCK cells were grown to 100% confluency on the coverslips in six-well plates and washed twice with PBS. The confluent coverslips were then aseptically transferred to new six well plates containing 900 µl serum free DMEM. Norleual, Hinge peptide, and/or HGF (20 ng/ml) were added to appropriate wells. Control wells received PBS vehicle. Plates were incubated at 37°C with 5% CO_2 for 48 hours. Media was removed and cells were fixed with methanol. Cells were stained with Diff-Quik Wright-Giemsa (Dade-Behring, Newark, DE) and digital images were taken. Coverslips were removed with forceps and more digital images were captured. Pixel quantification of images was achieved using Image J and statistics were performed using Prism 5 and InStat v.3.05.

Cell Viability/ Cell Death-Annexin V/Propidium Iodide Dual Staining. MDCK cells and B16F10 cells are serum starved for 24 hours. Four different treatment groups were included in each of two studies: (1) HGF alone, HGF+ 10^{-10}M Hinge, 10^{-10}M Hinge alone, and 10^{-12}M

Hinge alone, plus a control group receiving the PBS vehicle; and (2) HGF alone, HGF+ 10^{-10}M Norleual, 10^{-10}M Norleual alone, and 10^{-12}M Norleual alone, plus a control group receiving the PBS vehicle. After four days of treatment, cells are washed twice in cold PBS, and then resuspended in cold binding buffer to a concentration of $1x10^5$ to $1x10^6$ cells/ml. Ten µl of annexin V-FITC from a ApoScreen™ Annexin V Apoptosis Kit purchased from Southern Biotech (Birmingham, AL), was added to 100 µl of the prepared cell suspension. Annexin V-FITC cell mixtures were incubated for 15 minutes on ice in the dark. After incubation, an additional 380 µL of cold binding buffer was added to each tube along with 10µL of 50µg/ml Propidium Iodide (ApoScreen™ Annexin V Apoptosis Kit). Percentages of cells undergoing apoptosis and necrosis were determined by flow cytometry (FACSort Calibur 2). FlowJo (Tree Star, Ashland, OR), a flow cytometry analysis program.

Lung colony formation. Six to eight month old C57BL/6 mice were injected with 200,000 B16-F10 cells in 200 µl PBS by tail vein injection followed by daily ip. injections of either Hinge peptide or a PBS vehicle control. Two weeks later, mice were anesthetized and the lungs were perfused with PBS and removed. Photos were taken and the lungs solubilized in 1% Triton x-100, 20 mM Tris, 0.15 M NaCl, 2 mM EDTA, and 0.02% sodium azide. Samples were disrupted by sonicaton (Mixonix, Farmingdale, NY) and spun at 15,000g for 30 minutes. The supernatant was transferred to a 96 well plates and melanin absorbance at 410nm was measured using a Biotek Synergy 2 plate reader.

Statistics. Independent one-way analysis of variance (ANOVA) (InStat v.3.05) was used to determine differences among groups. Tukey-Kramar or Bonferroni's multiple comparison post-hoc tests were performed where necessary. Statistical comparisons of two groups were determined using the two-tailed Student's *t*-test (InStat v.3.05 and Prism 5).

2.4 Results

The Hinge peptide sequence binds HGF and Norleual competes with Hinge for HGF binding: Norleual [Nle-Tyr-Leu-Ψ-$(CH_2$-$NH_2)^{3-4}$-His-Pro-Phe] has been shown by our laboratory to act as an HGF/Met antagonist capable of blocking the binding of HGF to Met, inhibiting HGF-dependent activation of Met, and attenuating HGF-dependent cellular activities (Yamamoto et al., 2010). The exact mechanism responsible for this profound activity, however, has remained undetermined. We have proposed two possible mechanisms: (1) direct blockade of HGF binding to Met, and (2) sequestration of HGF in an inactive form. The second hypothesis posits that Norleual binding to HGF prevents it from dimerizing and thus acquiring the active conformation ultimately needed for Met activation. To begin to evaluate this idea, we first used a ^{3}H-Hinge peptide as a probe in a soluble binding assay to determine whether it was capable of binding HGF with high affinity**. Figure 2.1A** shows a representative saturation isotherm of ^{3}H-Hinge binding to HGF; pooled data indicate that Hinge does indeed bind to HGF with high affinity (K_d=13.92x10^{-12} M +/- 1.73x10^{-12}M; mean +/- SEM; N=9)). Using ^{3}H-Hinge as a probe to assess direct HGF binding, a competition study was initiated with Norleual. This study demonstrated that Norleual, acting as a Hinge-mimic, competes with Hinge for HGF binding and has a high affinity for HGF, with a K_i = 3.604x10^{-12} M (**Figure 2.1B**).

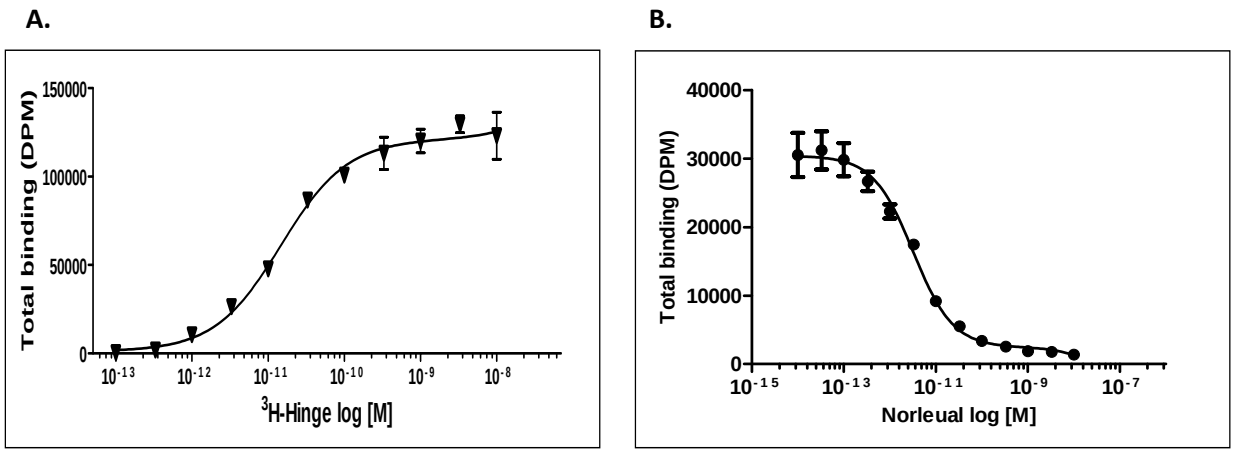

Figure 2.1: Hinge peptide and the Norleual bind directly to HGF. (**A**) Representative dose response curve for Hinge binding to HGF demonstrating the saturability of the binding. 3H-Hinge was incubated with 1.25ng of HGF for 40 minutes at 37oC in 0.25 ml of buffer. After the addition of different concentrations of 3H-Hinge (10^{-13}-10^{-8}M), HGF-bound 3H-Hinge was eluted from Bio-Gel P6 spin columns. Radioactivity of the eluted solution was quantitated by scintillation counting. Pooled data indicate that 3H-Hinge bound to HGF with high affinity (Kd=13.92x10^{-12} M +/- 1.73x10^{-12}M; mean +/- SEM; N=9). (**B**) A representative competition curve of Norleual for 3H-Hinge binding to HGF. Norleual and 3H-Hinge (13.3x10^{-12}M) were incubated with 1.25ng of HGF for 40 minutes at 37oC in 0.25 ml of buffer. HGF-bound Hinge was eluted from Bio-Gel P6 columns after the addition of different concentrations of Norleual (10^{-14} -10^{-8}M). The radioactivity of the eluted solution was quantitated using scintillation counting. These data demonstrate that Norleual competes with Hinge for binding to HGF with a (Ki= 3.604x10^{-12} M +/- 1.942x10^{-12} M); mean +/- SEM: N=16.

Norleual and the Hinge peptide block HGF-dimerization: Several reports have shown that HGF needs to form homodimers and/or other multimeric forms, as a prerequisite for its activation of Met (Gherardi et al., 2006; Youles et al., 2008). The Hinge region, a central feature of HGF, participates in the formation of the active HGF dimer; which possesses the correct conformation to enable activation of its receptor, Met (Gherardi et al., 2006; Youles et al., 2008).

A screen for possible transcripts having conserved sequences similar to AngIV identified partial homology with the Hinge region of the plasminogen family of proteins, which include plasminogen itself, its anti-angiogenic degradation product, angiostatin, and the protein hormones heptocyte growth factor and macrophage stimulating protein (Yamamoto et al., 2010). This homology, coupled with the above data indicating that both Norleual and the Hinge peptide bind directly to HGF with high affinity, supported our hypothesis that Norleual and now the Hinge peptide should be able to interfere with dimer formation. To test this supposition directly, we utilized PAGE and silver staining methods to determine whether Norleual and Hinge could disrupt dimerization. The data in **Figure 2.2** demonstrate that Norleual and the Hinge peptide almost completely block HGF dimer formation at concentrations of 10^{-10} M. Partial disruption of HGF dimer formation by both compounds was evident at concentrations as low as 10^{-12} M (data not shown).

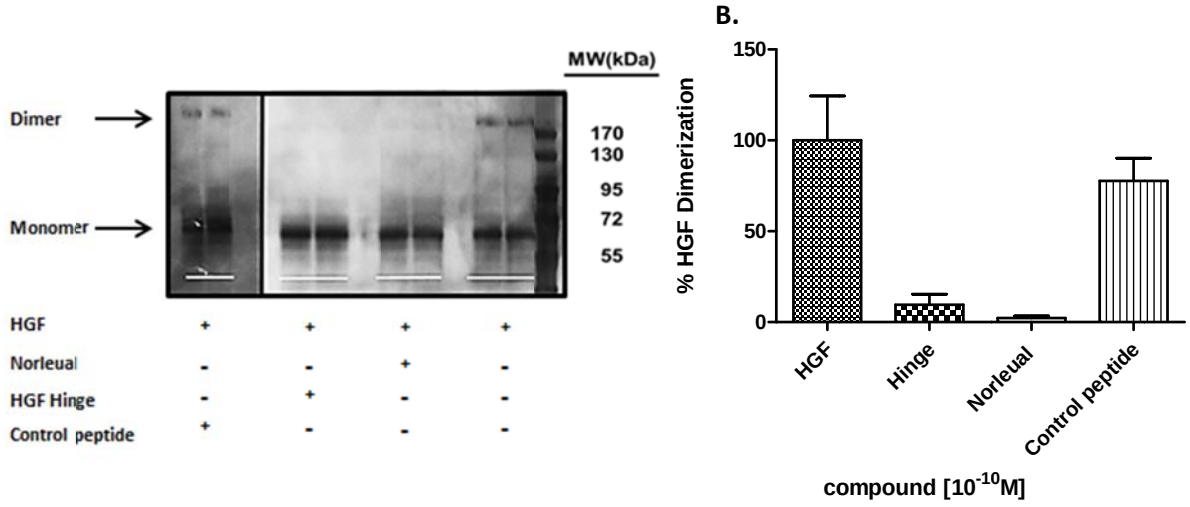

Figure 2.2: Norleual and the Hinge peptide inhibit HGF dimerization. HGF spontaneously dimerizes when incubated in PBS in the presence of heparin. HGF was incubated alone or with Hinge peptide, Norleual, or a control (negative control) peptide at 10^{-10}M. After 30 minute incubation, samples were

cross-linked with BS3, separated by gel electrophoresis, and silver stained. Band density was quantified and used to determine the level of HGF dimerization in each group. Both treatment groups (Norleual and Hinge) were statistically different than the HGF treated group ($p<0.01$), but not different from one another, the control peptide group, and the non-treated control group ($p >0.05$). Mean +/-SEM, N=8. (**A**) Representative gel. (**B**) Pooled and quantified data.

Hinge inhibits HGF dependent Met activation: To further test the notion that the AngIV analog, Norleual, can act as Hinge-mimic, its ability to block HGF-dependent Met activation was compared to that of the Hinge peptide. As can be seen in (**Figure 2.3A&B),** both Norleual and the Hinge similarly blocked HGF-dependent Met phosphorylation at 10^{-10} M. Gab1 is the cornerstone scaffolding adaptor that is responsible for mediating the HGF-dependent activation of multiple Met-dependent signaling pathways (Weidner et al., 1996; Sakkab et al., 2000), including: ERK, PI3K-Akt/PKB, Crk-Rap, and Rac-PAK, which are integral to Met's effects on cell survival and proliferation, cell motility, and cell morphology. During its activation Gab1 is phosphorylated in a Met-dependent manner. Thus, if Norleual is truly mimicking the Hinge region of HGF one would expect that like Norleual the Hinge peptide should attenuate HGF/Met-dependent phosphorylation and activation of Gab1. As anticipated, **Figure 2.3C&D** show that Norleual and the Hinge peptide both suppress HGF-dependent Gab1 phosphorylation equivalently at 10^{-10} M. Together; these data suggest an identical or convergent mechanism for the effects of Norleual and the Hinge on the Met receptor signaling pathway.

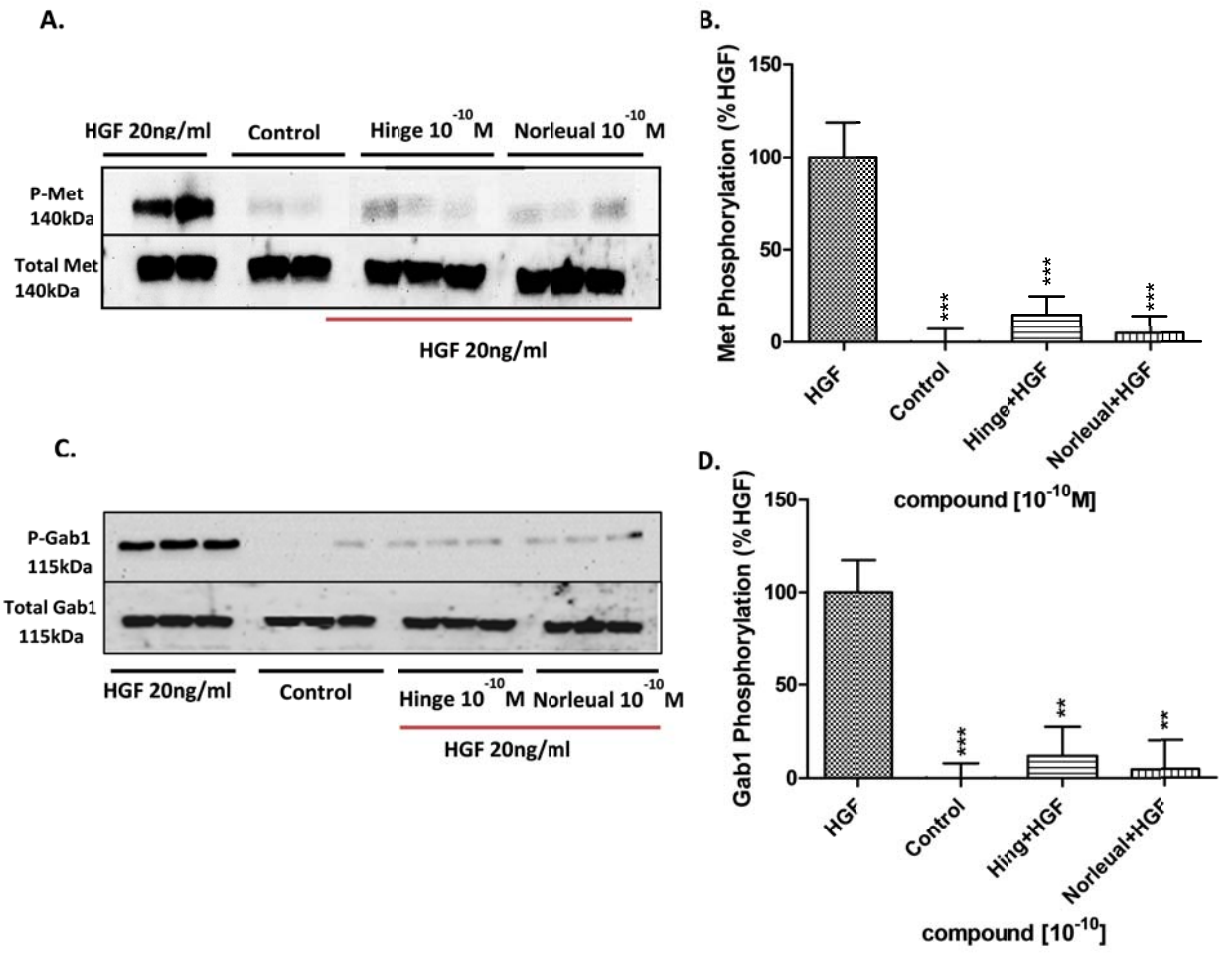

Figure 2.3: Norleual and the Hinge peptide inhibit HGF-dependent Met and Gab1 phosphorylation. (**A**) HEK293 cells were treated for 10 minutes with HGF+/- Nle (Norleual) or Hinge at the 10^{-10}M. HEK293 cell lysates were immunoblotted with anti-phospho-Met and anti-Met antibodies. (**B**) Both treatment groups (Nle and Hinge) were statistically different than the HGF treated group ($p<0.001$), but not different from one another or non-treated controls ($p>0.05$). Mean +/-SEM, N=6. (**C**) HEK293 cells were treated for 10 minutes with HGF+/- Nle (Norleual) or Hinge at 10^{-10}M. HEK293 cell lysates were immunoblotted with anti-phospho-Gab1 and anti-Gab1 antibodies. (**D**) Both treatment groups (Nle and Hinge) were statistically different than the HGF treated group ($P<0.001$), but not different from one another or non-treated controls ($p>0.05$). Mean +/-SEM, N=6.

Hinge inhibits HGF dependent scattering and proliferation in MDCK cells: The capacity of both Norleual and the Hinge peptide to block HGF-dependent Met signaling predicts that both molecules should be able to inhibit HGF-dependent cellular processes including proliferation, migration, invasion, and relief from anoikis (blockade of apoptosis). In this regard we have chosen to first compare the effects of Norleual and the Hinge peptide on HGF-dependent cell scattering, which is a hallmark cellular response to Met activation by HGF (Zhang and Vande Woude, 2003) that relies on the loss of cellular adhesion and increased motogenic activity. HGF-dependent scattering was assessed in Madin-Darby Canine Kidney (MDCK) cells, a standard cellular model for investigating the HGF/Met system (Stella and Comoglio, 1999) and well recognized for its robust scattering response to HGF. MDCK cells grown at a low cell density form colonies and demonstrate a "cobblestone" morphology, which is characterized by tight intercellular junctions. Application of HGF initiates a scattering response that occurs in two stages (Kopp, 1998; Comoglio and Boccaccio, 2001). First, the cells lose their cell-to-cell adhesion and become polarized. Second, they separate completely and migrate away from each other. If the Hinge peptide is indeed capable of disrupting HGF/Met initiated cellular activities in the manner observed with Norleual (Yamamoto et al., 2010), then it would be expected to attenuate scattering in MDCK cells stimulated with HGF. This expectation is verified in **Figure 2.4 A&B**, which illustrates the comparable ability of Norleual and the Hinge peptide to attenuate MDCK cell scattering. A maximum effect for the Hinge peptide was apparent at 10^{-10} M, with a threshold near 10^{-12} M (**Figure 2.4C**). As a second approach to evaluating the anti-HGF/Met effects of the Hinge peptide, its impact on MDCK proliferation was monitored. The data presented in **Figure 2.5** shows the dose-dependent inhibition of HGF-dependent MDCK proliferation by the Hinge peptide. The decrease in HGF-dependent MDCK

proliferation below control levels is not surprising since the experiment was carried in 2% serum, which likely contains some level of HGF. The suppression of cell numbers below control levels further suggests that Hinge in not only slowing MDCK cell proliferation but also inducing cell death. To test this notion directly we utilized Fluorescence-activated cell sorting (FACS) methods to assess the capacity of Hinge to induce both apoptotic and non-apoptotic cell death in MDCK cells. This study (**Figure 2.S1**) demonstrated that both 10^{-10}M and 10^{-12}M Hinge dramatically stimulated apoptotic cell death and decreased overall cell viability.

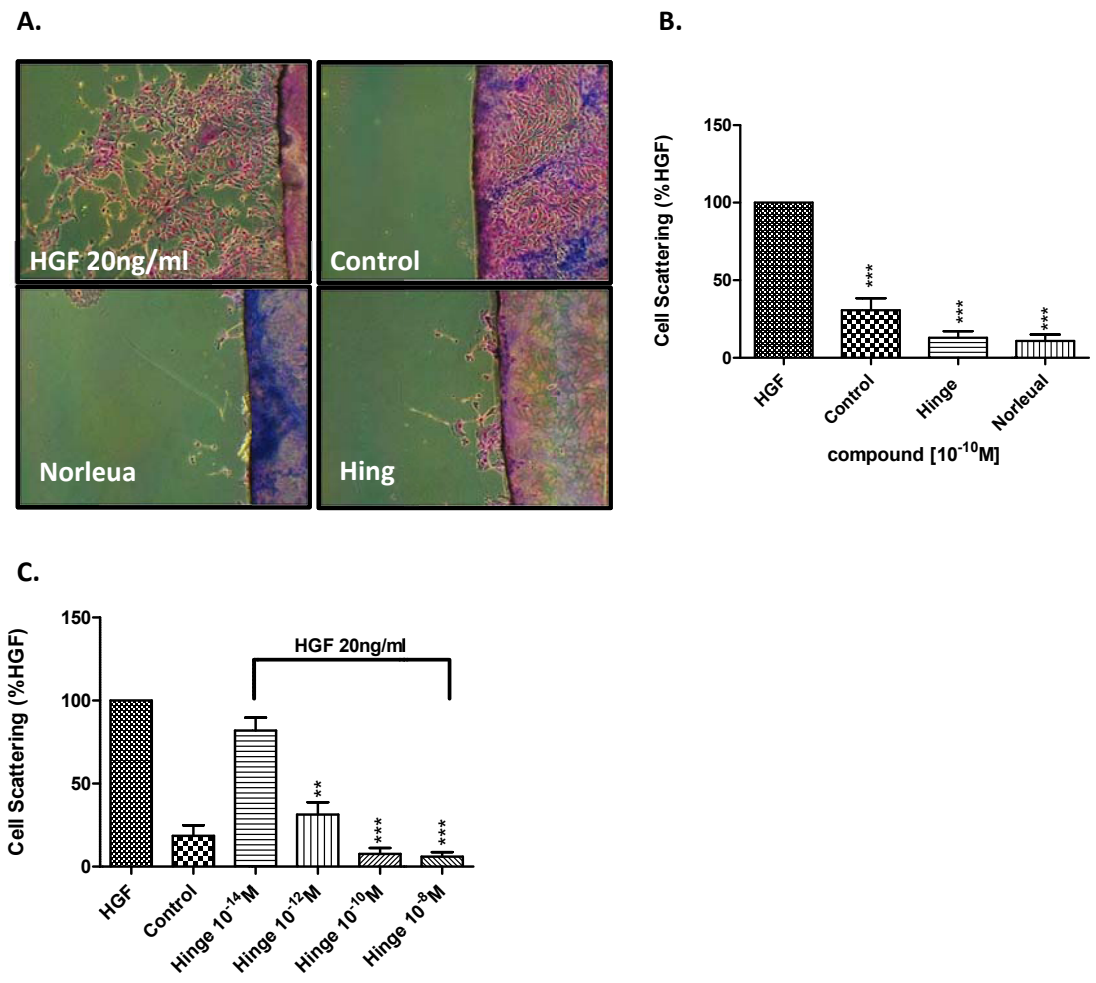

Figure 2.4: Norleual and the Hinge peptide inhibit HGF-dependent scattering in MDCK cells. Cell scattering, in which cells lose cell-to-cell contacts and then migrate rapidly is the classic response to HGF. MDCK cells, the usual cellular model for studying the HGF/Met system, were grown to 100% confluence on coverslips and then placed in a fresh culture dishes. The cells were stimulated to scatter off of the coverslip by adding 20 ng/ml of HGF to the media alone or in combination with Norleual or Hinge at 10^{-10}M. After 48 hours of scattering, the cells were fixed with methanol and stained with Diff-Quik. The coverslips were removed to reveal the ring of cells that had scattered off of the cover slip and onto the plate. (**A**) Picture of MDCK cells scattering of the coverslips. (**B**) The effect of HGF on scattering was quantitated by determining by densitometry of the digital images of scattered cells. ANOVA analysis indicates that both treatment groups (Norleual and Hinge) were statistically different than the HGF treated

group ($p<0.01$), but not different from one another or non-treated controls ($p>0.05$). (**C**) Shows the dose-response effect of Hinge on HGF-induced scattering. The data from the groups with HGF plus Hinge peptide at 10^{-8}M, 10^{-10}M, and 10^{-12}M were different from the HGF alone group ($p<0.001$) but not different from the untreated control group ($p>0.05$). The HGF plus 10^{-14}M Hinge peptide group was not different from the HGF alone group ($p>0.05$). Mean +/-SEM, N=8.

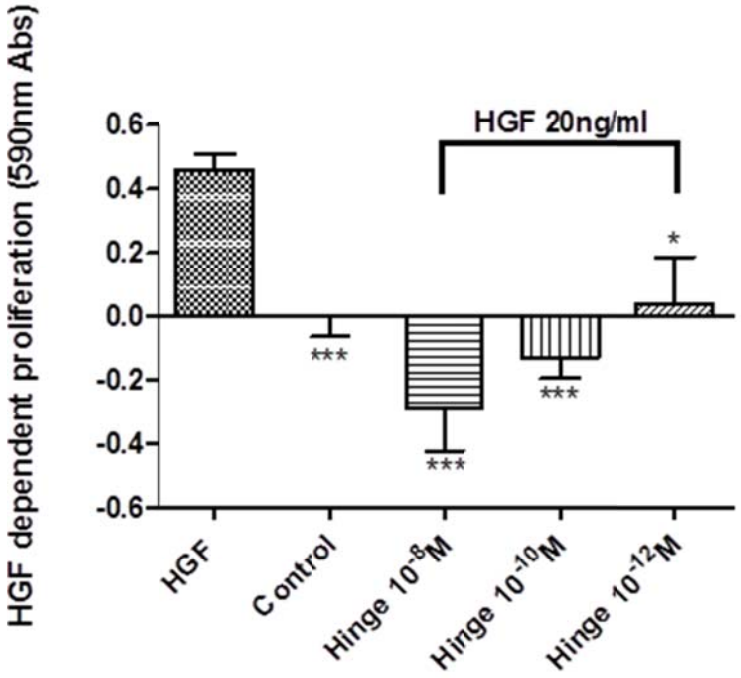

Figure 2.5: Hinge peptide inhibits HGF-dependent proliferation. MDCK cells maintained in 2% serum were treated with a PBS vehicle (negative controls), HGF, or HGF in combination with Hinge peptide at different concentrations. The cells were allowed to grow for four days. Cell numbers were estimated on the fourth day with an MTT assay by measuring absorbance at 590nm. Control values from cells that were not treated with HGF were subtracted from all values to determine the HGF-induced increase in cell proliferation. The 10^{-8}M, 10^{-10}M, and 10^{-12}M Hinge peptide groups were all significantly

reduced compared to the HGF group(***$p<0.001$) but not different from untreated controls ($p>0.05$). The 10^{-14}M Hinge peptide group was not different from the untreated control group ($p>0.05$). Mean +/-SEM, N=6.

Both Hinge and Norleual block the ability of HGF to protect from apoptosis: HGF has been reported to act as an anti-apoptotic, pro-survival agent for many cell types (Zeng et al., 2002; Derksen et al., 2003; Kakazu et al., 2004). In addition exaggerated anti-apoptotic activity, resulting from an over-active HGF/Met system, is thought to be a significant contributor to many malignancies. Thus, one would anticipate that the Hinge peptide should exhibit a pro-apoptotic effect on cell types whose survival is dependent on or positively impacted by HGF. FACS methods were used to assess the consequences of Hinge peptide application on the viability of B16F10 murine melanoma cells, which are known to have an over-active HGF/Met system (Halaban et al., 1992; Takayama et al., 1997; Ferraro et al., 2006). Dual fluorescent tags were employed to identify dead cells (propidium iodide; PI) and apoptotic cells (fluorescent anti-Annexin IV antibodies), and to distinguish between necrotic and apoptotic mechanisms of cell death. The top left panel in **Figure 2.6**, which shows data from B16F10 cells grown in culture for four days, indicates that 34% were dead or dying from a combination of apoptotic and non-apoptotic cell death mechanisms. After treatment with 20ng/ml of HGF, the number of B16F10 cells that were dead and dying dropped below 10% of the total. This dramatic anti-apoptotic effect of HGF was not only completely blocked by the addition of 10^{-10} M Hinge peptide but the percentage of dying cells and particularly those dying by apoptotic mechanisms increased markedly. Somewhat surprisingly, application of Hinge peptide alone at both 10^{-10} M and 10^{-12} M concentrations markedly increased B16F10 apoptosis and decreased overall cell viability

beyond the levels seen with the non-treated control group. These results suggest the presence of endogenous HGF derived from past exposure to serum or produced by the B16F10 cells themselves. FACS studies, in which a shorter 24-hour exposure to the Hinge peptide was employed, failed to induce B16F10 cell death, suggesting that the effects of Met blockade on B16F10 viability require more chronic, long-term inhibition (**Figure 2.S2**). Similar to Hinge, Norleual also abrogated the anti-apoptotic effect of HGF on B16F10 cells. (**Figure 2.S3**). This pro-apoptotic effect of Norleual was apparent both in the presence and absence of exogenous HGF.

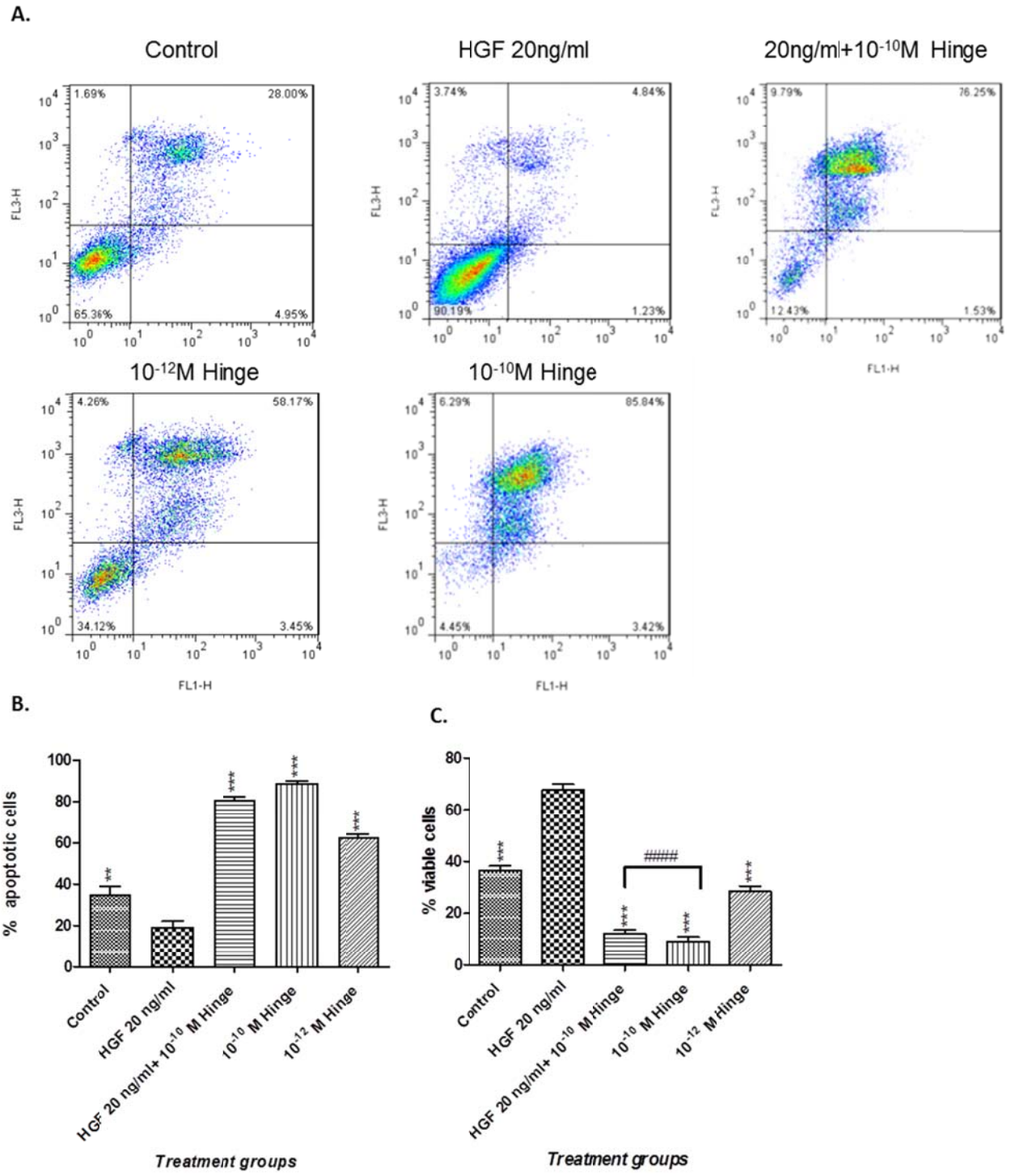

Figure 2.6: Hinge peptide inhibits HGF dependent cell survival and induces cell death. Five different groups of treated B16F10 murine melanoma cells received PBS (Control), HGF (20ng/ml) +/- 10^{-10}M

Hinge, or Hinge alone (at two different concentrations 10^{-10}M and 10^{-12}M), daily for four days. The percentage of cells undergoing necrosis and apoptosis was determined by flow cytometry (FACS). Panels in (**A**) show the staining profile for the different treatment groups. Cells that are undergoing apoptosis are dual stained with Annexin V and PI (right upper corner) while viable cells are at the lower left corner. Cells in the upper left corner are dead, most likely by necrotic mechanisms. Cells in the lower right corner are damaged and show initial signs of apoptosis. Panel (**B**) and (**C**) are the quantification of cells undergoing apoptosis and the number of viable cells respectively. The level of apoptosis of the HGF plus 10^{-10}M Hinge peptide, 10^{-10}M Hinge peptide, and 10^{-12}M Hinge peptide groups were all different from both the control and HGF alone groups (***$p<0.001$) but not different from one another ($p>0.05$). The number of viable cells is insignificantly lower in the HGF plus 10^{-10}M Hinge peptide, 10^{-10}M Hinge peptide, and 10^{-12}M Hinge peptide groups when compared to the HGF alone group (###$p<0.001$) while HGF plus 10^{-10}M Hinge peptide, 10^{-10}M Hinge peptide groups were lower than the non-treated control group ($P<0.001$). Mean +/-SEM; N=6.

Hinge inhibits B16-F10 melanoma lung colonization: A final test of the hypothesis that both Norleual and the Hinge peptide are acting as dominant negative Hinge mimics would be a demonstration that the Hinge peptide possessed in vivo anti-cancer activity similar to that reported previously for Norleual (Yamamoto et al., 2010). As such, the Hinge peptide was evaluated for its ability to suppress B16F10 murine melanoma lung colonization following tail vein injection of the cancer cells. The B16F10 model was chosen because these cells are known to rapidly and aggressively colonize the lung, thus emulating the formation of secondary metastatic tumors. Furthermore, Met signaling has been shown to be a critical participant in B16F10 migration, invasion, and metastasis (Sakkab et al., 2000). The data in **Figure 2.7** illustrate the capacity of the Hinge peptide to decrease B16-F10 lung colonization following

daily IP treatment at doses of 10μg/kg/day and 100μg/kg/day; a result reminiscent of Norleual at identical doses (Yamamoto et al., 2010).

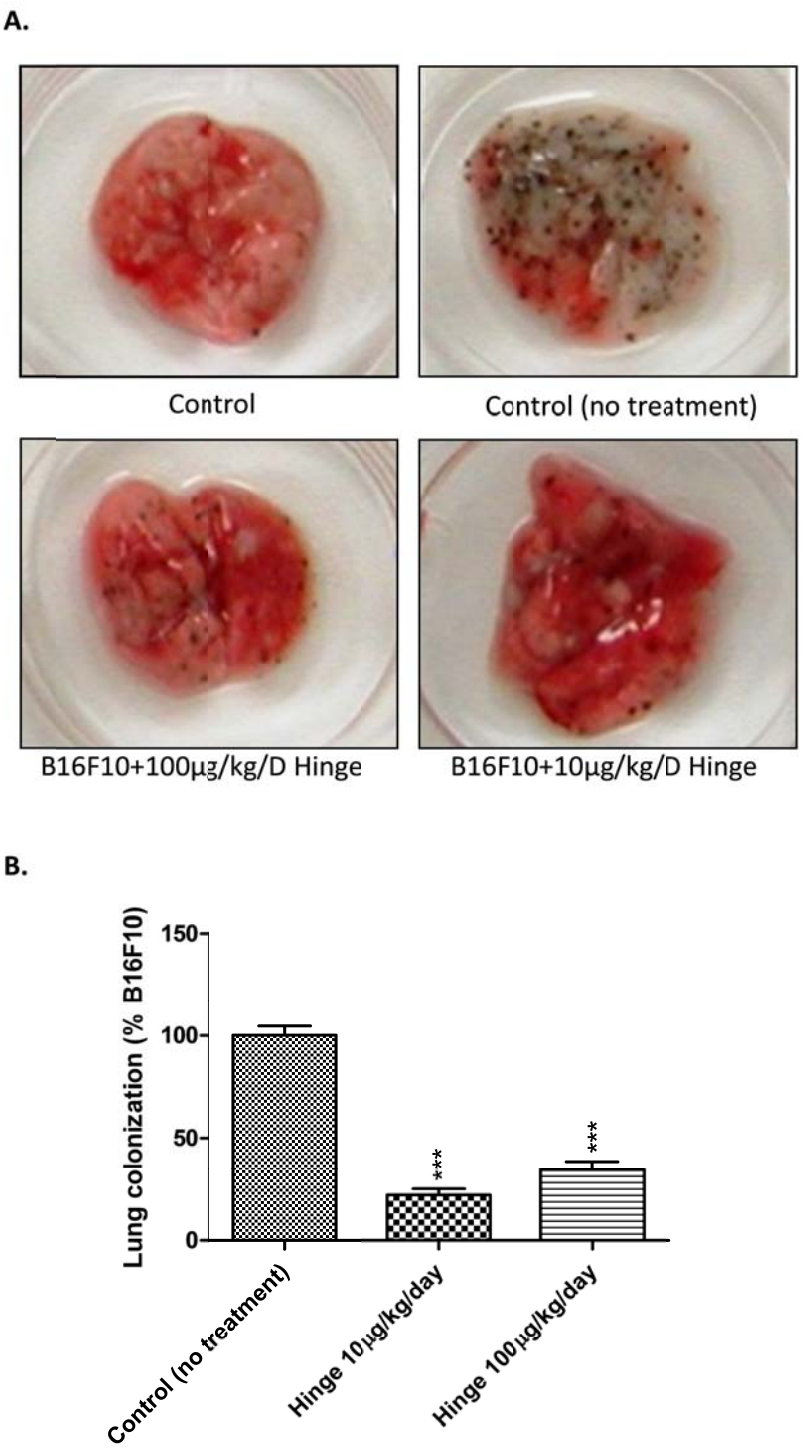

Figure 2.7: Hinge peptide inhibits B16-F10 melanoma lung colonization. 200,000 B16-F10 murine melanoma cells were treated in suspension with Hinge at 10^{-11} M or PBS vehicle for 30 minutes. The cells

were then injected into the tail vein of C57BL/6 mice after which mice received daily IP injections of Hinge (10μg/kg/day or 100μg/kg/day) or PBS vehicle. After fourteen days, the lungs from Hinge treated mice exhibited an obvious reduction in melanoma colonies when compared to untreated controls. After removal, lungs were homogenized and total melanin content was determined spectrophotometrically by measuring absorbance at 410nm. This was used to quantify total pulmonary melanoma colonization in vehicle treated and Hinge treated groups. Ungrafted age-matched control lungs exhibited a background absorbance at 410nm. N=5, Mean ± SEM; $*p<0.05$.

2.5 Discussion

Recent work in our laboratory (Yamamoto et al., 2010) has shown that Norleual, an angiotensin IV) analog, possesses potent anti-HGF/Met activity and displays marked anti-cancer activity. As part of the discussion of these results, two possible mechanisms were offered to explain this inhibition: 1) Norleual bound directly to Met acting as a classic competitive antagonist of HGF; and, 2) Norleual acted as a dimerization-domain (Hinge region) mimic and dominant negative resulting in the inhibition of HGF dimerization-dependent activation. Here we introduce a novel strategy for inhibiting the HGF/Met system, which exploits a semi-unique property of this system; namely the need for HGF to dimerize or multimerize prior to interacting with Met.

Since Norleual was proposed to act as a Hinge (dimerization domain) mimic, we asked whether a peptide representing the Hinge sequence would exhibit characteristics akin to Norleual. Investigations to probe this question demonstrated that the Hinge peptide, like Norleual, could block HGF-dependent Met and Gab1 phosphorylation, HGF-dependent cell scattering and proliferation, and HGF-dependent protection from cell death. The dramatic ability

of the Hinge peptide to both suppress the pro-survival effects of HGF on B16F10 cells, an HGF/Met-dependent murine melanoma, and induce apoptosis in these cells in the absence of exogenous HGF, encouraged us to examine the *in vivo* anti-cancer potential of the Hinge peptide. To probe the potential in vivo anti-cancer response for the Hinge peptide, we evaluated its capability to attenuate lung colonization by B16F10 cells. The results demonstrated that similar to Norleual the Hinge peptide could inhibit colonization when delivered intraperitoneally at a concentration as low as10 μg/kg/day. Since the structure of the Hinge peptide presents N- and C-termini that could be readily acted upon by exopeptidases, it was unclear whether robust anti-cancer activity would be evident with ip. delivery. The observed inhibition, however, argues that the extraordinary high affinity of the Hinge peptide for its HGF target counteracted any anticipated metabolic instability allowing sufficient compound to reach and inhibit the action of endogenous HGF. In order to neutralize any HGF that might be present in the cell preparation B16F10 cells were briefly pre-incubated with the Hinge peptide prior to their tail vein injection. This procedure, however, posed the question as to whether the observed inhibition with Hinge was primarily a manifestation of cell death induced by brief pre-exposure. This, nevertheless, seems an unlikely possibility given that a 24 hour exposure to Hinge failed to induce cell death as determined in the FACS studies.

While it appears clear that the Hinge peptide (KDYIRN) is capable of blocking the activation of Met by HGF these studies do not rule out the possibility that Hinge may interact with other targets, thus contributing to its in vitro and vivo effects. Although off target interactions may be a real possibility, studies in which single amino acid changes were incorporated into the Hinge peptide seem to decrease the likelihood of widespread cross-talk with other systems (Kawas and Harding, unpublished). These studies indicate that every amino

acid in the Hinge structure is essential for biological activity. Even though extensive non-HGF-related targets may be unlikely selected interactions to related molecules may still be occurring. One obvious potential interactor is macrophage stimulating protein (MSP), which resides in the same gene family as HGF and initiates some of the same biological actions (Accornero et al., 2010). Although no data yet exists confirming a dimerization process for MSP that is akin to HGF's, it is very intriguing that MSP possesses a homologous sequence (KDYVRT) that like HGF resides between its N-terminal and first kringle domains. Thus we are currently exploring both the necessity of a dimerization step in MSP's activation of its receptor, RON, and the potential of Hinge and other dimerization domain mimics to interact and modify the activity of this critical signaling system.

The specificity advantage of target-based therapy has drastically changed the way cancer is treated. Among the many possible therapeutic targets, Met and its ligand HGF have recently gained extensive attention. Numerous studies have shown that the HGF/Met pathway is one of the most often dysregulated pathways in human malignancies, which include, but are not limited to bladder, breast, cervical, colorectal, endometrial, esophageal, gastric, head and neck, kidney, liver, lung, nasopharyngeal, ovarian, pancreatic, prostate, and thyroid cancers (Liu et al., 2008). It is worth noting that activation of Met in some cancers, like osteosarcomas and globlastoma mutliforme, occurs most often through ligand-autocrine or paracrine activation (Caanadas et al., 2010), thus providing a strong rationale for the development of anti-HGF therapeutics.

Multiple therapeutic approaches have been investigated to inhibit HGF/Met system with each method targeting one of the steps that leads to Met-dependent cellular responses. The earliest step to be targeted in the Met activation process is the interaction between Met and HGF. HGF antagonists, like HGF directed antibodies (Burgess et al., 2006; Stabile et al., 2008) or

soluble fragments of Met extracellular domains, which act as 'decoy' molecules (Michieli et al., 2004), can interfere with this interaction act by sequestering HGF. Met neutralizing antibodies can also obstruct this step in the signaling cascade (Martens et al., 2006) by either directly blocking HGF access to Met or causing down regulation of Met by inducing receptor internalization. Similarly protein-based antagonists including fragments of HGF like NK4 can function as competitive antagonists of HGF binding to Met (Kuba et al., 2000; Matsumoto and Nakamura, 2008). A concentrated effort has recently been put forward to develop molecules that can block the receptor's catalytic activity. These 'kinase inhibitors" are small hydrophobic molecules that work intracellularly to compete for the binding of ATP site to the kinase domain of Met thus inhibiting receptor autophosphorylation (Morotti et al., 2002; Christensen et al., 2003; Sattler et al., 2003). Despite the promise of the biologic and kinase-inhibitor approaches, which are currently represented in clinical trials, both have limitations arising from toxicity or specificity considerations (Hansel et al., 2010; Maya, 2010).

The major implication of this study is that molecules, which target the dimerization domain of HGF, could represent novel and viable anti-cancer therapeutics. Furthermore, these data support the development of such molecules using Norleual and/or the Hinge peptide as synthetic templates. Given the metabolic instability ($t_{1/2}$ in blood< 5 minutes, Harding and McCoy unpublished) and pharmacokinetic limitations of these template molecules we expect that superior molecules can be designed with even higher in vivo potencies.

2.6 References

Accornero P, Pavone LM and Baratta M (2010) The scatter factor signaling pathways as therapeutic associated target in cancer treatment. *Curr Med Chem* **17**:2699-2712.

Birchmeier C, Birchmeier W, Gherardi E and Vande Woude GF (2003) Met, metastasis, motility and more. *Nature reviews. Molecular cell biology* **4**:915-925.

Burgess T, Coxon A, Meyer S, Sun J, Rex K, Tsuruda T, Chen Q, Ho SY, Li L, Kaufman S, McDorman K, Cattley RC, Elliott G, Zhang K, Feng X, Jia XC, Green L, Radinsky R and Kendall R (2006) Fully human monoclonal antibodies to hepatocyte growth factor with therapeutic potential against hepatocyte growth factor/Met-dependent human tumors. *Cancer research* **66**:1721-1729.

Caanadas I, Rojo F, Arumai-Uraia M, Rovira A, Albanell J and Arriola E (2010) MET as a new therapeutic target for the development of novel anticancer drugs. *Clinical and Translational Oncology* **12**:253-260.

Christensen JG, Schreck R, Burrows J, Kuruganti P, Chan E, Le P, Chen J, Wang X, Ruslim L, Blake R, Lipson KE, Ramphal J, Do S, Cui JJ, Cherrington JM and Mendel DB (2003) A selective small molecule inhibitor of Met kinase inhibits Met-dependent phenotypes in vitro and exhibits cytoreductive antitumor activity in vivo. *Cancer research* **63**:7345-7355.

Comoglio PM and Boccaccio C (2001) Scatter factors and invasive growth. *Seminars in cancer biology* **11**:153-165.

Cramer T, Schuppan D, Bauer M, Pfander D, Neuhaus P and Herbst H (2004) Hepatocyte growth factor and Met expression in rat and human liver fibrosis. *Liver International* **24**.

Danilkovitch-Miagkova A and Zbar B (2002) Dysregulation of Met receptor tyrosine kinase activity in invasive tumors. *The Journal of clinical investigation* **109**:863-867.

Derksen PW, de Gorter DJ, Meijer HP, Bende RJ, van Dijk M, Lokhorst HM, Bloem AC, Spaargaren M and Pals ST (2003) The hepatocyte growth factor/Met pathway controls proliferation and apoptosis in multiple myeloma. *Leukemia : official journal of the Leukemia Society of America, Leukemia Research Fund, U.K* **17**:764-774.

Ferraro D, Corso S, Fasano E, Panieri E, Santangelo R, Borrello S, Giordano S, Pani G and Galeotti T (2006) Pro-metastatic signaling by Met through RAC-1 and reactive oxygen species (ROS). *ONCOGENE -BASINGSTOKE-* **25**:3689-3698.

Gentile A, Trusolino L and Comoglio P (2008) The Met tyrosine kinase receptor in development and cancer. *Cancer and Metastasis Reviews* **27**:85-94.

Gherardi E, Sandin S, Petoukhov MV, Finch J, Youles ME, Ofverstedt LG, Miguel RN, Biundell TL, Vande Woude GF, Skoglund U and Svergun DI (2006) Structural basis of hepatocyte growth factor/scatter factor and MET signalling, in *Proceedings of the National Academy of Sciences of the United States of America* pp 4046-4051.

Halaban R, Rubin JS, Funasaka Y, Cobb M, Boulton T, Faletto D, Rosen E, Chan A, Yoko K, White W and et al. (1992) Met and hepatocyte growth factor/scatter factor signal transduction in normal melanocytes and melanoma cells. *Oncogene* **7**:2195-2206.

Hansel TT, Kropshofer H, Singer T, Mitchell JA and George AJ (2010) The safety and side effects of monoclonal antibodies. *Nature reviews. Drug discovery* **9**:325-338.

Kakazu A, Chandrasekher G and Bazan HE (2004) HGF protects corneal epithelial cells from apoptosis by the PI-3K/Akt-1/Bad- but not the ERK1/2-mediated signaling pathway. *Investigative ophthalmology & visual science* **45**:3485-3492.

Kanda S, Kanetake H and Miyata Y (2006) HGF-induced capillary morphogenesis of endothelial cells is regulated by Src. *Biochemical & Biophysical Research Communications* **344**.

Kopp JB (1998) Hepatocyte growth factor: Mesenchymal signal for epithelial homeostasis. *Kidney International* **54**.

Kuba K, Matsumoto K, Date K, Shimura H, Tanaka M and Nakamura T (2000) HGF/NK4, a four-kringle antagonist of hepatocyte growth factor, is an angiogenesis inhibitor that suppresses tumor growth and metastasis in mice. *Cancer research* **60**:6737-6743.

Liu X, Newton RC and Scherle PA (2010) Developing Met pathway inhibitors for cancer therapy: progress and challenges. *Trends in molecular medicine* **16**:37-45.

Liu X, Yao W, Newton RC and Scherle PA (2008) Targeting the Met signaling pathway for cancer therapy. *Expert opinion on investigational drugs* **17**:997-1011.

Maina F and Klein Rd (1999) Hepatocyte growth factor, a versatile signal for developing neurons. *Nature Neuroscience* **2**.

Martens T, Schmidt N-O, Eckerich C, Fillbrandt R, Merchant M, Schwall R, Westphal M and Lamszus K (2006) A Novel One-Armed Anti-Met Antibody Inhibits Glioblastoma Growth In vivo. *Clinical cancer research : an official journal of the American Association for Cancer Research.* **12**:6144.

Matsumoto K and Nakamura T (2008) NK4 gene therapy targeting HGF-Met and angiogenesis. *Frontiers in bioscience : a journal and virtual library* **13**:1943-1951.

Maya BL (2010) Endocrine side effects of broad-acting kinase inhibitors. *Endocrine-Related Cancer* **17**.

Michieli P, Mazzone M, Basilico C, Cavassa S, Sottile A, Naldini L and Comoglio PM (2004) Targeting the tumor and its microenvironment by a dual-function decoy Met receptor. *Cancer Cell* **6**.

Morotti, Mila, Accornero, Tagliabue, Ponzetto and Correspondence (2002) K252a inhibits the oncogenic properties of Met, the HGF receptor. *Oncogene* **21**:4885-4893.

Ratajczak MZ, Marlicz W, Ratajczak J, Wasik M, Machalinski B, Carter A and Gewirtz AM (1997) Effect of hepatocyte growth factor on early human haemopoietic cell development. *British Journal of Haematology* **99**:228.

Sakkab D, Lewitzky M, Posern G, Schaeper U, Sachs M, Birchmeier W and Feller SM (2000) Signaling of hepatocyte growth factor/scatter factor (HGF) to the small GTPase Rap1 via the large docking protein Gab1 and the adapter protein CRKL. *The Journal of biological chemistry* **275**:10772-10778.

Sattler M, Pride YB, Ma P, Gramlich JL, Chu SC, Quinnan LA, Shirazian S, Liang C, Podar K, Christensen JG and Salgia R (2003) A novel small molecule met inhibitor induces apoptosis in cells transformed by the oncogenic TPR-MET tyrosine kinase. *Cancer research* **63**:5462-5469.

Sengupta S, Gherardi E, Sellers LA, Wood JM, Sasisekharan R and Fan TP (2003) Hepatocyte growth factor/scatter factor can induce angiogenesis independently of vascular endothelial growth factor. *Arteriosclerosis, thrombosis, and vascular biology* **23**:69-75.

Stabile LP, Rothstein ME, Keohavong P, Jin J, Yin J, Land SR, Dacic S, Luong TM, Kim KJ, Dulak AM and Siegfried JM (2008) Therapeutic targeting of human hepatocyte growth factor with a single neutralizing monoclonal antibody reduces lung tumorigenesis. *Molecular cancer therapeutics* **7**:1913-1922.

Stella MC and Comoglio PM (1999) HGF: a multifunctional growth factor controlling cell scattering. *The international journal of biochemistry & cell biology.* **31**:1357-1362.

Takayama H, LaRochelle WJ, Sharp R, Otsuka T, Kriebel P, Anver M, Aaronson SA and Merlino G (1997) Diverse Tumorigenesis Associated with Aberrant Development in Mice Overexpressing Hepatocyte Growth Factor/Scatter Factor. *Proceedings of the National Academy of Sciences of the United States of America* **94**:701-706.

Thompson J, Dolcet X, Hilton M, Tolcos M and Davies AM (2004) HGF promotes survival and growth of maturing sympathetic neurons by PI-3 kinase- and MAP kinase-dependent mechanisms. *Molecular and cellular neurosciences* **27**:441-452.

Weidner KM, Di Cesare S, Sachs M, Brinkmann V, Behrens J and Birchmeier W (1996) Interaction between Gab1 and the Met receptor tyrosine kinase is responsible for epithelial morphogenesis. *Nature* **384**:173-176.

Yamamoto BJ, Elias PD, Masino JA, Hudson BD, McCoy AT, Anderson ZJ, Varnum MD, Sardinia MF, Wright JW and Harding JW (2010) The Angiotensin IV Analog Nle-Tyr-Leu-Ψ-(CH2-NH2)3-4-His-Pro-Phe (Norleual) Can Act as a Hepatocyte Growth Factor/Met Inhibitor. *The Journal of pharmacology and experimental therapeutics.* **333**:161.

Youles M, Holmes O, Petoukhov MV, Nessen MA, Stivala S, Svergun DI and Gherardi E (2008) Engineering the NK1 Fragment of Hepatocyte Growth Factor/Scatter Factor as a MET Receptor Antagonist, in *Journal of Molecular Biology* pp 616-622.

Zeng Q, McCauley LK and Wang CY (2002) Hepatocyte growth factor inhibits anoikis by induction of activator protein 1-dependent cyclooxygenase-2. Implication in head and

neck squamous cell carcinoma progression. *The Journal of biological chemistry* **277**:50137-50142.

Zhang YW, Su Y, Volpert OV and Vande Woude GF (2003) Hepatocyte growth factor/scatter factor mediates angiogenesis through positive VEGF and negative thrombospondin 1 regulation. *Proceedings of the National Academy of Sciences of the United States of America* **100**:12718-12723.

Zhang YW and Vande Woude GF (2003) HGF/SF-met signaling in the control of branching morphogenesis and invasion. *Journal of cellular biochemistry* **88**:408-417.

2.7 Supplementary Material

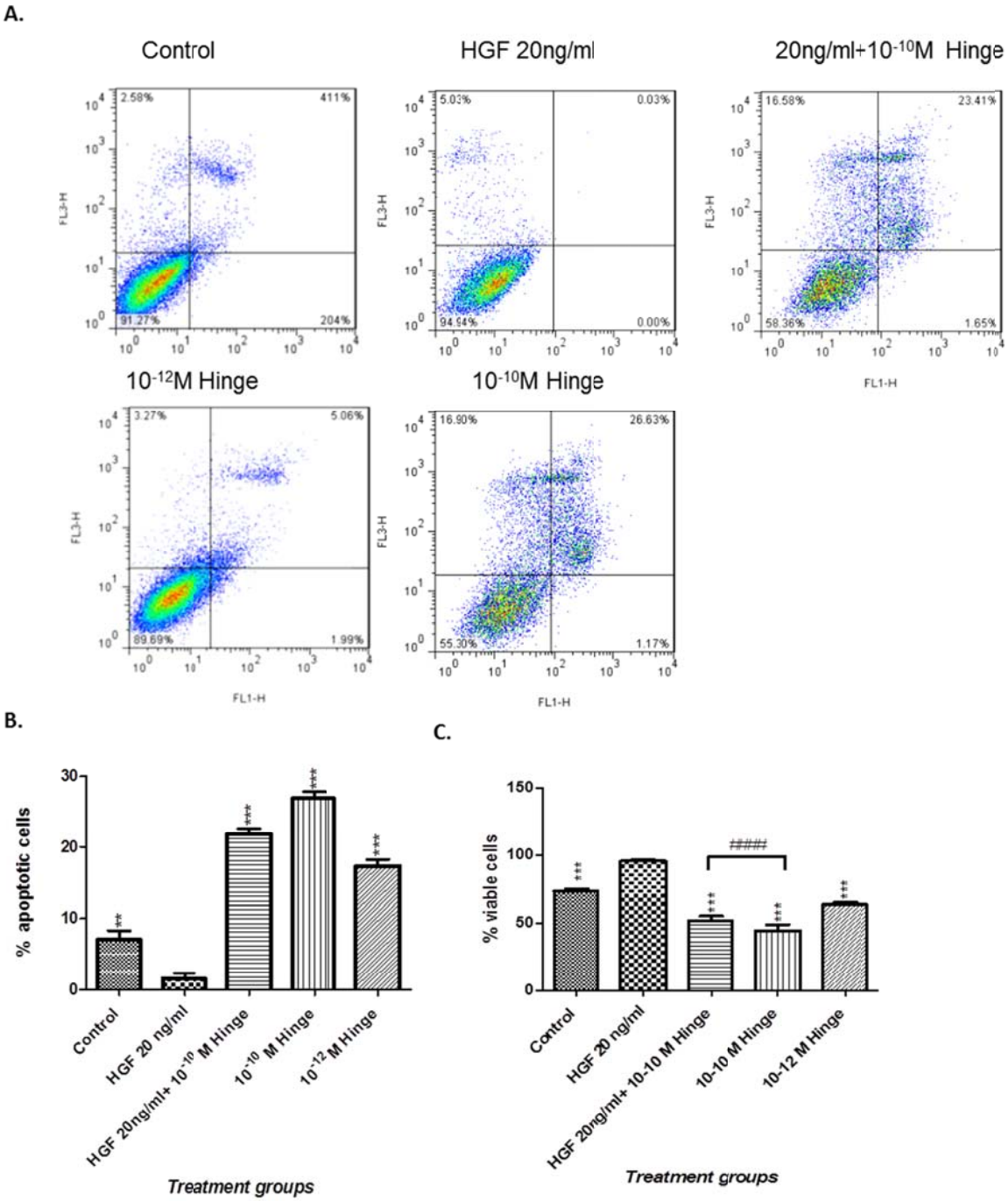

Figure 2.8 supplemental 1. Hinge peptide inhibits HGF dependent cell survival and induces cell death. Five different groups of treated MDCK (Madin-Darby Canine Kidney) cells received PBS

(Control), HGF(20ng/ml) +/- 10^{-10}M Hinge, or Hinge alone (at two different concentrations 10^{-10}M and 10^{-12}M), daily for four days. The percentage of cells undergoing necrosis and apoptosis was determined by flow cytometry (FACS). Panels in (**A**) show the staining profile for the different treatment groups. Cells that are undergoing apoptosis are dual stained with Annexin V and PI (right upper corner) while viable cells are at the lower left corner. Cells in the upper left corner are dead, most likely by necrotic mechanisms. Cells in the lower right corner are damaged and show initial signs of apoptosis. Panel (**B**) and (**C**) are the quantification of cells undergoing apoptosis and the number of viable cells respectively. The level of apoptosis of the HGF plus 10^{-10}M Hinge peptide, 10^{-10}M Hinge peptide, and 10^{-12}M Hinge peptide groups are were all different from HGF alone group (***p=<0.001) but not different from one another (P>0.05). The number of viable cells has insignificantly lower in the HGF plus 10^{-10}M Hinge peptide, 10^{-10}M Hinge peptide, and 10^{-12}M Hinge peptide groups when compared to the HGF alone group (###P=<0.001) while HGF plus 10^{-10}M Hinge peptide, 10^{-10}M Hinge peptide groups were lower than the non-treated control group (P<0.001). Mean +/-SEM; N=6.

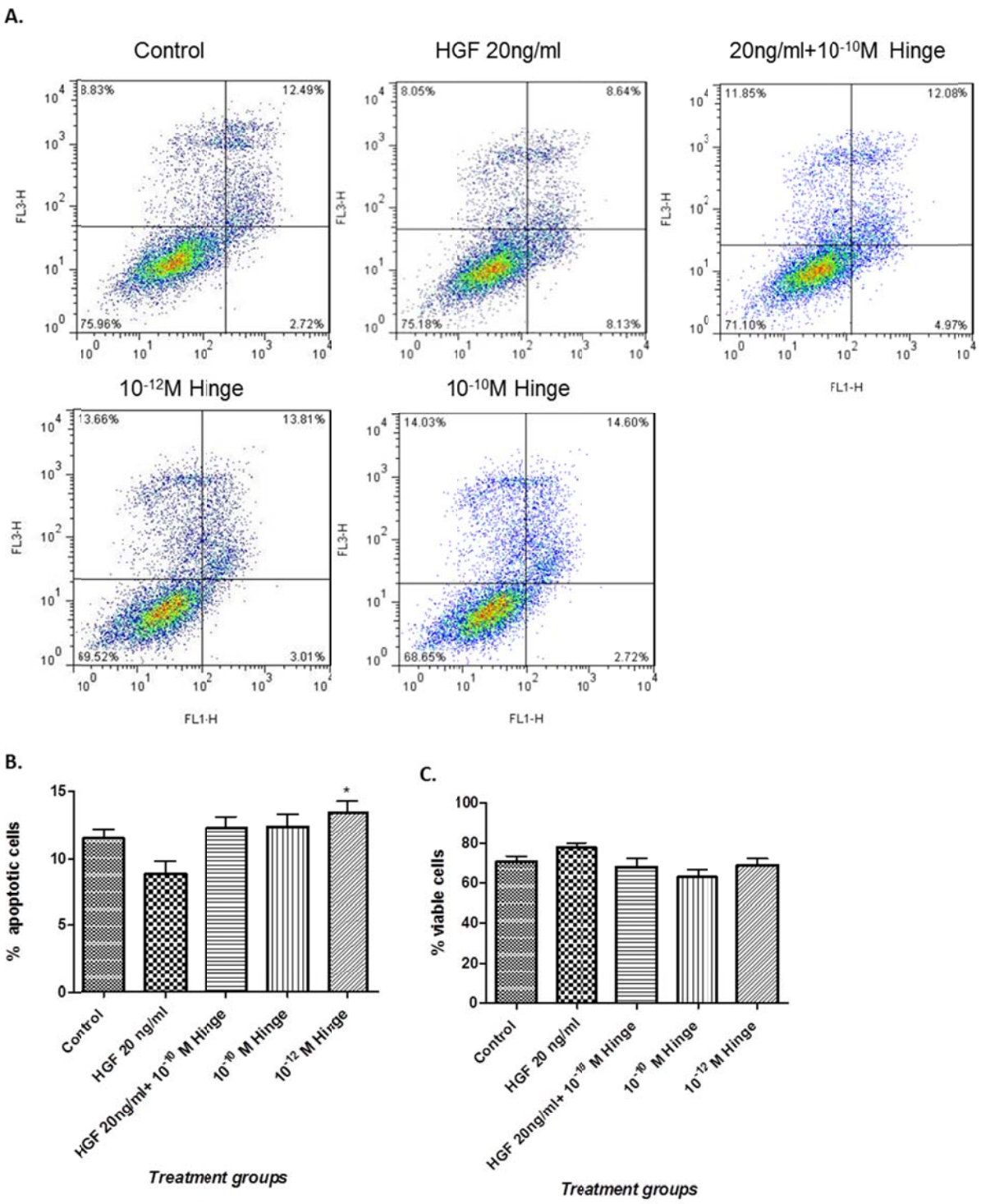

Figure 2.9 supplemental 2. B16-F10 short-term treatment with the Hinge peptide does not inhibit HGF dependent cell survival. Five different groups of treated MDCK (Madin-Darby Canine Kidney)

cells received PBS (Control), HGF(20ng/ml) +/- 10^{-10}M Hinge, or Hinge alone (at two different concentrations 10^{-10}M and 10^{-12}M),and incubated for 24 hours. The percentage of cells undergoing necrosis and apoptosis was determined by flow cytometry (FACS). Panels in (**A**) show the staining profile for the different treatment groups. Cells that are undergoing apoptosis are dual stained with Annexin V and PI (right upper corner) while viable cells are at the lower left corner. Cells in the upper left corner are dead, most likely by necrotic mechanisms. Cells in the lower right corner are damaged and show initial signs of apoptosis. Panel (**B**) and (**C**) are the quantification of cells undergoing apoptosis and the number of viable cells respectively. The level of apoptosis of the HGF plus 10^{-10}M Hinge peptide and 10^{-10}M Hinge peptide groups were not different from HGF alone group. HGF alone group, HGF plus 10^{-10}M Hinge peptide, 10^{-10}M Hinge peptide, and 10^{-12}M Hinge peptide were not different from the control group. HGF plus 10^{-10}M Hinge peptide, 10^{-10}M Hinge peptide, and 10^{-12}M Hinge peptide were not different from one another ($P>0.05$). The number of viable cells are insignificantly different between all groups. Mean +/-SEM; N=3.

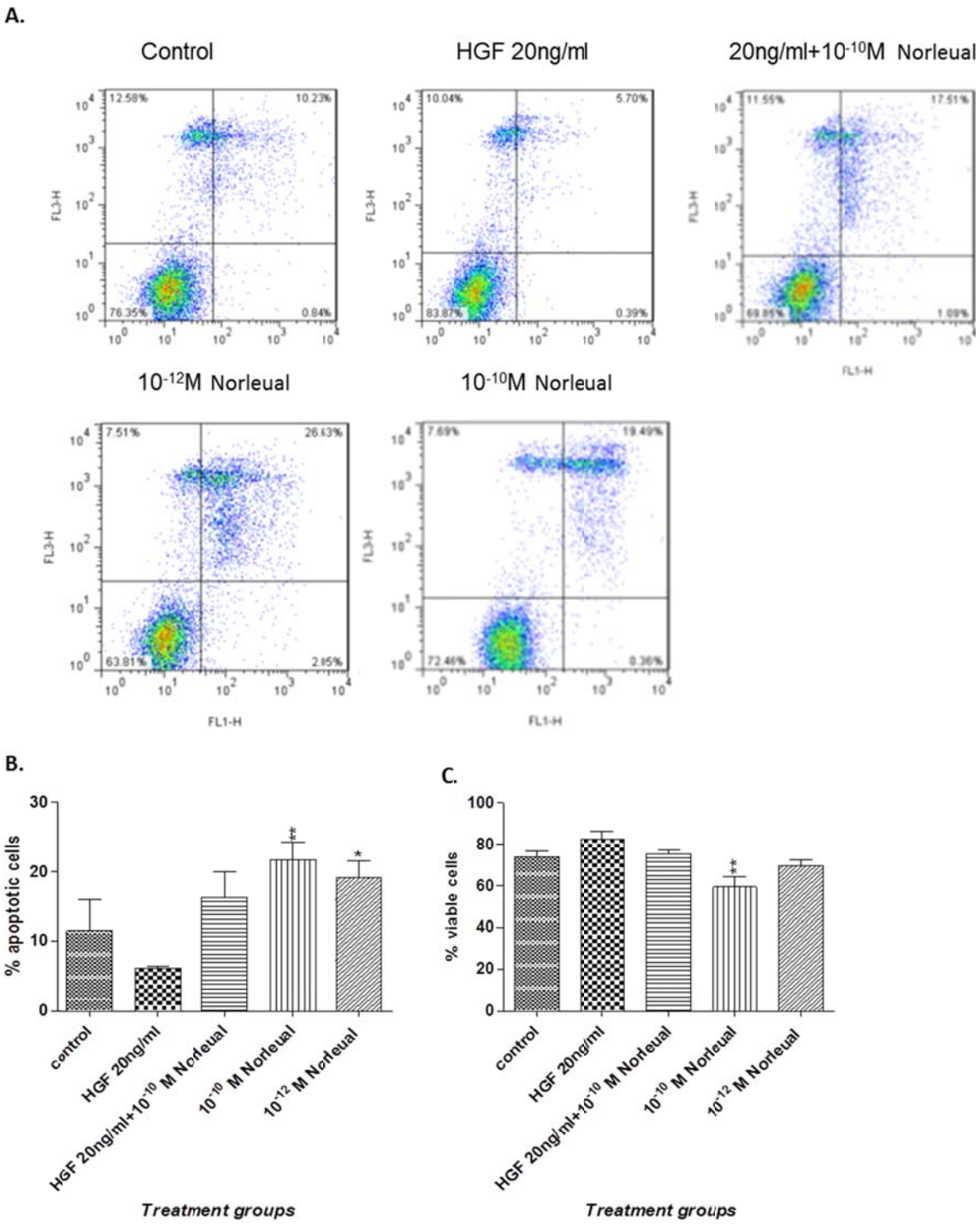

Figure 2.10 supplemental 3. Norleual peptide effects on HGF dependent cell survival and cell death.

Five different groups of treated B16F10 murine melanoma cells received PBS (Control), HGF(20ng/ml)

+/- 10^{-10}M Norleual, or Norleual alone (at two different concentrations 10^{-10}M and 10^{-12}M), daily for four days. The percentage of cells undergoing necrosis and apoptosis was determined by flow cytometry (FACS). Panels in (A) show the staining profile for the different treatment groups. Cells that are undergoing apoptosis are dual stained with Annexin V and PI (right upper corner) while viable cells are at the lower left corner. Cells in the upper left corner are dead, most likely by necrotic mechanisms. Cells in the lower right corner are damaged and show initial signs of apoptosis. Panel (B) and (C) are the quantification of cells undergoing apoptosis and the number of viable cells respectively. The level of apoptosis of 10^{-10}M Norleual peptide, and 10^{-12}M Norlual peptide groups were different from HGF alone group (**p=<0.01, **p=<0.05) but not different from one another (P>0.05). The number of viable cells has insignificantly lower in the 10^{-10}M Norleual peptide group when compared to the HGF alone group (*P=<0.05). Mean +/-SEM; N=4.

CHAPTER THREE

DEVELOPMENT OF ANGIOTENSIN IV ANALOGS AS HEPATOCYTE GROWTH FACTOR/MET MODIFIERS

3.1 Abstract

The 6-AH family [D-Nle-X-Ile-NH-$(CH_2)_5$-$CONH_2$; where X= various amino acids] of Angiotensin IV analogs, bind directly to Hepatocyte Growth Factor (HGF) and inhibit HGF's ability to form functional dimers. The metabolically stabilized 6-AH family member, D-Nle-Tyr-Ile-NH-$(CH_2)_5$-$CONH_2$, had a $t_{1/2}$ in blood of 80 minutes compared to the parent compound Norleual (Nle-Tyr-Leu-ψ-$(CH_2$-$NH_2)^{3-4}$-His-Pro-Phe), which had a $t_{1/2}$ in blood of < 5 Minutes. 6-AH family members were found to act as mimics of the dimerization domain of HGF (hinge region), and inhibited the interaction of an HGF molecule with a ^{3}H-hinge region peptide resulting in an attenuated capacity of HGF to activate its receptor Met. This interference translated into inhibition of HGF-dependent signaling, proliferation, and scattering in multiple cell types at concentrations reaching down into the low picomolar range. We also noted a significant correlation between the ability of the 6-AH family members to block HGF dimerization and inhibition of the cellular activity. Further, a member of the 6-AH family with cysteine at position 2, was a particularly effective antagonist of HGF-dependent cellular activities. This compound suppressed pulmonary colonization by B16-F10 murine melanoma cells, which are characterized by an overactive HGF/Met system. Together these data indicate that the 6-AH family of AngIV analogs exert their biological activity by modifying the activity

of the HGF/Met system and offer the potential as therapeutic agents in disorders that are dependent on or possess an over-activation of the HGF/Met system.

3.2 Introduction

The multifunctional growth factor hepatocyte growth factor (HGF) and its receptor Met are important mediators for mitogenesis, motogenesis, and morphogenesis in a wide range of cell types (Birchmeier et al., 2003) including epithelial (Kakazu et al., 2004), endothelial (Kanda et al., 2006), and hematopoietic cells (Ratajczak et al., 1997), neurons (Maina and Klein, 1999; Thompson et al., 2004), melanocytes (Halaban et al., 1992), and hepatocytes (Borowiak et al., 2004; Huh et al., 2004). Furthermore, dysregulation of the HGF/Met system often leads to neoplastic changes and to cancer (in both human and animal) where it contributes to tumor formation, cancer cell metastasis, and tumor angiogenesis (Christensen et al., 2005; Liu et al., 2008). Over-activation of this signaling system is routinely linked to poor patient prognosis (Liu et al., 2010). Therefore molecules that inhibit the HGF/Met system can be expected to exhibit anti-cancer activity and attenuate malignant and metastatic transformations.

HGF is a vertebrate heteromeric polypeptide growth factor with a domain structure that closely resembles the proteinases of the plasminogen family (Donate et al., 1994). HGF consists of seven domains: an amino terminal domain, a dimerization-linker domain, four kringle domains (K1-K4), and a serine proteinase homology (SPH) domain (Lokker et al., 1992; Chirgadze et al., 1999). The single chain pro-polypeptide is proteolytically processed by convertases to yield a mature α (heavy chain 55 KDa), and β (light chain 34 KDa) heterodimer, which are bound together by a disulfide link (Stella and Comoglio, 1999; Birchmeier et al., 2003; Gherardi et al., 2006). In addition to proteolytic processing, HGF requires dimerization to be

fully activated (Lokker et al., 1992; Chirgadze et al., 1999; Youles et al., 2008). Several reports have shown that HGF forms dimers and/or multimers, which are arranged in a head-to-tail orientation, prior to its interaction with Met (Gherardi et al., 2006). The dimer interface, which encompasses the inter-domain linker amino acids (K122, D123, Y124, I125, R126, and N127) is referred to as the hinge region (Gherardi et al., 2006; Youles et al., 2008). Although both pre-pro-HGF and the active disulfide-linked heterodimer bind Met with high affinity, it is only the heterodimer that is capable of activating Met (Lokker et al., 1992; Sheth et al., 2008).

Recent studies from our laboratory (Yamamoto et al., 2010) have shown that picomolar concentrations of the AngIV analog, Norleual (Nle-Tyr-Leu-ψ-$(CH2-NH2)^{3-4}$-His-Pro-Phe), are capable of potently inhibiting the HGF/Met system and bind directly to the hinge region of HGF blocking its dimerization (Kawas et al., 2011). Moreover, a hexapeptide representing the actual hinge region possessed biochemical and pharmacological properties identical to Norleual's (Kawas et al., 2011). The major implication of those studies was that molecules, which target the dimerization domain of HGF, could represent novel and viable anti-cancer therapeutics. Additionally, these data support the development of such molecules using Norleual and/or the Hinge peptide as synthetic templates.

Despite its marked anti-cancer profile Norleual is highly unstable making its transition to clinical use problematic. Thus a family of metabolically stable Ang IV-related analogs has been developed in our laboratory, which are referred to here as the 6-AH family because of 6-amnio hexanoic amide substituted at the C-terminal position. This substitution along with D-norleucine at the N-terminal enhances the metabolic resistance of family members.

Here we demonstrate that 6-AH family members have superior metabolic stability when compared to Norleual, bind to HGF with high affinity, and act as hinge region mimics; thus

preventing HGF dimerization and activation. This interference translates into inhibition of HGF-dependent signaling, proliferation, and scattering in multiple cell types at concentration in the picomolar range. A positive correlation was evident between the ability to block dimerization and the inhibition of the cellular outcomes of HGF activation. Finally D-Nle-Cys-Ile-NH-$(CH2)_5$-$CONH_2$, a member of the 6-AH family suppressed pulmonary colonization by B16-F10 murine melanoma cells, which are characterized by an overactive HGF/Met system.

These studies highlight the ability of AngIV-like molecules to bind to HGF, block HGF dimerization, and inhibit the HGF/Met system. Moreover, these data encourage the development of AngIV-related pharmaceuticals as therapeutic agents in disorders where inhibition of the HGF/Met system would be clinically advantageous.

3.3 Materials &Methods

Animals. C57BL/6 mice from Taconic farms were used in the lung colonization studies. Male Sprague-Dawley rats (250+ g) were obtained from Harlan Laboratories (CA, USA) for use in pharmacokinetic studies. Animals were housed and cared for in accordance with NIH guidelines as described in the "Guide for the Care and Use of Laboratory Animals".

Compounds. D-Nle-X-Ile-NH-$(CH_2)_5$-COOH; where X= various amino acids and Norleual (Nle-Tyr-Leu-ψ-$(CH_2$-$NH_2)^{3-4}$-His-Pro-Phe) were synthesized using Fmoc based solid phase methods in the Harding laboratory and purified by reverse phase HPLC. Purity and structure were verified by LC-MS. Hepatocyte growth factor (HGF) was purchased from R&D Systems (Minneapolis, MN).

Antibodies. Anti-Met was purchased from Cell Signaling Technology (Beverly, MA). And the phospho-Met antibody was purchased from AbCam, Inc (Cambridge,MA).

Cell culture. Human embryonic kidney cells 293 (HEK293) and Madin Darby canine kidney cells (MDCK) were grown in DMEM, 10% fetal bovine serum (FBS). Cells were grown to 100% confluency before use. HEK and MDCK cells were serum starved for 2-24 hours prior to the initiation of drug treatment.

Blood Stability Studies. To compare the blood stability of Norleual and D-Nle-Tyr-Ile-NH-$(CH_2)_5$-$CONH_2$, a representative member of the 6-AH family, 20 µL of compound-containing vehicle (water [Norleual] or 30% ethanol [D-Nle-Tyr-Ile-NH-$(CH_2)_5$-$CONH_2$]) was added to 180 µL of heparinized blood and incubated at 37^{o}C for various times. For Norleual, 37^{o}C incubations were stopped at 0, 20, 40, and 60 minutes, and for D-Nle-Tyr-Ile-NH-$(CH_2)_5$-$CONH_2$, incubations were stopped at 0, 1, 3 and 5 hours.

At the end of each incubation 20 µL of Nle^1- AngIV (100 µg/ mL) was added to each sample as an internal standard. D-Nle-Tyr-Ile-NH-$(CH_2)_5$-$CONH_2$ samples were centrifuged at 4^{o}C for 5 minutes at 5000 RPM to pellet erythrocytes, and the serum was transferred to clean tubes. The Norleual and D-Nle-Tyr-Ile-NH-$(CH_2)_5$-$CONH_2$ samples were precipitated by adding three volumes of ice-cold acetonitrile (ACN) and the samples were vortexed vigorously. All samples were centrifuged at 4^{o}C, 5000 RPM for 5 minutes and the supernatants were transferred to clean tubes. Samples were then evaporated to dryness in a Savant SpeedVac® concentrator (Thermo Fisher Scientific, Waltham, MA), the residue was reconstituted in 225 µl 35% methanol, vortexed briefly, transferred to HPLC auto-sampler vials, and 100 µl injected into the HPLC system.

Samples were then separated by HPLC on an Econosphere C18 (100mm x 2.1mm) from Grace Davison Discovery Science (Deerfield, IL). Peaks were detected and analyzed by mass spectrographic methods using a LCMS-2010EV mass spectrometer (Shimadzu, Kyoto Japan). The mobile phase consisted of HPLC water (Sigma St. Louis, MO) with 0.1% trifluoroacetic or 0.1% heptafluorobutyric acid (Sigma St. Louis, MO) and varying concentrations of ACN or methanol. Separation was carried out using a gradient method, at ambient temperature and a flow rate of 0.3 mL/min (see below for more information). Stability half-lives were determined assuming a normal single phase exponential decay using Prism 5 graphical/statistical program (GraphPad, San Diego, CA).

IV Pharmacokinetics. *Surgerical Procedures.* Male Sprague-Dawley rats (250+ g) were allowed food (Harlan Teklad rodent diet) and water *ad libitum* in our AAALAC certified animal facility. Rats were housed in temperature-controlled rooms with a 12 hour light/dark cycle. The right jugular veins of the rats were catheterized with sterile polyurethane Hydrocoat^{TM} catheters (Access Technologies, Skokie, IL, USA) under ketamine (Fort Dodge Animal Health, Fort Dodge, IA, USA) and isoflurane (Vet One^{TM}, MWI, Meridian, ID, USA) anesthesia. The catheters were exteriorized through the dorsal skin. The catheters were flushed with heparinized saline before and after blood sample collection and filled with heparin-glycerol locking solution (6 mL glycerol, 3 mL saline, 0.5 mL gentamycin (100mg/mL), 0.5 mL heparin (10,000 u/mL)) when not used for more than 8 hours. The animals were allowed to recover from surgery for several days before use in any experiment, and were fasted overnight prior to the pharmacokinetic experiment.

Pharmacokinetic Study. Catheterized rats were placed in metabolic cages prior to the start of the study and time zero blood samples were collected. Animals were then dosed

intravenously via the jugular vein catheters, with D-Nle-Tyr-Ile-NH-$(CH_2)_5$-$CONH_2$ (24mg/kg) in 30% ethanol. After dosing, blood samples were collected as follows (times and blood volumes collected are listed in chronological order):

Table 3.1: Pharmacokinetics dosing regime

Compound	Time (minutes)	Blood Volume Collected (µl)
D-Nle-Tyr-Ile-NH-$(CH_2)_5$-$CONH_2$	0, 12, 30, 60, 90, 120,180, 240, 300	200, 200, 200, 200, 200, 300, 400, 500, 500

After each blood sample was taken, the catheter was flushed with saline solution and a volume of saline equal to the volume of blood taken was injected (to maintain total blood volume).

Blood Sample Preparation. Upon collection, samples were immediately centrifuged at 4°C, 5000 RPM for 5 minutes and the serum transferred into polypropylene microcentrifuge tubes. A volume of internal standard (Nle^1-AngIV, 100 µg/mL) equal to 0.1 times the sample serum volume was added. A volume of ice-cold acetonitrile equal to four times the sample serum volume was then added and the sample vortexed vigorously for 30 seconds. The supernatants were transferred to clean tubes and samples were then held on ice until the end of the experiment and stored at 4ºC afterward until further processing.

Serial dilutions of D-Nle-Tyr-Ile-NH-$(CH_2)_5$-$CONH_2$ in 30% ethanol were prepared from the stock used to dose the animals for standard curves. 20 µL of each serial dilution was added to 180 µL of blood on ice for final concentrations of 0.01µg/mL, 0.1µg/mL, 1µg/mL and 10µg/mL.

The samples were centrifuged at 4°C, 5000 RPM for 5 minutes and the serum transferred into polypropylene microcentrifuge tubes. A volume of internal standard (Nle^1-AngIV, 100µg/mL) equal to 0.1 times the sample serum volume was added. A volume of ice-cold acetonitrile equal to four times the sample serum volume was then added and the sample vortexed vigorously for 30 seconds. The supernatants were transferred to clean tubes and samples stored at 4ºC and processed alongside the pharmacokinetic study samples. All samples were evaporated to dryness in a Savant SpeedVac® concentrator. The residue was reconstituted in 225 µl 35% methanol and vortexed briefly. The samples were then transferred to HPLC autosampler vials and 100 µl was injected into the HPLC system a total of 2 times (2 HPLC/MS analyses) for each sample.

Chromatographic System and Conditions. The HPLC/MS system used was from Shimadzu (Kyoto, Japan), consisting of a CBM-20A communications bus module, LC-20AD pumps, SIL-20AC auto sampler, SPD-M20A diode array detector and LCMS-2010EV mass spectrometer. Data collection and integration were achieved using Shimadzu LCMS solution software. The analytical column used was an Econosphere C18 (100mm x 2.1mm) from Grace Davison Discovery Science (Deerfield, IL, USA). The mobile phase consisted of HPLC grade methanol and water with 0.1% trifluoroacetic acid. Separation was carried out using a non-isocratic method (40% - 50% methanol over 10 minutes) at ambient temperature and a flow rate of 0.3 mL/min. For MS analysis, a positive ion mode (Scan) was used to monitor the m/z of D-Nle-Tyr-Ile-NH-$(CH_2)_5$-$CONH_2$ at 542 and the m/z of Nle^1-AngIV (used for internal standard) at 395. Good separation of D-Nle-Tyr-Ile-NH-$(CH_2)_5$-$CONH_2$ and the internal standard in blood was successfully achieved. No interfering peaks co-eluted with the analyte or internal standard. Peak purity analysis revealed a peak purity index for D-Nle-Tyr-Ile-NH-$(CH_2)_5$-$CONH_2$ of 0.95 and the internal standard of 0.94. D-Nle-Tyr-Ile-NH-$(CH_2)_5$-$CONH_2$ eluted at 5.06 minutes and

the internal standard at 4.31 minutes. Data were normalized based on the recovery of the internal standard.

Pharmacokinetic Analysis. Pharmacokinetic analysis was performed using data from individual rats. The mean and standard deviation (SD) were calculated for the group. Non-compartmental pharmacokinetic parameters were calculated from serum drug concentration-time profiles by use of WinNonlin® software (Pharsight, Mountain View, CA, USA). The following relevant parameters were determined where possible: area under the concentration-time curve from time zero to the last time point ($AUC_{0\text{-last}}$) or extrapolated to infinity ($AUC_{0\text{-}\infty}$), C_{max} concentration in plasma extrapolated to time zero (C_0), terminal elimination half-life ($t_{1/2}$), volume of distribution (Vd), and clearance (CL).

Microsomal Metabolism. Male rat liver microsomes were obtained from Celsis (Baltimore, MD, USA). The protocol from Celsis for assessing microsomal- dependent drug metabolism was followed with minor adaptations. An NADPH regenerating system (NRS) was prepared as follows: 1.7 mg/mL NADP, 7.8 mg/mL glucose-6-phosphate and 6 units/mL glucose-6-phosphate dehydrogenase were added to 10 mL 2% sodium bicarbonate and used immediately. 500 µM solutions of Norleual, D-Nle-Tyr-Ile-NH-$(CH_2)_5$-$CONH_2$, piroxicam, verapamil and 7-ethoxycoumarin (low, moderate and highly metabolized controls, respectively) were prepared in acetonitrile. Microsomes were suspended in 0.1M Tris buffer (pH 7.38) at 0.5 mg/mL and 100 µL of the microsomal suspension was added to pre-chilled microcentrifuge tubes on ice. To each sample, 640 µL 0.1M Tris buffer, 10 µL 500 µM test compound, and 250 µL of NRS was added. Samples were incubated in a rotisserie hybridization oven at 37ºC for the appropriate incubation times (10, 20, 30, 40 or 60 minutes). 500 µL from each sample was transferred to tubes containing 500 µL ice-cold acetonitrile with internal standard per incubation

sample. Standard curve samples were prepared in incubation buffer and 500 µL added to 500 µL ice-cold acetonitrile with internal standard. All samples were then analyzed by high performance liquid chromatography/mass spectrometry. Drug concentrations were determined and loss of parent relative to negative control samples containing no microsomes was calculated. Clearance was determined by nonlinear regression analysis for k_e and $t_{1/2}$ and the equation $Cl_{int} = k_e$ Vd. For in vitro-in vivo correlation, Cl_{int} per kg body weight was calculated using the following measurements for Sprague-Dawley rats: 44.8 mg of protein per g of liver, 40 g of liver per kg of body weight (obtained from Naritomi, 2001).

HGF Binding. The binding of 6-AH analogs to HGF was assessed by competition using a soluble binding assay. 250µl of PBS containing human HGF (1.25ng) were incubated with ^{3}H-Hinge, the central dimerization domain of HGF, in the presence of varying concentrations of 6-AH analogs between 10^{-13} M to 10^{-7}M (half-log dilutions) for 40 minutes at 37^0C. The incubates were then spun through Bio-Gel P6 spin columns (400 µl packed volume) for 1 minute to separate free and bound ^{3}H-Hinge and the eluent was collected. Five milliliters of scintillation fluid was added to the eluent, which contained the HGF bound ^{3}H-Hinge, and was then counted using scintillation counter. Total disintegrations per minute of bound ^{3}H-Hinge were calculated based on machine counting efficiency. The Ki values for the binding of the peptides were determined using the Prism 5. Competition binding curves were performed in triplicate. Preliminary kinetic studies indicated that equilibrium binding was reached by 40 minutes of incubation at 37^0C. ^{3}H- Hinge has recently been shown to bind to HGF with high affinity (Kawas et al., 2011).

HGF Dimerization. HGF dimerization was assessed using PAGE followed by silver staining (Kawas et al.,2011). Human HGF at a concentration of 0.08ng/µl with or without 6-AH

analogs was incubated with heparin at a final concentration of 5μg/ml. Loading buffer was then added to each sample and the mixture separated by native PAGE using gradient Criterion XT precast gels (4-12% Bis-Tris; Biorad Laboratories, Hercules, CA). Next the gel was silver stained for the detection of the HGF monomers and dimers. Bands were quantitated from digital images using a UVP phosphoimager (Upland, CA).

Western blotting. HEK293 cells were seeded in 6 well tissue culture plates and grown to 95% confluency in DMEM containing 10% FBS. The cells were serum deprived for 24 hours prior to the treatment to reduce the basal levels of phospho-Met. Following serum starvation, cocktails comprised of vehicle and HGF with/without 6-AH analogs were prepared and pre-incubated for 30 minutes at room temperature. The cocktail was then added to the cells for 10 minutes to stimulate the Met receptor and downstream proteins. Cells were harvested using RIPA lysis buffer (Millipore; Billerica, MA) fortified with phosphatase inhibitor cocktails 1 and 2 (Sigma-Aldrich; St. Louis, MO). The lysate was clarified by centrifugation at 15,000 g for 15 minutes, protein concentrations were determined using the BCA total protein assay (Pierce), and then appropriate volumes of the lysates were diluted with 2x reducing Laemmli buffer and heated for ten minutes at 95° C. Samples containing identical amounts of protein were resolved using SDS-PAGE (Criterion, BioRad Laboratories), transferred to nitrocellulose, and blocked in Tris-buffered saline (TBS) containing 5% milk for one hour at room temperature. The phospho-Met antibody were added to the blocking buffer at a final concentration of 1:1000 and incubated at 4° C overnight with gentle agitation. The membranes were then washed several times with water and TBS (PBS, 0.05% Tween-20), a 1:5000 dilution of horseradish-peroxidase conjugated goat anti-rabbit antiserum was added, and the membranes further incubated for one hour at room temperature. Proteins were visualized using the Supersignal West Pico Chemiluminescent

Substrate system (Pierce, Fenton, MO) and molecular weights determined by comparison to protein ladders (BenchMark, Invitrogen, and Kaleidoscope, BioRad). Film images were digitized and analyzed using a UVP phosphoimager.

Cell proliferation. 5000 MDCK cells were seeded into the wells of a 96 well plates in 10% FBS DMEM. To induce cellular quiescence, the cells were serum deprived for twenty-four hours prior to initiating the treatments. Following serum starvation, 10 ng/ml HGF alone and with various concentrations of 6-AH analogs or PBS vehicle were added to the media. The cells were allowed to grow under these conditions for four days with a daily addition of 6-AH analogs. On the fourth day, 1 mg/ml of 1-(4, 5-Dimethylthiazol-2-yl) 3, 5-diphenylformazan reagent (MTT, Sigma-Aldrich) prepared in PBS was added to the cells and incubated for four hours. Dimethyl sulfoxide diluted in a .01M glycine buffer was added to solubilize the cell membranes and the absorbance of reduced MTT in the buffer was quantitated at 590 nm using a plate reader (Biotek Synergy 2, Winooski, VT). HGF-dependent proliferation was determined by subtracting the basal proliferation (in the absence of HGF) from total proliferation rates in groups containing HGF.

Scattering assay. MDCK cells were grown to 100% confluency on the coverslips in six-well plates and washed twice with PBS. The confluent coverslips were then aseptically transferred to new six well plates containing 900 µl serum free DMEM. Norleual, Hinge peptide, and/or HGF (20 ng/ml) were added to appropriate wells. Control wells received PBS vehicle. Plates were incubated at 37°C with 5% CO_2 for 48 hours. Media was removed and cells were fixed with methanol. Cells were stained with Diff-Quik Wright-Giemsa (Dade-Behring, Newark, DE) and digital images were taken. Coverslips were removed with forceps and more digital images were captured. Pixel quantification of images was achieved using

Image J and statistics were performed using Prism 5 and InStat v.3.05 (GraphPad; San Diego, CA).

Lung colony formation. Six to eight month old C57BL/6 mice were injected with 400,000 B16-F10 cells in 200 µl PBS by tail vein injection and subsequently received daily intraperitoneal injections of either D-Nle-X-Cys-NH-$(CH_2)_5$-$CONH_2$ (10 µg/kg and 100µg/kg) or a PBS vehicle control. Two weeks later, mice were anesthetized and lungs were perfused with PBS and removed. Photos were taken and lungs were solubilized in 1% Triton x-100, 20 mM Tris, 0.15 M NaCl, 2 mM EDTA, and 0.02% sodium azide. Samples were disrupted by sonication (Mixonix, Farmingdale, NY) and spun. The supernatant was transferred to a 96 well plate and melanin absorbance at 410nm was measured using a plate reader.

Statistics. Independent one-way analysis of variance (ANOVA) (InStat v.3.05 and Prism 5) was used to determine differences among groups. Tukey-Kramar or Bonferroni's multiple comparison post-hoc tests were performed where necessary. Statistical comparisons of two groups were determined using the two-tailed Student's *t*-test (InStat v.3.05 and Prism 5).

3.4 Results

The AngIV analog D-Nle-Tyr-Ile-NH-$(CH_2)_5$-$CONH_2$ is more metabolically stable than Norleual (Nle-Tyr-Leu-ψ-$(CH_2$-$NH_2)^{3-4}$-His-Pro-Phe): The AngIV-related peptidomimetic Norleual was previously shown to possess, anti-HGF/Met, anti-angiogenic, and anti-cancer activities (Yamamoto et al., 2010). The presence of unprotected peptide bonds at both the N- and C-terminal linkages predicts that Norleual should have poor metabolic stability and rapid clearance for the circulation, properties that may limit its clinical utility. In an attempt to overcome this limitation, a family of compounds, the 6-AH family was designed and synthesized

to offer defense against exopeptidases. **Figure 3.1** demonstrates that as expected Norleual is unstable in blood while D-Nle-Tyr-Ile-NH-$(CH_2)_5$-$CONH_2$ exhibited improved stability.

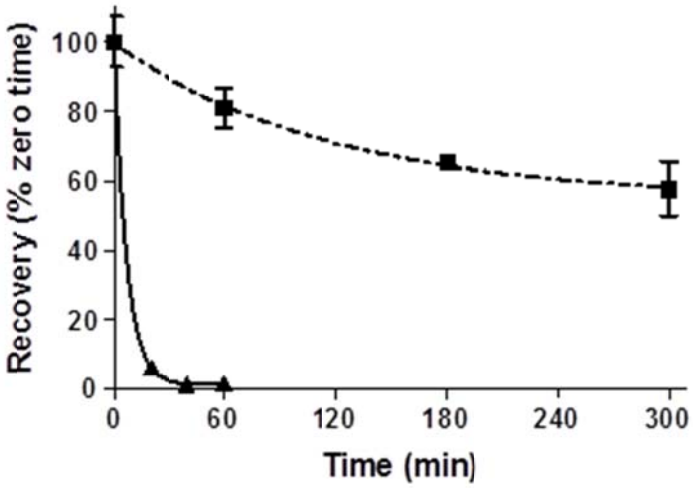

Figure 3.1: Stability of Norleual in rat blood as compared to D-Nle-Tyr-Ile-NH-$(CH_2)_5$-$CONH_2$. ▲ Norleual and ■ D-Nle-Tyr-Ile-NH-$(CH_2)_5$-$CONH_2$ were stored in rat blood at 37ºC; the figure shows percent recovery over time (mean ± SD). The calculated stability $t_{1/2}$ based on single phase exponential decay for Norleual was 4.6 minutes and for D-Nle-Tyr-Ile-NH-$(CH_2)_5$-$CONH_2$ stability $t_{1/2}$ was 79.97 minutes.

The AngIV analog D-Nle-Tyr-Ile-NH-$(CH_2)_5$-$CONH_2$ has a much longer circulating half-life than Norleual (Nle-Tyr-Leu-ψ-$(CH_2$-$NH_2)^{3-4}$-His-Pro-Phe): As anticipated from the *in-vitro* blood stability data, D-Nle-Tyr-Ile-NH-$(CH_2)_5$-$CONH_2$ exhibited an extended *in-vivo* elimination half-life of 1012 minutes after IV injection in rats. Other relevant pharmacokinetic parameters of D-Nle-Tyr-Ile-NH-$(CH_2)_5$-$CONH_2$ after a single IV bolus dose are summarized in

Table 3.2. Serum data was modeled using WinNonlin® software to perform non-compartmental analysis. D-Nle-Tyr-Ile-NH-$(CH_2)_5$-$CONH_2$ appeared to be extensively distributed outside the central blood compartment and/or bound within the tissues as evidenced by its large volume of distribution (Vd). D-Nle-Tyr-Ile-NH-$(CH_2)_5$-$CONH_2$ is not expected to be highly bound to plasma proteins according to quantitative structure-activity relationship (QSAR) modeling (discussed below) and since total recovery from serum was greater than 35 percent. These results, which suggest that D-Nle-Tyr-Ile-NH-$(CH_2)_5$-$CONH_2$ is likely to be relatively hydrophobic, are in agreement with the outcome of QSAR modeling estimates generated by ADMET Predictor® that calculated an octanol:water partition coefficient of 28.18 for D-Nle-Tyr-Ile-NH-$(CH_2)_5$-$CONH_2$ (**Table 3.3**).

Table 3.2: WinNonlin® estimated pharmacokinetic parameters for D-Nle-Tyr-Ile-NH-$(CH_2)_5$-$CONH_2$ after intravenous administration in adult male Sprague-Dawley rats (n = 5). $AUC_{0-\infty}$ = area under the curve. Vd= volume of distribution. Cp^0= initial concentration of drug in plasma. t1/2= biological half-life. KE= rate of elimination. CL= clearance rate.

Pharmacokinetic Parameter	D-Nle-Tyr-Ile-NH-$(CH_2)_5$-$CONH_2$ (Mean ± SEM)
AUC0-∞ (min.ng/mL)	692.5 ± 293.2
Vd (L/kg)	104186.8 ± 65034.3
Cp^0 (ng/mL)	68.2 ± 32.2
t1/2 (min)	1012.0 ± 391.4
KE (min-1)	0.001 ± 0.0002
CL (L/min/kg)	58.3 ± 15.6

Not surprisingly because of its stability, hydrophobic character, and small size, D-Nle-Tyr-Ile-NH-$(CH_2)_5$-$CONH_2$ was predicted to be orally bioavailable. The P_{eff} value represents the predicted effective human jejunal permeability of the molecule. The predicted P_{eff} value for D-Nle-Tyr-Ile-NH-$(CH_2)_5$-$CONH_2$ (1.53) is intermediate between the predicted P_{eff} values for enalapril (1.25) and piroxicam (2.14), two orally bioavailable drugs. D-Nle-Tyr-Ile-NH-$(CH_2)_5$-$CONH_2$ was also predicted to be 42.68 percent unbound to plasma proteins in circulation, thus making it available for distribution into the tissues.

Also contributing to its slow removal from the blood was a lack of Phase I metabolism for D-Nle-Tyr-Ile-NH-$(CH_2)_5$-$CONH_2$. D-Nle-Tyr-Ile-NH-$(CH_2)_5$-$CONH_2$ exhibited no detectable metabolism over 90 minutes in an in-vitro metabolism assay using rat liver microsomes (data not shown).

Table 3.3: Predicted physiochemical properties of D-Nle-Tyr-Ile-NH-$(CH_2)_5$-$CONH_2$. The physiochemical properties of D-Nle-Tyr-Ile-NH-$(CH_2)_5$-$CONH_2$ were estimated following modeling with ADMET Predictor® software.

Physicochemical Property	**Predicted Value**
logP	1.45
P_{eff}	1.53
P_{avg}	0.39
Pr_{Unbnd}	42.68

Together these data indicate that D-Nle-Tyr-Ile-NH-$(CH_2)_5$-$CONH_2$ is more metabolically stable than Norleual, possesses an elongated half-life in the circulation and

penetrates tissue effectively. Overall these favorable pharmacokinetic properties justify the mechanistic and therapeutic evaluation of D-Nle-Tyr-Ile-NH-$(CH_2)_5$-$CONH_2$ and related molecules.

D-Nle-X-Ile-NH-$(CH_2)_5$-$CONH_2$ analogs bind HGF and compete with the ^{3}H-Hinge peptide for HGF binding: Several members of the D-Nle-X-Ile-NH-$(CH_2)_5$-$CONH_2$, 6-AH family, were analyzed for the capacity to compete for ^{3}H-Hinge binding to HGF. As will be evident below, members of the 6-AH family display a varied ability to block the biological action of HGF. As such, the HGF binding properties of a selection of analogs with varying biological activity was assessed to determine if there was a relationship between inhibitory activity and affinity for HGF. The hypothesis that was put forth was that analogs are binding directly to HGF and affecting the sequestration of HGF in an inactive form. To begin the evaluation of this idea, we used a ^{3}H-Hinge peptide as a probe to assess direct HGF binding of the peptides. The use of ^{3}H-Hinge to probe the interaction was based on the ability of ^{3}H-Hinge to bind specifically and with high affinity to HGF (Kawas et al., 2011). A competition study was initiated with several derivatives of the D-Nle-X-Ile-NH-$(CH_2)_5$-$CONH_2$ family. This study demonstrated that different analogs have variable abilities to bind HGF, and that the analogs showing antagonism to HGF are acting as a Hinge mimics. D-Nle-X-Ile-NH-$(CH_2)_5$-$CONH_2$ derivatives were found to compete with Hinge for HGF binding and exhibited a range of affinities for HGF, with K_is ranging from $1.37x10^{-7}$- $1.33x10^{-10}$M (**Figure 3.2**). As expected there is appears to be relationship between a compound's ability to bind HGF and its capacity to block dimerization and inhibit HGF-dependent activities (see **Figures 3.4, 3.5, 3.6**).

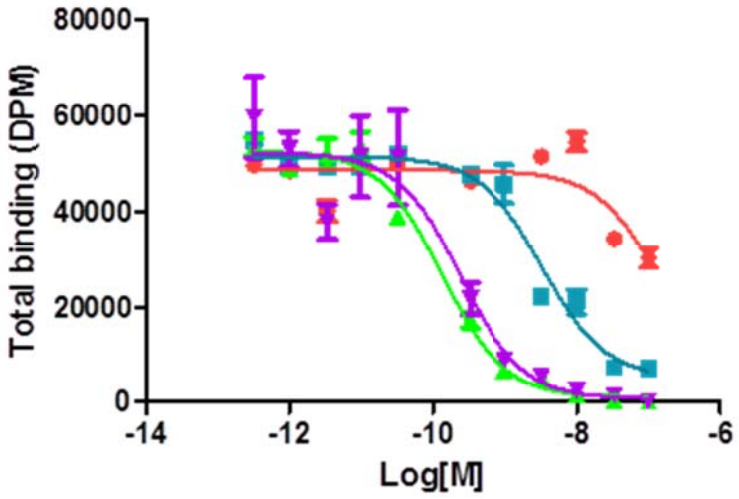

Figure 3.2: The D-Nle-X-Ile-NH-$(CH_2)_5$-$CONH_2$ analogs bind directly to HGF. Representative curves illustrating the competition of D-Nle-X-Ile-NH-$(CH_2)_5$-$CONH_2$ analogs for ^{3}H-Hinge binding to HGF. The D-Nle-X-Ile-NH-$(CH_2)_5$-$CONH_2$ analogs and ^{3}H-Hinge ($13.3x10^{-12}$M) were incubated with 1.25ng of HGF for 40 minutes at 37^{o}C in 0.25 ml of buffer. HGF-bound Hinge was eluted from Bio-Gel P6 columns after the addition of different concentrations of the D-Nle-X-Ile-NH-$(CH_2)_5$-$CONH_2$ analogs (10^{-13} -10^{-7}M). The radioactivity of the eluted solutions was quantitated using scintillation counting. These data demonstrate that the D-Nle-X-Ile-NH-$(CH_2)_5$-$CONH_2$ analogs exhibit a range of affinities for HGF. The K_is for the Met, Trp, Cys , and Tyr analogs were respectively determined to be: $1.375x10^{-07}$M , $3.372x10^{-09}$M, $1.330x10^{-10}$M, and $2.426x10^{-10}$ M; N=9. D-Nle-Cys-Ile-NH-$(CH_2)_5$-$CONH_2$, D-Nle-Met-Ile-NH-$(CH_2)_5$-$CONH_2$, D-Nle-Trp-Ile-NH-$(CH_2)_5$- CONH2, D-Nle-Tyr-Ile-NH-$(CH_2)_5$- $CONH_2$.

D-Nle-X-Ile-NH-$(CH_2)_5$-$CONH_2$ analogs block HGF Dimerization: Several reports have shown that HGF needs to form homodimers and/or multimers, prior to its activation of Met (Chirgadze et al., 1999a; Gherardi et al., 2006). This dimer is arranged in a head to tail orientation; the dimer interface comprises a central region, the hinge region that is important for the proper dimer formation and orientation. A homologous sequence-conservation screen against all possible transcripts that were independent of and not derived from angiotensinogen looking for similarities to AngIV identified partial homology with the hinge region (Yamamoto et al., 2010) of the plasminogen family of proteins, which include plasminogen itself, its anti-angiogenic degradation product, angiostatin, and the protein hormones heptocyte growth factor (HGF) and macrophage stimulating protein (MSP). Moreover, the AngIV analog Norleual, which is a potent inhibitor of the HGF/Met system, was shown to bind to HGF and block its dimerization (Kawas et al., 2011). This knowledge coupled with the demonstration that some members of the 6-AH family bound with high affinity to the hinge region of HGF led to the expectation that other active AngIV analogs, like 6-AH family members, could be expected to inhibit HGF dimerization and that the ability of an individual analog to bind HGF and inhibit HGF-dependent processes should be reflected in its capacity to attenuate dimerization. The data in **Figure 3.3** confirm this expectation by demonstrating that D-Nle-Cys-Ile-NH-$(CH_2)_5$-$CONH_2$ and D-Nle-Tyr-Ile-NH-$(CH_2)_5$-$CONH_2$, which bind HGF with high affinity (**Figure 3.2**) and effectively attenuate HGF-dependent processes (**Figures 3.4, 3.5, 3.6**) completely block HGF dimer formation. Conversely D-Nle-Met-Ile-NH-$(CH_2)_5$-$CONH_2$, which has low affinity for HGF (**Figure 3.2**) and exhibits little anti-HGF/Met activity, is unable to block dimerization at the concentration tested. The D-Nle-Trp-Ile-NH-$(CH_2)_5$-$CONH_2$ analog, which exhibits intermediate inhibition of dimerization, predictably has a moderate affinity for HGF and a moderate ability to

inhibit HGF-dependent processes (**Figures 3.4, 3.5, 3.6**). Together these data confirm the expectation that active 6-AH analogs can block dimerization and further that dimerization inhibitory potential of an analog translates, at least qualitatively, to its capacity to block HGF-dependent processes.

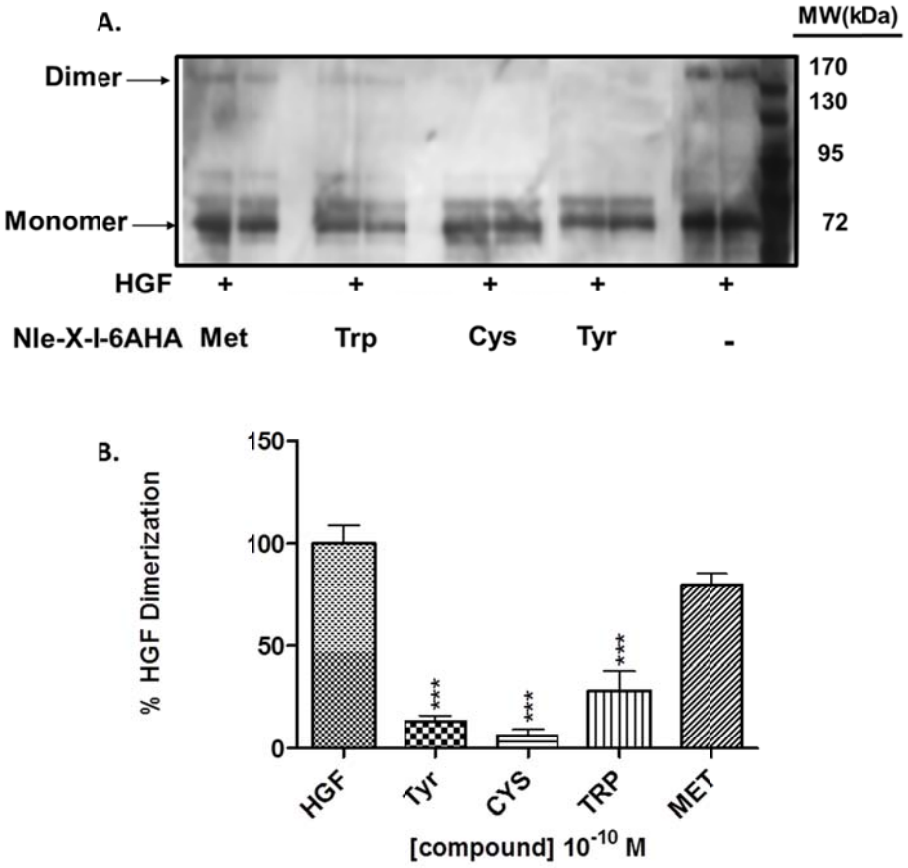

Figure 3.3: Inhibition of HGF dimerization. HGF spontaneously dimerizes when incubated in PBS in the presence of heparin. HGF was incubated without (control) or with various drug candidates at 10^{-10}M. These include the derivatives of D-Nle-X-Ile- (6) amino-hexanoic amide, an AngIV-based analog family, where X= Tyr, Cys, Trp, and Met. After 30 minute incubation, samples were cross-linked with BS3, separated by gel electrophoresis, and silver stained. Band density was quantified and used to determine

the level of HGF dimerization in each group. Treatment groups (Tyr, Cys, Trp) were statistically different than the HGF treated group ($P<0.05$; N=8) (**A**) Representative gel. (**B**) Pooled and quantified data.

D-Nle-X-Ile-NH-$(CH_2)_5$-$CONH_2$ analogs attenuates HGF-dependent Met signaling:

After establishing that the 6-AH family members exhibit a range of HGF binding and dimerization inhibitory profiles, we next determined whether these properties would parallel a compound's ability to inhibit Met signaling. Characteristic of tyrosine kinase-linked growth factor receptors like Met is a requisite tyrosine residue auto-phosphorylation step, which is essential for the eventual recruitment of various SH2 domain signaling proteins. Thus we evaluated the ability of several 6-AH analogs to induce Met tyrosine phosphorylation. As anticipated, the data in **Figure 3.4** demonstrate that both D-Nle-Cys-Ile-NH-$(CH_2)_5$-$CONH_2$ and D-Nle-Tyr-Ile-NH-$(CH_2)_5$-$CONH_2$, which bind HGF with high affinity (**Figure 3.2**) and effectively block its dimerization (**Figure 3.3**) were able to block Met auto-phosphorylation. The D-Nle-Trp-Ile-NH-$(CH_2)_5$-$CONH_2$ analog had intermediate inhibitory activity, and the D-Nle-Met-Ile-NH-$(CH_2)_5$-$CONH_2$ analog showed no ability to effect on Met activation. Together, these data indicate that the capacity of 6-AH analogs to inhibit HGF-dependent Met activation paralleled their HGF binding affinity and their capacity to block dimerization.

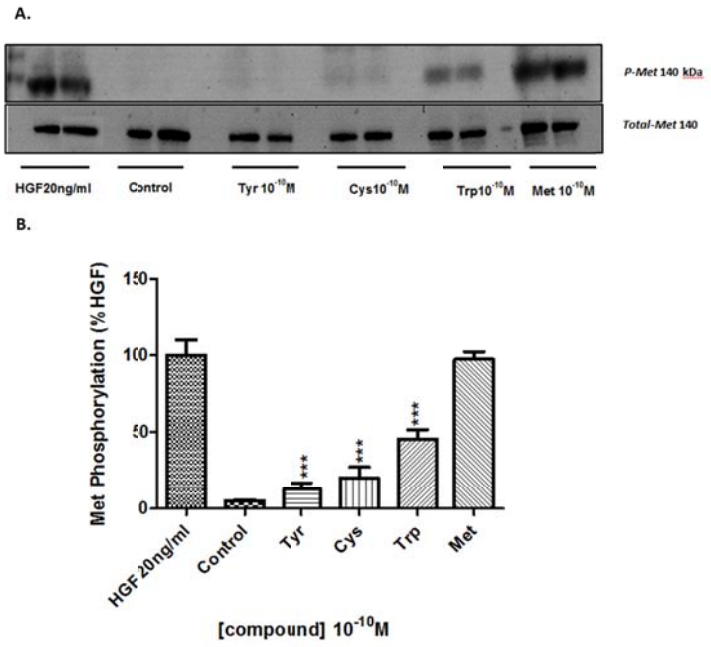

Figure 3.4: Nle-X-Ile-(6) aminohexanoic amide analogs inhibition of Met phosphorylation.

HEK293 cells were treated for 10 minutes with HGF+/- Nle-X-Ile-(6) aminohexanoic amide analogs at the indicated concentrations. HEK293 cell lysates were immunoblotted with anti-phospho-Met and anti-Met antibodies. The differences in the mean values for Met phosphorylation among the indicated treatment groups (Nle-X-Ile-(6) aminohexanoic amide analogs) compared to the HGF treated group were greater than would be expected by chance ($P < 0.05$; N=6). The Met group was not different than the HGF group ($P > 0.05$; N=6).

D-Nle-X-Ile-NH-$(CH_2)_5$-COOH analogs affect HGF/Met stimulated MDCK cell proliferation: Met activation initiates multiple cellular responses including increased proliferation and motility, enhanced survival, and differentiation (Zhang and Vande Woude, 2003). As an initial test of the ability of 6-AH family members to alter HGF-dependent cellular activity we evaluated the capacity of several members of the family to modify the proliferative activity of Madin-Darby canine kidney (MDCK) cells, a standard cellular model for investigating the HGF/Met system (Stella and Comoglio, 1999). As seen in **Figure 3.5** there is a

wide range of inhibitory activity against HGF dependent cellular proliferation. Similar to the results from the binding and dimerization experiments the Cys^2 and Tyr^2 analogs exhibited marked inhibitory activity. The Asp^2 analog, which had not been evaluated in the earlier studies, also exhibited pronounced inhibitory activity. The Trp^2, Phe^2, and Ser^2 analogs all showed inhibitory activity, albeit less than that observed with the most potent analogs. The decrease in HGF-dependent MDCK proliferation below control levels for some compounds is not surprising since the experiment was carried in 2% serum, which likely contains some level of HGF. The Hinge peptide (KDYIRN), which represents the dimerization domain of HGF, was included as a positive control. A recent study has demonstrated that Hinge binds to HGF with high affinity blocking its dimerization and acting as a potent inhibitor of HGF-dependent cellular activities including MDCK proliferation (Kawas et al., 2011).

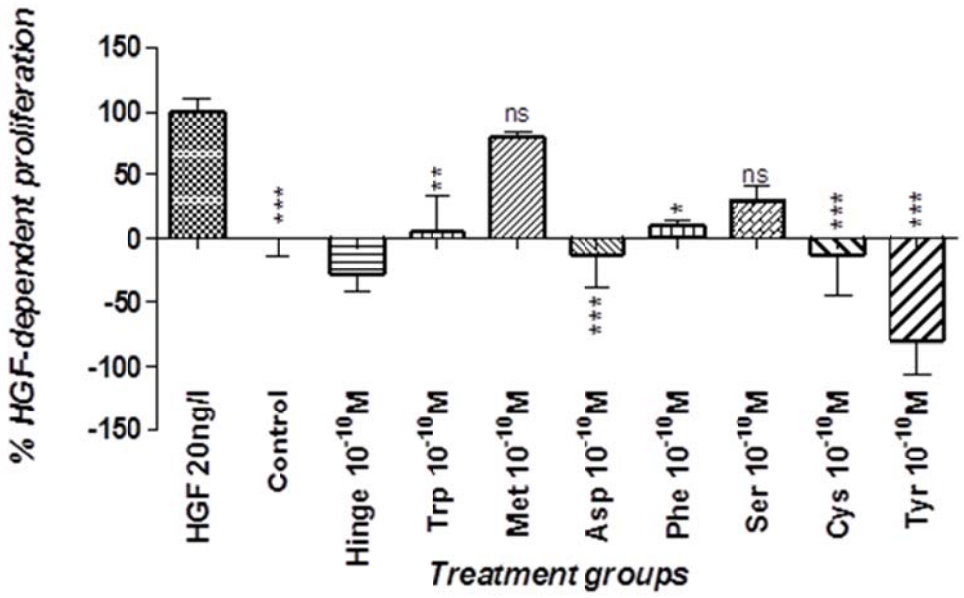

Figure 3.5: Nle-X-Ile-(6) aminohexanoic amide analogs effects on MDCK cells proliferation. MDCK cells were treated with a PBS vehicle (negative control), HGF, or HGF in combination with Nle-X-Ile-

(6)-aminohexanoic amide analogs (X= L-amino acid) at 10^{-10}M concentration. The Hinge peptide (KDYIRN), which represents the dimerization domain of HGF, was included as a positive control. The cells were allowed to grow for four days. Cell numbers were estimated on the fourth day with an MTT assay by measuring absorbance at 590. % HGF-dependent proliferation: control values were subtracted from all values to determine HGF-induced increase in cell proliferation. N=6. *** $p<0.001$. ** $p<0.001$, * $p<0.05$, ns: not significant.

D-Nle-X-Ile-NH-$(CH_2)_5$-COOH analogs modify HGF/Met mediated cell scattering in MDCK cells: Cell scattering is the hallmark effect of HGF/Met signaling; a process characterized by decreased cell adhesion, increased motility, and increased proliferation. The treatment of MDCK cells with HGF initiates a scattering response that occurs in two stages. First, the cells lose their cell-to-cell adhesion and become polarized. Second, they separate completely and migrate away from each other. It is expected that if the 6AH family members are capable of inhibiting the HGF/Met system then they should be able to modify HGF dependent MDCK cell scattering.

Figures 3.6 A & B indicate that those analogs that were previously found to block HGF dimerization were effective inhibitor of HGF/Met mediated cell scattering in MDCK cells, while those analogs with poor affinity for HGF were ineffective. **Figure 3.7** shows a correlation between the blockade of HGF dimerization and HGF binding affinity and the ability to prevent MDCK cell scattering.

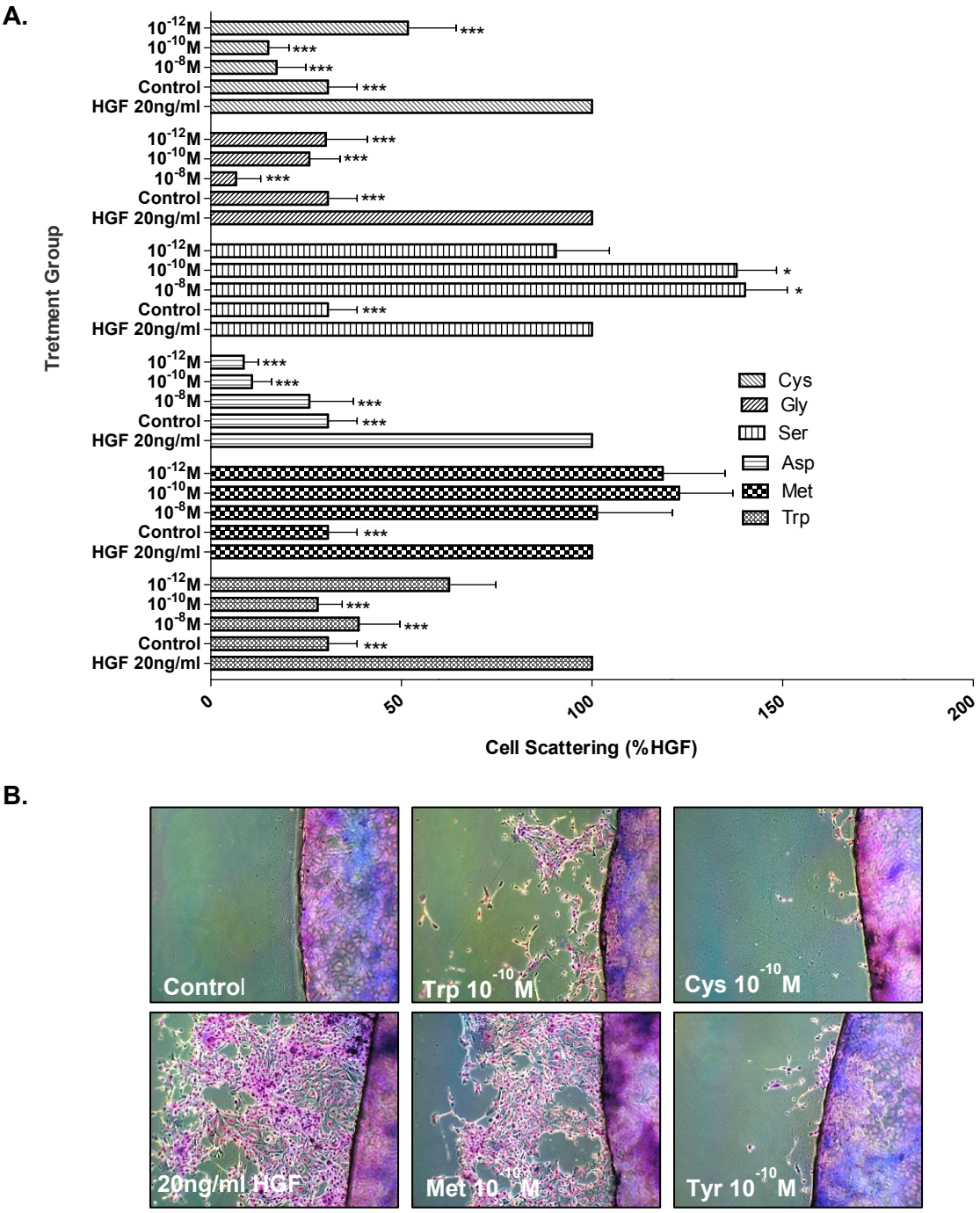

Figure 3.6: Effect of Nle-X-Ile-(6) aminohexanoic amide analogs on HGF-dependent scattering in MDCK cells. Cell scattering in which cells lose the cell-to-cell contacts and then migrate rapidly is the

classic response to HGF. MDCK cells, the gold standard cellular model for studying the HGF/Met system, were grown to 100% confluence on cover slips and then placed in a clean plate. The cells were stimulated to scatter off of the cover slip by adding 20 ng/ml of HGF to the media alone or in combination with Nle-X-Ile-(6) aminohexanoic amide analogs (X= L-amino acid). After 48 hours of scattering, the cells were fixed with methanol and stained with Diff-Quik. The coverslips were removed to reveal the ring of cells that had scattered off of the cover slip and onto the plate. (**A**) The effect of HGF on scattering was quantitated by determining by densitometry of the digital images from scattered cells. ANOVA analysis indicates that the Tyr + HGF, Cys + HGF, and Trp + HGF treated groups were different from the HGF alone group but not different from the control group. The HGF and HGF + Met groups were not different. N=8, $p<0.05$ (**B**) Representative pictures of MDCK cells scattering off the coverslips.

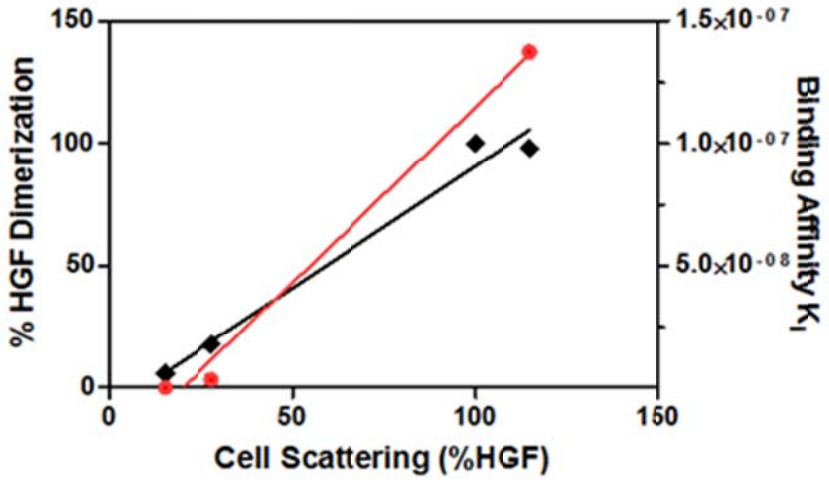

Figure 3.7: Correlation between inhibition of MDCK cell scattering and interference with dimerization and the affinity to bind HGF. Three derivatives of the D-Nle-X-Ile-(6)amino-hexanoic amide, where X is: Cys, Trp, or Met were examined to determine whether the percent of inhibition of dimerization and the binding affinity for each compound for HGF could be correlated to in vitro cellular activity, namely inhibition of MDCK cell scattering. The figure shows a strong correlation between

percent inhibition of HGF dimerization (◆; R^2=0.9809) and for binding affinity to HGF (●; K_i Values; R^2=0.9903) and percent inhibition of HGF-dependent cell scattering.

D-Nle-Cys-Ile-NH-$(CH_2)_5$-COOH inhibits B16-F10 murine melanoma cell migration and lung colony formation: To evaluate the prospective utility of the 6AH family members' as potential therapeutics, we examined the capacity of [D-Nle-Cys-Ile-NH-$(CH_2)_5$-COOH], an analog that exhibits a strong inhibitory profile against HGF-dependent Met activation, to suppress the migratory and lung colony-forming capacity of B16-F10 murine melanoma cells. B16 melanoma cells over-express Met (Ferraro et al., 2006), and were chosen for these studies because Met signaling is critical for their migration, invasion, and metastasis. As a final test for the physiological significance of the 6AH family blockade of Met-dependent cellular outcomes, we evaluated the ability of D-Nle-Cys-Ile-NH-$(CH_2)_5$-COOH to inhibit the formation of pulmonary colonies by B16-F10 cells after tail vein injection in mice. **Figure 3.8a** illustrates the inhibitory response that was observed with daily intraperitoneal injections at two doses (10μg/kg/day and 100μg/kg/day) of [D-Nle-Cys-Ile-NH-$(CH_2)_5$-COOH]. **Figure 3.8b** provides a quantitative assessment of pulmonary colonization by measuring melanin content, which reflects the level of melanoma colonization. Together these data demonstrate that treatment of melanoma cells with D-Nle-Cys-Ile-NH-$(CH_2)_5$-COOH radically prevented lung colonization and highlight the potential utility of the use of 6-AH analogs as potential anti-cancer agents.

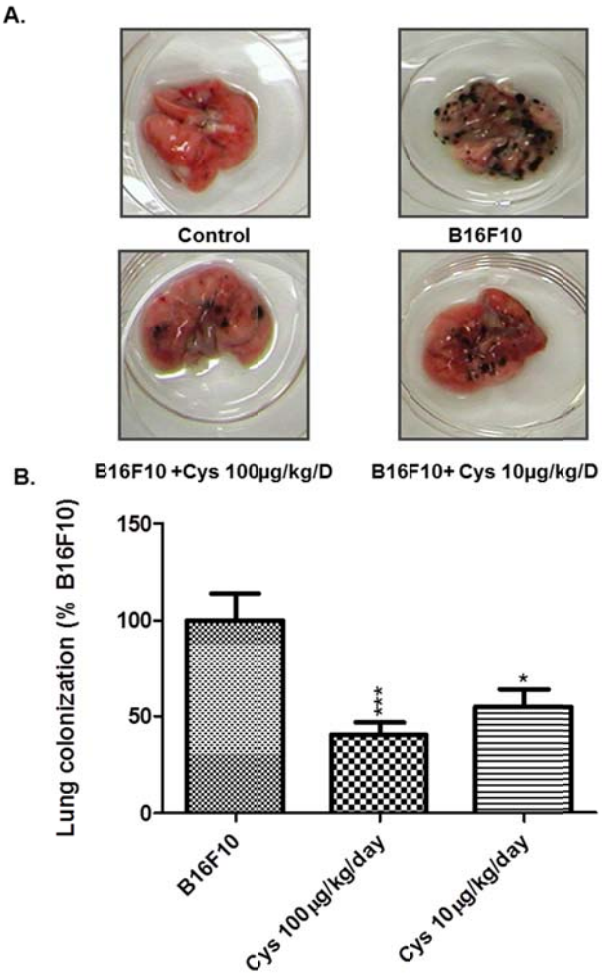

Figure 3.8: D-Nle-Cys-Ile-(6)-amino-hexanoic amide inhibits B16-F10 melanoma lung colonization. 400,000 B16-F10 murine melanoma cells were injected into the tail vein of C57BL/6 mice. Mice received daily IP injections of D-Nle-Cys-Ile-(6)-amino-hexanoic amide (10µg/kg/day or 100µg/kg/day) or PBS vehicle. (**A**) After fourteen days, the lungs from D-Nle-Cys-Ile-(6)-amino-hexanoic amide treated mice exhibited an obvious reduction in melanoma colonies when compared to untreated controls. (**B**) After removal, lungs were homogenized and total melanin content was determined spectrophotometrically and used to quantify total pulmonary melanoma colonization in vehicle treated and D-Nle-Cys-Ile-(6)-amino-hexanoic amide treated. Ungrafted age-matched control lungs exhibited a background absorbance at 410nm. N=15, Mean ± SEM; * $P<0.05$, *** $P<0.001$.

3.5 Discussion

The specificity advantage of target-based treatments has drastically changed the way cancer is treated. While the effectiveness of these types of molecules can't be denied their utility is often limited to a relatively small number of cancer patients. Thus, the cancer research community has been searching for a target that is not only critical to but also widespread among cancer types. One such target, which meets these criteria and has moved to the forefront of research and development, is the hepatocyte growth factor (HGF)/Met (its tyrosine kinase receptor) system (Comoglio et al., 2008; Eder et al., 2009). Three specific characteristics of this system have ignited an explosion of development activity. First, a wide range of malignancies including bladder, breast, cervical, colorectal, endometrial, esophageal, gastric, head and neck, kidney, liver, lung, nasopharyngeal, ovarian, pancreatic, prostate, and thyroid cancers (http://www.vai.org/met/) display unrelenting Met stimulation because of over-expression of Met and/or HGF or the presence of gain-of-function mutations resulting in ligand-dependent autocrine or paracrine mechanisms. Osteosarcomas and globlastoma mutliforme, which over-express both Met and HGF are examples of neoplasms that are characterized by dysfunctional autocrine control of the HGF/Met system. Second, HGF/Met signaling activates a number of cellular responses such as proliferation, migration, invasion, and scattering, which are essential for tumor growth and the transition to a metastatic phenotype. Many studies have shown that HGF/Met activation augments mitogenic and invasive activity in ovarian, glioma, gastric, and lung carcinomas. Ectopic over-expression of HGF and/or Met in mouse and human cell lines leads them to develop tumorigenic and metastatic phenotypes (Rong et al., 1994). Because of the ability of HGF to encourage multiple pro-neoplastic cellular activities, HGF over- or miss-expression often correlates with poor patient prognosis (Danilkovitch-Miagkova and Zbar,

2002). And third, HGF/Met is a critical regulator of angiogenesis, the process of blood vessel growth. The recruitment of a dedicated blood supply, which provides access to oxygen and nutrients, is essential for tumor growth. Defects in the integrity of this new tumor vasculature facilitate the shedding of primary tumor cells into the general vasculature thus supporting the metastatic process. In fact, angiogenic inhibitors like bevacizumab, a VEGF antibody, are commonly used as an adjunct treatment option (e.g., Iwamoto et al., 2010).

Currently the pharmaceutical industry is employing two general approaches to block Met-dependent cellular activities (Eder et al., 2009; Liu X et al 2010). The first involves the development of single-arm humanized antibodies to HGF (Burgess et al., 2006; Stabile et al., 2008) or Met (Martens et al., 2006). The second approach being advanced is the use of "kinase inhibitors", which block the intracellular consequences of Met activation. These 'kinase inhibitors" are small hydrophobic molecules that work intracellularly to compete for the binding of ATP site to the kinase domain of Met thus inhibiting receptor autophosphorylation (Morotti et al., 2002; Christensen et al., 2003; Sattler et al., 2003). Despite the promise of the biologic and kinase-inhibitor approaches, which are currently represented in clinical trials, both have limitations arising from toxicity or specificity considerations and/or cost(Hansel et al., 2010; Maya, 2010).

A third approach, which our laboratory has been pursuing exploits a step in the actvivation process of the HGF-Met system; namely the need for HGF to pre-dimerize before it is able to activate Met. Thus we have targeted the dimerization process by developing molecules that mimic the dimerization domain, the hinge region, with idea that they can act as dominant negative replacements. Recent studies have validated this general approach demonstrating that molecules designed around angiotensin IV (Yamamoto et al, 2010) or the hinge sequence itself (

Kawas et al., 2011) can bind HGF, block its dimerization, and attenuate HGF-dependent cellular actions. The studies described herein represent a first step toward producing useful therapeutics targeted at HGF dimerization. The primary focus of this study was to improve the pharmacokinetic characteristics of a parent compound, Norleual (Yamamoto et al., 2010) while maintaining biological activity. To this end we successfully synthesized and evaluated a family of new molecules, the 6-AH family [D-Nle-X-Ile-NH-$(CH_2)_5$-COOH]. A subset of these molecules not only not had improved metabolic stability and circulating $t_{1/2}$ but exhibited excellent in vitro and in vivo activity.

In addition to characterizing a new family of HGF/Met antagonists, the present investigation demonstrated a qualitative relationship between the ability of a compound to bind HGF and block HGF dimerization and its observed in vitro biological activity. Moreover these studies provide initial structure-activity data and pave the way for more extensive evaluation. The chemical modifications that were made at the N- and C-terminals of the AngIV molecule and the resultant improvement in metabolic stability highlight the critical role played by exopeptidases in the metabolism of AngIV-derived molecules. The demonstrated importance of protecting the terminals to pharmacokinetic characteristics suggests numerous additional synthetic approaches that may be applicable including the insertion of non-peptide linkages (see Sardinia et al., 1996) between the first and second amino acids, the replacement of the N-terminal amino acid with a non-α amino acid, and N-terminal acylatio.

In sum these studies further validate the notion that targeting the dimerization domain of HGF is an effective means of inhibiting the HGF/Met system. Further they demonstrate that molecules with favorable pharmacokinetic characteristics can be produced thus highlighting their potential clinical utility.

3.6 References

Birchmeier C, Birchmeier W, Gherardi E and Vande Woude GF (2003) MET, METASTASIS, MOTILITY AND MORE, in Nature Reviews Molecular Cell Biology pp 915-925, Nature Publishing Group.

Borowiak M, Garratt AN, WÃ¼stefeld T, Strehle M, Trautwein C and Birchmeier C (2004) Met provides essential signals for liver regeneration. Proceedings of the National Academy of Sciences of the United States of America 101.

Chirgadze DY, Hepple JP, Zhou H, Byrd RA, Blundell TL and Gherardi E (1999) Crystal structure of the NK1 fragment of HGF/SF suggests a novel mode for growth factor dimerization and receptor binding. Nature Structural Biology 6.

Christensen JG, Burrows J and Salgia R (2005) Met as a target for human cancer and characterization of inhibitors for therapeutic intervention. Cancer Letters 225.

Danilkovitch-Miagkova A and Zbar B (2002) Dysregulation of Met receptor tyrosine kinase activity in invasive tumors. The Journal of clinical investigation 109:863-867.

Donate LE, Gherardi E, Srinivasan N, Sowdhamini R, Aparicio S and Blundell TL (1994) Molecular evolution and domain structure of plasminogen-related growth factors (HGF/SF and HGF1/MSP). Protein science : a publication of the Protein Society 3:2378-2394.

Ferraro D, Corso S, Fasano E, Panieri E, Santangelo R, Borrello S, Giordano S, Pani G and Galeotti T (2006) Pro-metastatic signaling by Met through RAC-1 and reactive oxygen species (ROS). ONCOGENE -BASINGSTOKE- 25:3689-3698.

Gherardi E, Sandin S, Petoukhov MV, Finch J, Youles ME, Ã”Fverstedt L-Gr, Miguel RN, Biundell TL, Vande Woude GF, Skoglund U and Svergun DI (2006) Structural basis of hepatocyte growth factor/scatter factor and MET signalling, in Proceedings of the National Academy of Sciences of the United States of America pp 4046-4051.

Halaban R, Rubin JS, Funasaka Y, Cobb M, Boulton T, Faletto D, Rosen E, Chan A, Yoko K, White W and et al. (1992) Met and hepatocyte growth factor/scatter factor signal transduction in normal melanocytes and melanoma cells. Oncogene 7:2195-2206.

Huh C-G, Factor VM, SÃ¡nchez An, Uchida K, Conner EA, Thorgeirsson SS and Woude GFV (2004) Hepatocyte Growth Factor/Met Signaling Pathway Is Required for Efficient Liver Regeneration and Repair. Proceedings of the National Academy of Sciences of the United States of America 101:4477-4482.

Kakazu A, Chandrasekher G and Bazan HE (2004) HGF protects corneal epithelial cells from apoptosis by the PI-3K/Akt-1/Bad- but not the ERK1/2-mediated signaling pathway. Investigative ophthalmology & visual science 45:3485-3492.

Kanda S, Kanetake H and Miyata Y (2006) HGF-induced capillary morphogenesis of endothelial cells is regulated by Src. Biochemical & Biophysical Research Communications 344.

Kawas LH, Yamamoto BJ, Wright JW and Harding JW (2011) Mimics of the dimerization domain of hepatocyte growth factor exhibit anti-met and anti-cancer activity. The Journal of pharmacology and experimental therapeutics. *(In-press)*

Liu X, Newton RC and Scherle PA (2010) Developing Met pathway inhibitors for cancer therapy: progress and challenges. Trends in molecular medicine 16:37-45.

Liu X, Yao W, Newton RC and Scherle PA (2008) Targeting the Met signaling pathway for cancer therapy. Expert opinion on investigational drugs 17:997-1011.

Lokker NA, Mark MR, Luis EA, Bennett GL, Robbins KA, Baker JB and Godowski PJ (1992) Structure-function analysis of hepatocyte growth factor: identification of variants that lack mitogenic activity yet retain high affinity receptor binding. The EMBO journal 11:2503-2510.

Maina F and Klein Rd (1999) Hepatocyte growth factor, a versatile signal for developing neurons. Nature Neuroscience 2.

Ratajczak MZ, Marlicz W, Ratajczak J, Wasik M, Machalinski B, Carter A and Gewirtz AM (1997) Effect of hepatocyte growth factor on early human haemopoietic cell development. British Journal of Haematology 99:228.

Rong S, Segal S, Anver M, Resau JH and Woude GFV (1994) Invasiveness and Metastasis of NIH 3T3 Cells Induced by Met-Hepatocyte Growth Factor/Scatter Factor Autocrine Stimulation. Proceedings of the National Academy of Sciences of the United States of America 91:4731-4735.

Sheth PR, Hays JL, Elferink LA and Watowich SJ (2008) Biochemical Basis for the Functional Switch That Regulates Hepatocyte Growth Factor Receptor Tyrosine Kinase Activation, in Biochemistry pp 4028-4038.

Stella MC and Comoglio PM (1999) HGF: a multifunctional growth factor controlling cell scattering. The international journal of biochemistry & cell biology. 31:1357-1362.

Thompson J, Dolcet X, Hilton M, Tolcos M and Davies AM (2004) HGF promotes survival and growth of maturing sympathetic neurons by PI-3 kinase- and MAP kinase-dependent mechanisms. Molecular and cellular neurosciences 27:441-452.

Wright JW, Stubley L, Pederson ES, Kramár EA, Hanesworth JM and Harding JW (1999) Contributions of the brain angiotensin IV-AT4 receptor subtype system to spatial learning. The Journal of neuroscience : the official journal of the Society for Neuroscience 19:3952-3961.

Yamamoto BJ, Elias PD, Masino JA, Hudson BD, McCoy AT, Anderson ZJ, Varnum MD, Sardinia MF, Wright JW and Harding JW (2010) The Angiotensin IV Analog Nle-Tyr-Leu-Ψ-CH2-NH2)3-4-His-Pro-Phe (Norleual) Can Act as a Hepatocyte Growth Factor/Met Inhibitor. The Journal of pharmacology and experimental therapeutics. 333:161.

Youles M, Holmes O, Petoukhov MV, Nessen MA, Stivala S, Svergun DI and Gherardi E (2008) Engineering the NK1 Fragment of Hepatocyte Growth Factor/Scatter Factor as a MET Receptor Antagonist. Journal of Molecular Biology 377.

Zhang YW and Vande Woude GF (2003) HGF/SF-met signaling in the control of branching morphogenesis and invasion. Journal of cellular biochemistry 88:408-417.

CHAPTER FOUR

NANOSCALE MAPPING OF THE MET RECEPTOR ON HIPPOCAMPAL NEURONS BY AFM (ATOMIC FORCE MICROSCOPY) AND CONFOCAL MICROSCOPY

4.1 Abstract

Hepatocyte growth factor (HGF), a neurotrophic protein, acting through its tyrosine kinase receptor, Met, facilitates learning, long-term potentiation, neurite outgrowth and provides neuroprotection against toxicants. In concert with the recognized role of the HGF/Met system in synaptic plasticity we demonstrate that Met is localized to brain regions, like the hippocampus and prefrontal cortex, which undergo extensive synaptic remodeling, and that Met activation results in an increase in dendritic spine density and functional synapses. Based on these functions we hypothesized that Met should be associated with post-synaptic elements found on dendritic spines where it would be positioned to perform its role as a determinant of synaptic connectivity. Thus, the ultimate focus of this study was to ascertain the sub-cellular localization of Met on hippocampal neurons and to distinguish between activated and non-activated Met receptors. Using atomic force microscopy (AFM) and an AFM tip coated with a specific Met antibody we mapped the location of activated and non-activated Met to different sub-cellular compartments of hippocampal pyramidal neurons. As anticipated, activated Met was found concentrated in the dendritic compartment while non-activated Met was prominent in the soma. Elucidating and comparing the detailed sub-cellular localization of activated and non-activated Met on hippocampal neurons derived from normal brains and brains from individuals with neurodegenerative disorders like Alzheimer's disease, may provide insights into Met's potential role in the synaptic dysfunction commonly observed.

4.2 Introduction

Hepatocyte growth factor (HGF), which was first recognized as a potent regulator of hepatocyte growth and survival (Borowiak, et al., 2004; Jiang, Hallett, & Puntis, 1993) mediates its cellular actions via the type I tyrosine kinase receptor Met (Halaban, et al., 1992). The HGF/Met system is now well recognized to support mitogenic, motogenic, morphogenic and anti-apoptotic activities in a variety of cells types (Matsumoto & Nakamura, 1997; Nakamura, Nawa, & Ichihara, 1984; Nakamura, et al., 1989). HGF is synthesized and secreted as an inactive pro-form. After secretion, it is cleaved by extracellular proteases to form the mature heterodimer, which consists of the 69 kDa α-chain and the 34 kDa β-chain (Naka, et al., 1992; Naldini, et al., 1992). This mature heterodimeric form of HGF further dimerizes to form the biologically active tetramer. Binding of the active form of HGF to Met induces receptor multimerize into its activated form and trans-tyrosine autophosphorylation activating multiple pathways to induce proliferation, differentiation, motility, and survival (Miller & Leonard, 1998; Naldini, et al., 1991; Rodrigues & Park, 1994). The combined impact of these HGF-dependent activities has proven critical for the development, maintenance, and repair of many peripheral organs and tissues.

Attention has recently expanded from the periphery to the involvement of the HGF/Met system in the brain where it has neuro-protective(Akimoto, et al., 2004; Date, et al., 2004; Hayashi, Abe, Sakurai, & Itoyama, 1998; Miyazawa, et al., 1998; Tyndall & Walikonis, 2007) and neuro-regenerative effects on many neuronal cell types including: hippocampal, cerebral cortical, midbrain dopaminergic, cerebellar granular, and sensory neurons as well as , motoneurons and

sympathetic neuroblasts (Honda, et al., 1995; Maina & Klein, 1999). HGF and Met are expressed in both the adult and developing central nervous system (Achim, et al., 1997; Maina & Klein, 1999; Matsumoto & Nakamura, 1997) where HGF is recognized as a neurotrophic factor (Hamanoue, et al., 1996; Honda, et al., 1995) that plays an essential role in the development, maintenance, and activity dependent modulation of the nervous system (Funakoshi, et al., 1995; Ibanez, 1998). In addition to its neuro-protective actions the HGF/Met system has been implicated as a crucial regulator of synaptic plasticity as evidenced by its role in learning and long-term potentiation, which is one of the major cellular mechanisms underlying cognitive processing and its ability to enhance dendritic sprouting (Tyndall & Walikonis, 2007). These HGF-dependent synaptic actions anticipate the localization of HGF and activated Met at functional synapses where they can regulate the synaptic reorganization requisite for plasticity. As initial test of this prediction we show that Met is present in those areas of the brain most noted for their involvement in processes that require extensive neural plasticity, like learning. In addition we demonstrate that, as expected, HGF supports synaptic remodeling as evident by its capacity to induce dramatic increases in the number of dendritic spines present on cultured hippocampal neurons. These findings further predict that activated Met should be localized to postsynaptic densities found on dendritic spines.

In order to evaluate this hypothesis we have for the first time used atomic force microscopy (AFM), a techniques that enables a high resolution assessment of protein-protein interactions, to probe the sub-cellular location of a growth factor receptor; in this case Met on hippocampal neurons. The specificity of the interactions between the Met receptor and its antibody was exploited to map the localization of Met on neuronal cell surfaces. Numerous groups have effectively utilized AFM to quantifying the interaction forces between

complementary biomolecular pairs, such as those observed between an antigen and its specific antibody (Allen, et al., 1997; Binnig & Quate, 1986; Dammer, et al., 1996; Hinterdorfer, Baumgartner, Gruber, Schilcher, & Schindler, 1996; Ros, et al., 1998).

The growing popularity of AFM to quantify bimolecular interactions and provide high resolution topographic information is based on several inherent advantages that it has over standard microscopic techniques. First, AFM is capable of providing high spatial resolution-three dimensional images of localized proteins on cells. Second, AFM has made it possible to calculate physical parameters in biological samples, such as intramolecular and intermolecular forces associated within the biological systems (Florin, Moy, & Gaub, 1994; Hinterdorfer, et al., 1996; Hinterdorfer & Duáfrne, 2006; Lee & Chrisey, 1994). Finally, AFM has the unique capacity to measure adhesion events that result from individual molecular interactions in liquid environments and is thus capable of mimicking the in vivo physiological conditions.
In this study, we have used a Met antibody functionalized AFM tip to probe the pattern of Met distribution and association on hippocampal neuronal cells. As anticipated, Met was found to be differentially localized at the dendrites when compared to the soma regions of the neurons. Moreover, the higher force measurements recorded at the dendrite, when compared to the soma, are consistent with target multimerization, which for Met would indicate the presence of the activated form.

4.3 Material & Methods

Hippocampal Cell Culture Preparation. Hippocampal neurons ($2x10^5$ cells per square cm) were cultured from P1 Sprague Dawley rats over coverslips coated with poly-L-lysine from

Sigma (St.Louis, MO; molecular weight 300,000) and placed in a 24 well culture plates. Neurons were maintained in Neurobasal A media from Invitrogen (Carlsbad, CA) supplemented at 2 days *in vitro* with B27 from Invitrogen, 0.5 mM L-glutamine, and 5mM cytosine-D-arabinofuranoside from Sigma then an additional 3–7 days to enable dendrites to mature and specify. At that point dendritic proteins will translocate from the cell soma to their functional location at the dendrites. Next cells were either treated with HGF (R&D Systems Inc. Minneapolis, MN) and then fixed for twenty minutes at room temperature for immunocytochemistry using a mixture of 4% paraformaldehyde, 3% sucrose, 60 mM PIPES, 25 mM HEPES, 5 mM EGTA and 1 mM $MgCl_2$ at pH 7.4), or fixed using the same mixture above for 0.5-1 minutes and prepared for AFM analysis as will be described later.

Transfection/ Spine Quantitation. Neurons were transfected with mRFP-β-actin on day *in vitro* 6 (DIV6) using LipofectAMINE 2000 (Invitrogen) according to the manufacturer's protocol. This protocol yielded the desired 3-5% transfection efficiency thus enabling the visualization of individual neurons. Higher efficiencies obscured the dendritic arbor of individual neurons. Expression of fluorescently tagged actin allowed clear visualization of dendritic spines, as dendritic spines are enriched in actin. On DIV7 the cells were treated with vehicle (H_2O) or HGF (as described in the text) which was added to media. On DIV12 the neurons were fixed (4% paraformaldehyde, 3% sucrose, 60 mM PIPES, 25 mM HEPES, 5 mM EGTA, 1 mM $MgCl_2$, pH 7.4) for 20 min at room temperature and mounted.

Slides were dried for at least 20 hours at 4°C and fluorescent images were obtained with Slidebook 4.2 Digital Microscopy Software driving an Olympus IX81 inverted confocal microscope with a 60X oil immersion lens, NA 1.4 and resolution 0.280 μm. Dendritic spine density was measured on primary and secondary dendrites at a distance of at least 150 μm from

the soma. Five 50 μm long segments of dendrites from at least 10 neurons were analyzed for each data point reported. Each experiment was repeated at least three times using independent culture preparations. Spines were manually counted.

Gel Electrophoresis and Western Blotting. Tissue extracts prepared from tissue taken from different regions of the brain were quantified for protein concentration using the BCA (Bicinchoninic acid) method (Pierce, Rockford, IL) and subsequently adjusted to match the protein concentration of the most dilute sample. Equal volumes of samples were then mixed with SDS-PAGE (sodium dodecyl sulfate polyacrylamide gel electrophoresis) buffer and boiled for 10 minutes before loading onto 4-12% Bis-Tris pre-cast gels (Invitrogen, Carlsbad, CA) for electrophoresis. After electrophoresis, proteins were transferred onto PVDF (Polyvinylidene Fluoride) membranes (Bio Rad, Hercules, CA) and blocked with AquaBlock™ (New England Biolabs, Ipswich, MA) for one hour at room temperature (RT). Primary antibody incubation was done in AquaBlock™ with rabbit anti-Met (1:1000, Millipore, Billerica, MA) overnight at 4°C. Alternating washes were done with PBS (Phosphate buffered saline) and PBST (Phosphate buffered saline-Tween) to remove excess and non-specific binding of the primary antibody. Secondary antibody (IRDye) (Rockland, Gilbertsville, PA) incubations were done in AquaBlock™ for one hour at RT. Western blots were imaged using LI-COR Odyssey Infrared Imaging System (LI-COR Biosciences, Lincoln, NE).

Immunocytochemistry. Hippocampal neurons were treated with 10ng/ml HGF or with the vehicle PBS and fixed as described above. Following fixation, cells were rinsed in PBS, permeabilized with 0.1% Triton X-100 detergent (Bio-Rad; Hercules, CA), rinsed twice with PBS, and blocked with 8% bovine serum albumin (Intergen Company; Burlington, MA) in PBS for one hour. Cells were again rinsed with PBS, followed by a 24 hour incubation period at 4°C

with primary anti-rabbit phospho-Met (Tyr1234/1235) (Cell Signaling Technology, Danvers, MA). Subsequently, cells were rinsed 3 times with PBS, incubated for two hours at RT in Alexafluor 488 goat-anti-rabbit antibody (Invitrogen: Carlsbad, CA) following the manufacturer's protocol. Cells were then finally rinsed in PBS and mounted on slides with ProLong Gold anti-fade reagent (Invitrogen; Carlsbad, CA). Fluorescent images were obtained with Slidebook 4.2 Digital Microscopy Software driving an Olympus IX81 inverted confocal microscope with a 60X oil immersion lens, NA 1.4.

AFM Tip Functionalization with Anti-Met Antibody. To study the distribution of Met proteins on neuronal cell surfaces, a Met monoclonal Met antibody (mAB Met) was chemically bound to an AFM gold-coated silicon nitride Si_3N_4 tip and substrate as described below. Si_3N_4 cantilevers (Bruker Corp., Bruker AXS Inc., Santa Barbra, CA) and disks (Ted Pella Inc., Redding, CA) were sputter-coated with a 5nm Cr adhesive layer followed by 40 nm of gold using a BOC Edwards Auto 306 sputter system under 2×10^{-7} Torr. The gold-coated cantilevers and disks were then cleaned sequentially in ethanol and deionized water (18 MΩ.cm) before drying in a stream of N_2 gas. ω-substituted alkanethiolated self-assembled monolayers (SAMs) of 16-mercaptohexadecanoic acid (MHA) (Aldrich, Milwaukee, WI) were deposited on the gold-coated cantilevers and disks *via* a thiol-gold linkage by incubation in a saturated 1mM solution of MHA dissolved in dimethylformamide (DMF) for 30 minutes. To remove any low affinity associated multilayers the cantilevers were washed with ethanol. Terminal COOH groups in the MHA SAM layer were activated by reacting them sequentially with 0.1 M N-hydroxysuccinimide (NHS) (Aldrich, St. Louis, MO) and 0.4 M 1-[3-(dimethylamio)propyl]-3-ethylcarbodiimide (EDC) (sigma-Aldrich, St. Louis, MO) in deionized water for 30 minutes each at room temperature. Si_3N_4 cantilevers and disks were then incubated with 25µg/ml of mAb Met

(Millipore, Billerica, MA) for one hour to allow for amine coupling. After incubation, surfaces were rinsed and kept hydrated in PBS solution and stored at 40ºC until use. The successful functionalization of the COOH-activated Si_3N_4 disks with mAb Met was confirmed *via* high-resolution AFM imaging acquired with a bare silicon nitride tip (**Figure 4.1A**). As shown in Figure 1A, a layer of the antibody (bright spots, size ranges from 7.5-15 nm) was shown to homogeneously cover the gold substrate, in contrast to the bare substrate. The contrast and sizes of our antibody in the acquired AFM images is similar to other reports of pure antibodies modified on a substrate in a similar manner (San Paulo and GarcÃ-a, 2000; Mart et al., 2008). The presence of antibodies on the chemically modified Si_3N_4 disks using the same protocols employed to functionalize the Si_3N_4 cantilevers assured the successful functionalization of our cantilevers with the mAB Met. Further confirmation of the chemical functionalization of the AFM cantilevers with the mAB Met was established *via* force measurements as described below.

Atomic Force Microscopy. All AFM experiments were performed with a PicoForce™ scanning probe microscope with Nanoscope IIIa controller and extender module (Bruker Corp., Bruker AXS Inc., Santa Barbara, CA). The force constant of each cantilever was determined at the beginning of each experiment based on the power spectral density of the thermal noise fluctuations in Hanks balanced salt solution (HBSS). On average, the spring constant for the mAB Met functionalized cantilevers was found to be 0.09 ± 0.01 N/m ($n = 3$). Prior to force measurements, hippocampal neurons were imaged using mAB Met functionalized cantilevers and bare cantilevers (control) in TappingMode™ under HBSS at a scan speed of 0.5 Hz at a resolution of 256 pixels per line and 256 lines per image (**Figure 4.1B**). Real-time images were used to locate the cells, ensure the population homogeneity, and correct cellular morphology. Once a cell had been located *via* topographical scanning, the oscillation of the cantilever was

stopped and the extending and retracting deflection-displacement curves were recorded on fifteen cells taken from two different cultures (3-7) days old. For each neuron investigated, multiple points contact points covering the soma and dendritic regions of the neuron were selected for force measurements using the point and shoot feature of the AFM software (**Figure 4.1C**). Retraction curves were measured at a rate of 580 nm/sec to minimize hydrodynamic drag forces (Cox, 2007) and a resolution of 4096 points. 300-600 nm ramp sizes were generally used during force measurements.

Analysis of Retraction Curves. Retraction curves are generally used to quantify the adhesion strength and interaction specificity between two given surfaces. In our study, adhesion forces were measured between a mAb-Met modified tip and its Met receptor on the neuron surface as well as between a bare Si_3N_4 cantilever and cell surfaces (control). As the mAB-Met modified tip scanned specific locations on cell surfaces (**Figure 4.1C**), retraction curves such as that shown in Figure 2 were recorded and further analyzed to identify the location of the Met proteins on various regions of the neuronal cell surfaces. In general, retraction curves recorded between the mAB-Met cantilever and cell surfaces displayed multiple adhesion peaks, confirming the chemical modification of the cantilever with the Met monoclonal antibody. The retraction curves typically started with adhesion peaks characterized with forces on the order of several nano-Newton's (**Figure 4.2 A** black line). These forces were considered nonspecific forces resulting from non-covalent interactions measured between the chemically modified tip and various species on the cell surface. These high adhesion forces lacked a distinct snap-off point, characteristic of nonspecific interactions. Forces quickly decreased to magnitudes less than 0.5 nN (**Figure 4.2A** red line) indicating specific forces resulting from the successful binding of a mAB-Met to its Met receptor or multiple receptors on the neuronal cell surface (**Figure 4.1D**).

The location at which a specific binding is detected indicates the presence of Met protein at that point on the cell surface. By comparing the force curves of Met-antibody functionalized tip to the control force curves and to previous reports we predicted that the most probable individual unbinding force between single antibody and a Met molecule to be equal to a modal value= 0.05 nN. The appearance of force peaks equal to integer multiples of .05 nN and the absence of these peaks in the control curves indicated that 0.05 nN is the likely binding force between a single mAB-Met molecule and a single Met protein. Typical intermolecular specific binding forces in the literature have been reported to fall in the range of 10^{-11} to 10^{-9}N. The predicted 0.05 nN binding force between Met and a Met-antibody falls well within this range. In analogous AFM studies: Lehenkari and Horton projected a binding force of 0.127 nN between F11 antibody and the avβ3 integrin dimer (Lehenkari and Horton, 1999); Osada et al. estimated a binding force of 0.05 nN between lectin and GalNAc (Osada et al., 1999); and, Gad et al. stated the interaction force between concanavalin A and mannose to be in the range of 0.075–0.2 nN(Gad et al., 1997).

In comparison, force curves that were measured between a bare Si_3N_4 cantilever and cell surfaces displayed no adhesion forces 63% of the time and retraction curves were featureless displaying profiles fluctuating around zero force. This is an indicative of the repulsive force expected between the negatively charged bare Si_3N_4 cantilever and the negatively charged cell surface (**Figure 4.2 B**). The rest of the curves had peaks in the non-specific range (**Figure 4.2 C**), similar to the non-specific range of the functionalized cantilever (**Figure 4.2 A** black line), thus confirming the non-specificity of these unbinding peaks. Curves from the controls revealed peaks in the specific range with a modal value= 0.125 nM. More importantly none of them exhibited a specific force of 0.05 nN or multiples of this force. Another characteristic that

differentiated specific and non-specific interactions was that the later lacked the featured shape and slope of a specific interaction (**Figure 4.2A** red line).

Modeling of Retraction curves: Statistical Distributions of Adhesion Affinities. The adhesion affinities between the Met-mAb functionalized cantilever and the Met proteins distributed on the neuronal surfaces were distributed over a wide range due to the heterogeneous nature of the neuronal cells. A log-normal probability distribution function with four fitting parameters was applied to the adhesion affinity data. The log-normal asymmetric probability peak distribution is described as the single-tailed probability distribution of any random variable whose logarithm is normally distributed (Aitchison and Brown, 1957). The log-normal distribution of the adhesion forces (F) is described by

$$f(a,b,c,d) = a + b\exp\left(\frac{-(\ln F / c)^2}{2d^2}\right) \qquad (1)$$

where a is the intercept of the log-normal distribution, b is the amplitude of the distribution and predicts the maximum probability of occurrences, c is the adhesion force with the maximum probability, and d is a fitting parameter that indicates the width of the distribution function. Sigma Plot version 10.0 (Systat software, Inc., 2006) was used to estimate the fitting parameters and the quality of the fit for all data sets.

Statistical Description of AFM Data. Statistical tests were used to determine if the adhesion strength is different among the soma and dendrites regions of the neuronal cells. The non-parametric group comparisons Dunn's ranks test available in Sigma Stat 2.03 (Jandel Scientific) was applied to the data.

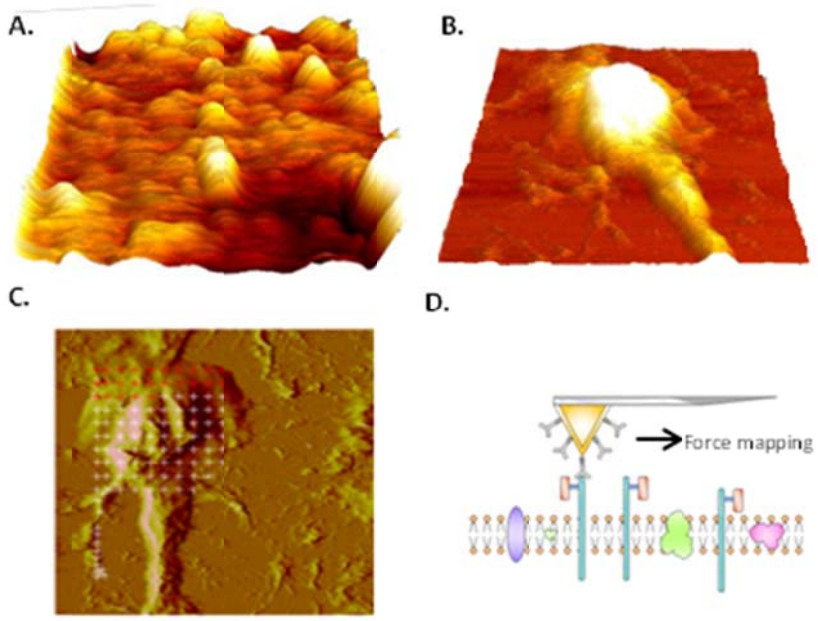

Figure 4.1: Experimental setup: tip functionalization and force mapping. (**A**) 3D high resolution TappingMode image of a COOH-activated Si3N4 disk with a monoclonal antibody against Met. The image is 500X500 nm^2 and 7.5 nm high. (**B**) 3D height Tapping Mode image of a hippocampal neuronal cell attached to poly-L-lysine coated coverslip. The image is 50X50μm^2 and 2.5 μm high (**C**) A representative example of how points are selected for force measurements. The image shows standard grid selection for locations on soma where force measurements were performed. (**D**) A schematic representation of how a Met receptor can be identified on hippocampal neurons cells membranes using a Met antibody-modified AFM tip.

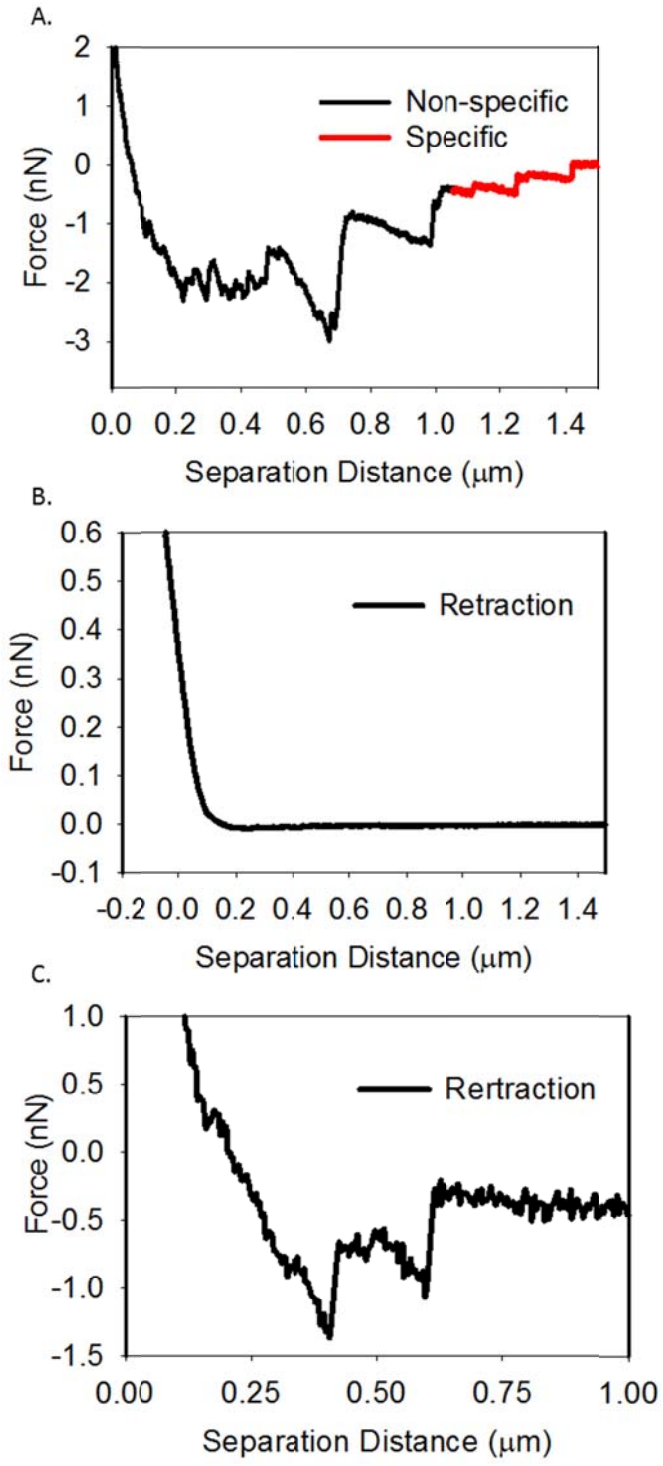

Figure 4.2: Retraction force-distance curves. Each peak in the retraction curve has two coordinates (pull-off distance /separation distance, pull-off force). The pull-off distance indicates the location at

which the cantilever contacted the neuronal cell surface. The pull-off force is equivalent to the adhesion force and represents the sum of all interaction forces between the neuronal cell surface and the AFM cantilever. The baseline for each peak was taken at zero force and only peaks that had magnitudes larger than 0.025 nN were counted. The 0.025 nN value was chosen as the force limit since it represents the minimal force that could be clearly identified with the resolution of our microscope. (**A**) Force-distance curve from Met-mAb decorated AFM cantilever. Black peaks represent non-specific events, while read peaks are the predicted specific interaction between Met-mAb and cell surface Met. (**B**) Force distance curves from a control experiment using a bare AFM cantilever, 63% of all the force-distance curves from bare cantilevers showed no peaks and curves fluctuated around zero force. (**C**) Depicts non-specific interactions between the bare cantilevers and the cell surface similar to the first part (black peaks) in (**A**). None of the curves recorded from the control experiment exhibited similar specific adhesion forces as those seen in the red part of (**A**).

4.4 Results

***Distribution and Activation of Met Expressed in Rat Brain Regions*.** We show here that Met is expressed in the cerebellum, cortex, mid-brain, hippocampus, and the prefrontal cortex (**Figure 4.3**). In addition to confirming the localization of Met to brain regions critical for directing processes like learning and memory consolidation that require synaptic remodeling, these data demonstrate the high specifically of the monoclonal Met antibody used in subsequent studies. The blot presented depicts a single species with a molecular weight of approximately 185 kDa, corresponds to the molecular weight of Met.

The functionality of the Met tyrosine kinase receptor expressed in the hippocampal neurons used for the AFM study was evaluated. Cultures were treated with 10 ng/ml HGF and

stained for phospho-Met (**Figure 4.4**) using a validated anti-phospho-Met antibody (Kawas et al., 2011). Figure 4B indicates that phospho-Met is present in the culture and that application of 10 ng/ml HGF appears to induce a general increase in Met phosphorylation.

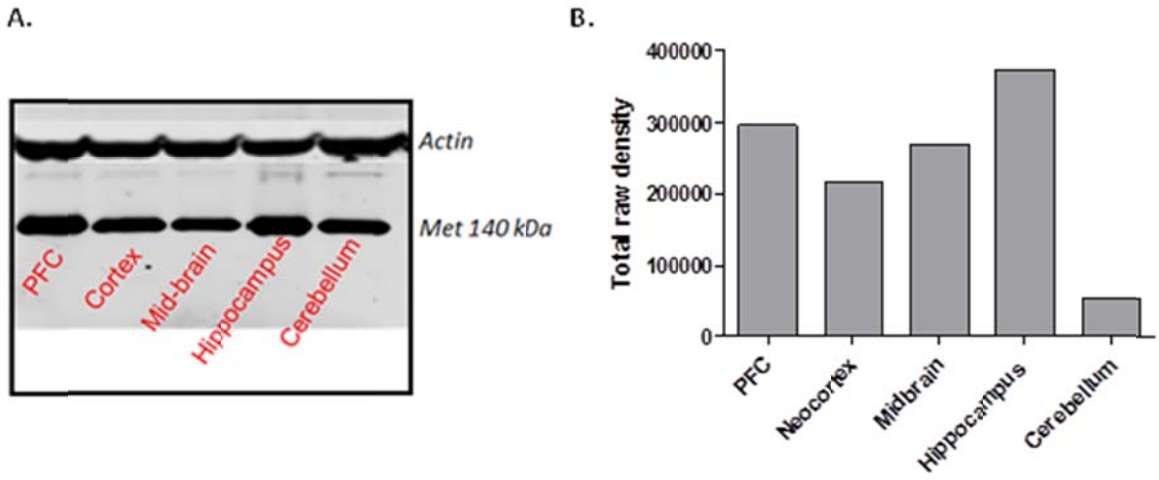

Figure 4.3: Distribution of Met in the rat brain. (**A**) A representative blot of the brain samples probed against Met with actin serving as a loading control. (**B**) Quantification of the Met protein in various brain regions. Equal amounts of protein were loaded in each lane based on BCA protein determinations.

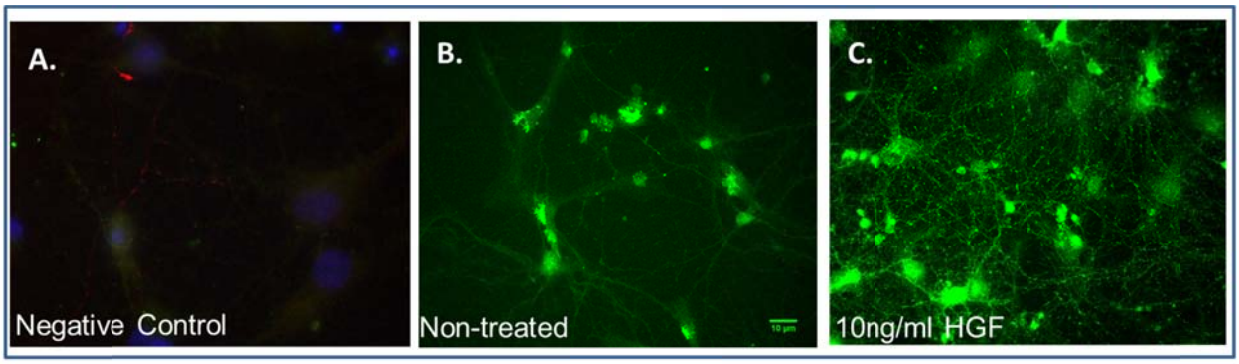

Figure 4.4: Distribution of phospho-Met in the dissociated neuronal hippocampal cultures. Representative confocal microscopy fluorescent images of immunocytochemistry images against phospho-Met are shown. (**A**) Negative control stain only secondry anti-serum (**B**) Control receiving only vehicle (PBS) and (**C**) HGF-treated Hippocampal neuronal cultures. Note that prominent dendritic staining following the addition of endogenous HGF.

Density of Dendritic Spines on Dissociated Hippocampus Neurons Following HGF Application. To further establish the functionality of Met in the neuronal cultures and to demonstrate that activation of Met has physiological consequences relevant to its purported role as a modulator of synaptic plasticity we examined the impact of HGF application on the number of dendritic spines apparent on the cultured neurons. Not surprisingly, hippocampal neurons treated with 10ng/ml HGF induced the production of new dendritic spines resulting in a significantly higher density of spines ($P<0.001$) than that observed on non-treated control neurons (**Figure 4.5**). The functionality of these new spines and by association the dendritic Met receptors was verified by demonstrating a concomitant increase in the frequency of miniature excitatory postsynaptic currents (data not shown). The presence of significant numbers of spines in neurons that were not treated with exogenous HGF and the presence of phospho-Met on untreated neurons (**Figure 4.4**) is consistent with the presence of HGF in control cultures

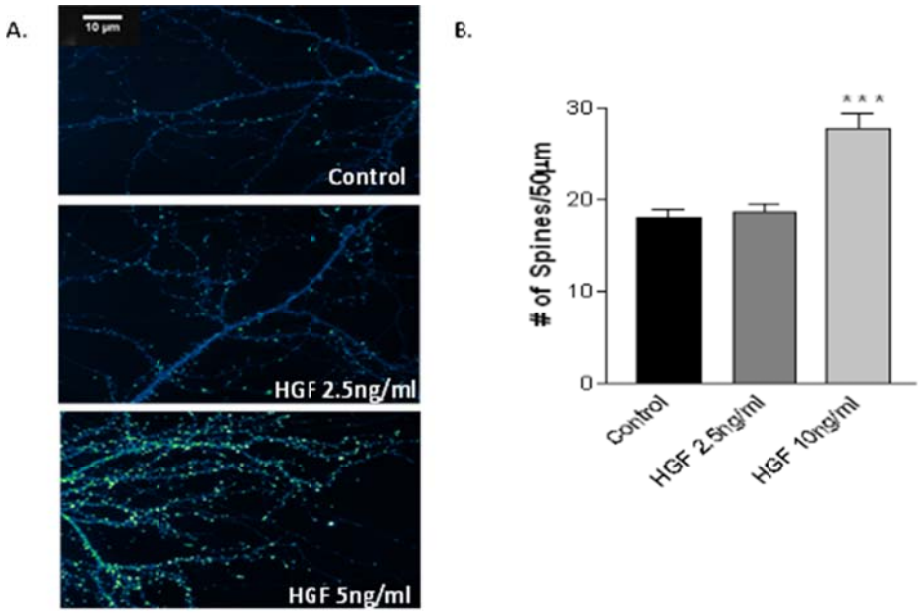

Figure 4.5: HGF-dependent Induction of dendritic spines in dissociated hippocampus neuronal cultures. Dissociated hippocampal neurons from 1 or 2 day old rats were transfected with mRFP-β-actin and stimulated with HGF for 5 days. (**A**) Representative confocal microscopy fluorescent images for the control and treatment groups. Control groups which only received the vehicle (PBS), show the basal level of spine formation. Treatment with 2.5 ng/ml HGF did not affect basal spine numbers and was considered sub-threshold. Treatment with 10 ng/ml significantly increased the number of functional synapse. N=50; Mean +/- SEM; *** P<0.001.

Distribution of Adhesion Forces. Biological surfaces are inherently heterogeneous due to topographic variability and their unequal distribution of membrane constituents. This complexity is exemplified by the wide range of adhesive forces (0.025-0.5 nN) that are observed for neuronal dendrites and somas. This unevenness in adhesive force is evident in Figure 6 where variability manifests as broad force probability distribution curves. **Figure 4.6 A**, which shows the distribution of specific forces on the dendrites, indicates that the distribution of the

magnitude of the forces is quite evenly distributed over the force range with a modal value of .05 nN. Multiples of the 0.05 nN force, which appear as intermediate peaks on the histogram are consistent with forces generated by multiple antibody-Met interactions. Forces corresponding to 0.1, 0.2, and 0.3 nN could be interpreted to represent the presence of Met dimers, tetramers, and hexamers. Unlike the even distribution of forces evident at the dendrites the force probability distribution for specific interactions on the cell soma (**Figure 4.6B**) indicates a marked skew with most of the forces concentrating at the lower force range. Unlike the dendrites no intermediate peaks are represented at the higher multiples of 0.05 nN on the somas suggesting that the dimers and multimers that dominate the dendrites are absent from cell somas. Together these data indicate that higher forces, including those that are multiples of the unitary 0.05nN, are more concentrated on the dendrites. This suggests that these higher forces measured on the dendrite correspond to multiple antibodies-Met interactions, indicative of the selective presence of activated Met aggregates.

Figure 4.6 D-F shows the probability distributions for the non-specific range of adhesive forces. Unlike the specific forces described above the observed distributions of non-specific forces appear similar for the dendrites and somas with both possessing a negative skew (1-2 nN). These forces result from the non-specific binding of components of the extracellular matrix, membranous, and cytoskeleton elements to the cantilever. Although the total non-specific force is significantly greater than the specific force generated between Met and its antibody, it should be noted that the non-specific force is a summed force that is represents the conglomeration of vast numbers of low affinity interactions.

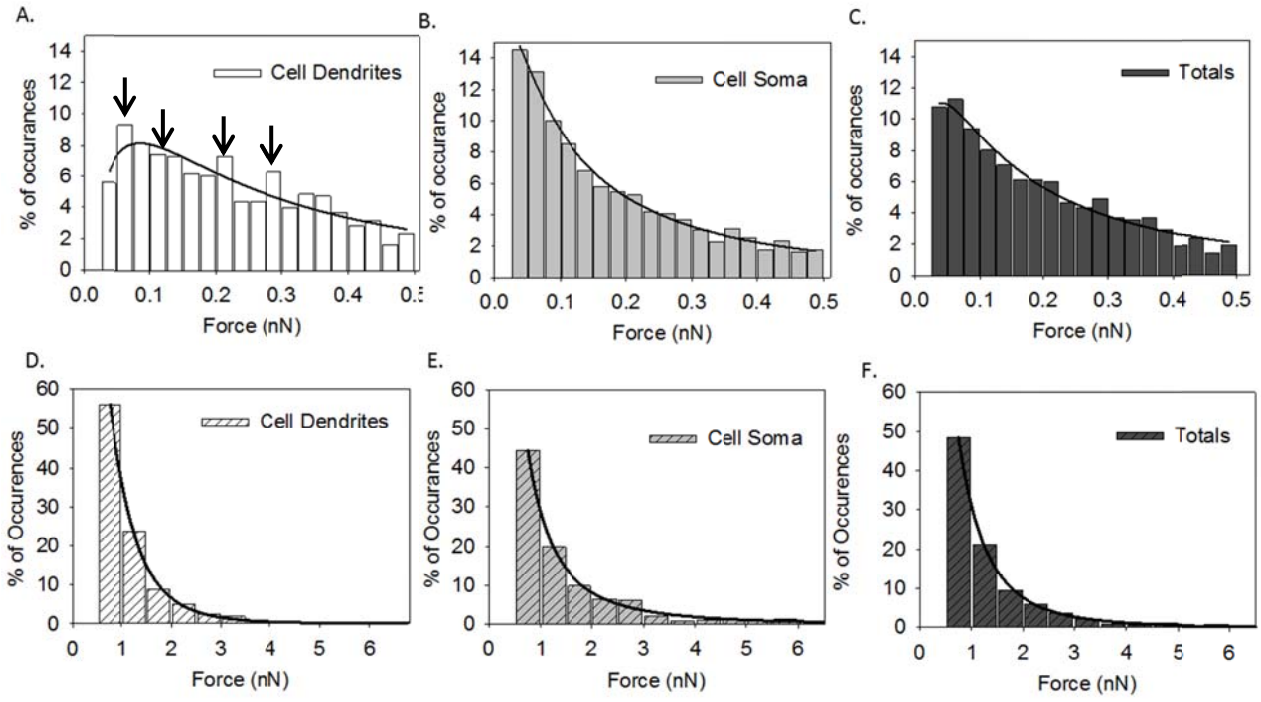

Figure 4.6: Force measurements between Met-antibody modified tips and the cell-surfaces of hippocampal neuronal cells. (**A**) Specific forces detected from the neuronal dendrites only, numerous recording were multiples of 0.05 nN, signifying accumulation of Met at local regions in the dendrites. (**B**) Specific forces recorded from the neuronal soma only. Most of the forces are at the lower range indicating a monomeric confirmation for Met. (**C**) Total specific forces recorded from hippocampal neurons membranes arrows denote unitary force, 0.05 nN and multiples at 0.10nN, 0.20nN, and 0.3nN which are postulated to represent dimeric, tetrameric, and hexameric forms of Met respectively. (**D-F**) Nonspecific adhesion forces for the total, cell soma and dendrites respectively.

Table 4.1 indicates the number of cells and dendrites used in this study, the number of peaks analyzed, and the average, median, mode, and range for the specific analyzed peaks. The means of specific forces from the dendrites is statistically different from the mean of the specific forces measured for the soma cell bodies of the neurons (***P≤ 0.001). This difference not only emphasizes the differential distribution of Met but also indicates a difference in the mechanical properties of the surfaces of the soma cell body and the dendrites. Despite the localization of Met

multimers in the dendrites the density of total Met receptor in the various cellular compartments was not directly addressed. Nevertheless, given the far greater area of a typical hippocampal soma in comparison to its dendritic area (Henze et al., 1996) and the frequency that adhesive events were encountered during force measurements in the somas and dendrites, it was our impression that the density of Met, regardless of it polymeric structure, was far greater in the dendrite than in the soma.

Table 4.1: A summary of AFM force-distance retraction data measured between cantilevers decorated with Met-mAb and Met distributed on the cell-surfaces of hippocampal neuronal cells in HBSS.

	Total (Cell Body +Dendrites)	**Cell Body**	**Dendrites**
# of Cells	15	15	41
# of peaks	3094	2081	1013
Average	0.15	0.12	0.20
Median	0.11	0.08	0.18
Mode	0.05	0.03	0.05
Range	(0.025- 0.5)	(0.025- 0.5)	(0.025- 0.5)

4.5 Discussion

The primary goals of this study were to evaluate the utility of AFM as a tool for mapping the neuronal localization of receptor proteins, determining their polymeric structure, and independently verifying the localization of an activated receptor on postsynaptic elements found on dendrites. The model system of choice for these studies was the hepatocyte growth factor/Met system, which has become a recent focus of our laboratory group(Yamamoto et al., 2010; Kawas et al., 2011). Our interest in the HGF/Met system stems from its increasingly recognized role in synaptic plasticity (Lim and Walikonis, 2008) and its anticipated localization to postsynaptic elements that are concentrated on neuronal dendrites(Frotscher et al., 2000; Calabrese et al., 2006). Several preliminary studies were carried out to solidify this expectation. First we used Western blotting methods to demonstrate a broad distribution of Met protein in the brain including brain areas known to be sites of extensive synaptic remodeling (Foster, 1999). To support the predicted localization of activated (phosphorylated) Met to dendrites, cultured hippocampal neurons were stimulated with HGF and probed for phospho-Met. As expected this study revealed an extensive distribution of phospho-Met on these neurons including their dendritic trees. Finally, in an attempt to both verify the physiological significance of these dendritic Met receptors and link their activation to synaptic plasticity we demonstrated that their activation by HGF produced a marked increase in the number of dendritic spines.

With the results of these initial studies supporting the predicted localization of Met on dendrites the AFM studies were initiated. The expected outcomes of these studies were: 1) to provide a quantitative description of Met distribution throughout the neuron; 2) to demonstrate the preferred localization of activated Met at the dendrites; 3) to elucidate the polymeric structure of these dendritic receptors; and 4) to compare the structure of dendritic Met to Met found on

neuronal soma. Using AFM we were able to show that Met is distributed on both the dendrites and the soma of the neuron but that the character of the adhesive force measured on the dendrites and soma were much different from one another. Most notably the force distribution data from the dendrite revealed a broad pattern of forces that were characterized by intermediate peaks at 0.1, 0.2, and 0.3nN; a pattern not found on the soma. Interestingly, these higher forces were exact multiples of the minimum force measured, 0.05nN. This pattern of forces suggests that 0.05nN is the unitary force generated between a single Met protein and a single anti-Met antibody on the cantilever. Even more intriguing is the possibility that the 0.05nN multiples result from the interaction of anti-Met antibodies with dimeric, tetrameric, and hexameric forms of Met, which may represent activated Met. While it is well appreciated that HGF induces Met dimerization, which is required for downstream intracellular signaling (Tolbert et al., 2007), the presence of larger defined and prominent multimeric forms of Met represents a novel observation.

Force distribution histograms indicate that the vast majority of Met found outside the dendrites is in a monomeric conformation and is thus inactive. This result was also expected and suggests that Met found in the soma is being synthesized and processed before transport to the dendrites and is still in its momomeric inactive form. These observations generate many additional questions that beg to be explored. For example: 1) Are there functional differences among the various multimers regarding their ability to modulate intracellular signaling cascades? 2) Is the pattern of multimers dependent upon the concentration of HGF or the presence of various co-receptors? And 3) is the spatial distribution of specific multimers different from one another?

As stated above, the appearance of adhesive forces that are multiples of 0.05nN allows us to tentatively assign 0.05 nN as the unitary specific binding force. A comparison of these experimental results with the force values for specific interactions between various biomolecular pairs reported by others indicates that the 0.05nN measured here falls within the reported force range of of 10^{-11} to 10^{-9}N(Reddy et al., 2004); additionally supporting our contention that the unitary specific binding force measured between a single Met protein and its antibody is 0.05nN. Forces smaller than 0.03 most probably result from weak non-covalent interactions between the cantilever tip and the cell surfaces (i.e., Van der Waals and hydrogen bonding forces) while forces greater than the upper limit most likely corresponding to multiple binding events.

A characteristic of cell surfaces, especially after cells have been collapsed by drying, is their heterogeneity. This variability, which can be attributed to the differential distribution of molecules on the membrane surfaces; the indentation to the cell membrane; inconsistent cytoskeletal structure; and a highly changeable extracellular matrix, is reflected in non-specific adhesion force heterogeneity. This heterogeneity is even more pronounced when dealing with of the specific Met interactions because the structural features of Met change with the level of activation. As indicated previously when HGF binds to its tyrosine kinase receptor Met it induces receptor dimerization and/or multimerization. Additionally, the level of processing of the Met receptor or the stage of maturation of the protein structure, and the degree of membrane incorporation may affect the antibody interaction with Met.

Although very labor intensive, one of the potential outcomes of an AFM evaluation is the generation of three dimensional force maps. It is our ultimate intention to generate this type of map for the distribution of Met on hippocampal neurons. Moreover, it is possible to map a single force level, like those proposed to be associated with Met in its dimeric, tetrameic, or hexameric

arrangement; thus addressing question (3) posed above. Additional future studies that are planned include probing with an antibody that binds phospho-Met and simultaneously probing for other proteins that may be physically or functionally linked to Met. These data should provide independent validation of some of the conclusions that were drawn from this initial study and detail the topographic relationship between Met (or specific mutlimeric forms) and protein interactors.

In sum we have used AFM to demonstrate the differential localization of Met multimers to the dendrites of rat hippocampal neurons. The distribution of these multimers, which we postulate to represent "active" forms of the receptor, in the dendrites and the ability of HGF to stimulate the growth of dendritic spines supports a role for the HGF/Met system as a regulator of synaptic remodeling and function. Furthermore this study highlights the potential utility of AFM to quantitatively address difficult questions regarding the sub-cellular distribution, structural form, and ultimately functional significance of receptor proteins.

.

4.6 References

Achim CL, Katyal S, Wiley CA, Shiratori M, Wang G, Oshika E, Petersen BE, Li JM and Michalopoulos GK (1997) Expression of HGF and cMet in the developing and adult brain. *Brain research. Developmental brain research* **102**:299-303.

Aitchison J and Brown JAC (1957) *The Lognormal Distribution, with Special Reference to its Use in Economics*. Cambridge University Press, New York

Akimoto M, Baba A, Ikeda-Matsuo Y, Yamada MK, Itamura R, Nishiyama N, Ikegaya Y and Matsuki N (2004) Hepatocyte growth factor as an enhancer of nmda currents and synaptic plasticity in the hippocampus. *Neuroscience* **128**:155-162.

Allen S, Chen X, Davies J, Davies MC, Dawkes AC, Edwards JC, Roberts CJ, Sefton J, Tendler SJ and Williams PM (1997) Detection of antigen-antibody binding events with the atomic force microscope. *Biochemistry* **36**:7457-7463.

Binnig G and Quate CF (1986) Atomic Force Microscope. *Phys. Rev. Lett. Physical Review Letters* **56**:930-933.

Borowiak M, Garratt AN, WÃ¼stefeld T, Strehle M, Trautwein C, Birchmeier C and Wigler MH (2004) Met Provides Essential Signals for Liver Regeneration. *Proceedings of the National Academy of Sciences of the United States of America* **101**:10608-10613.

Calabrese B, Wilson MS and Halpain S (2006) Development and regulation of dendritic spine synapses. *Physiology (Bethesda, Md.)* **21**:38-47.

Cox MG (2007) The area under a curve specified by measured values. *Metrologia* **44**:365-378.

Dammer U, Hegner M, Anselmetti D, Wagner P, Dreier M, Huber W and GÃ¼ntherodt HJ (1996) Specific antigen/antibody interactions measured by force microscopy. *Biophysical journal* **70**:2437-2441.

Date I, Takagi N, Takagi K, Kago T, Matsumoto K, Nakamura T and Takeo S (2004) Hepatocyte growth factor improved learning and memory dysfunction of microsphere-embolized rats. *Journal of neuroscience research* **78**:442-453.

Florin EL, Moy VT and Gaub HE (1994) Adhesion forces between individual ligand-receptor pairs. *Science (New York, N.Y.)* **264**:415-417.

Foster TC (1999) Involvement of hippocampal synaptic plasticity in age-related memory decline. *BRAIN RESEARCH REVIEWS* **30**:236-249.

Frotscher M, Drakew A and Heimrich B (2000) Role of afferent innervation and neuronal activity in dendritic development and spine maturation of fascia dentata granule cells. *Cerebral cortex (New York, N.Y. : 1991)* **10**:946-951.

Funakoshi H, Belluardo N, Arenas E, Yamamoto Y, Casabona A, Persson H and Ibanez C (1995) Muscle-derived neurotrophin-4 as an activity-dependent trophic signal for adult motor neurons. *Science Science* **268**:1495-1499.

Gad M, Itoh A and Ikai A (1997) Mapping cell wall polysaccharides of living microbial cells using atomic force microscopy. *Cell biology international* **21**:697-706.

Halaban R, Rubin JS, Funasaka Y, Cobb M, Boulton T, Faletto D, Rosen E, Chan A, Yoko K, White W and et al. (1992) Met and hepatocyte growth factor/scatter factor signal transduction in normal melanocytes and melanoma cells. *Oncogene* **7**:2195-2206.

Hamanoue M, Takemoto N, Matsumoto K, Nakamura T, Nakajima K and Kohsaka S (1996) Neurotrophic effect of hepatocyte growth factor on central nervous system neurons in vitro. *Journal of neuroscience research* **43**:554-564.

Hayashi T, Abe K, Sakurai M and Itoyama Y (1998) Inductions of hepatocyte growth factor and its activator in rat brain with permanent middle cerebral artery occlusion. *Brain research* **799**:311-316.

Henze DA, Cameron WE and Barrionuevo G (1996) Dendritic morphology and its effects on the amplitude and rise-time of synaptic signals in hippocampal CA3 pyramidal cells. *The Journal of comparative neurology* **369**:331-344.

Hinterdorfer P, Baumgartner W, Gruber HJ, Schilcher K and Schindler H (1996) Detection and Localization of Individual Antibody-Antigen Recognition Events by Atomic Force Microscopy. *Proceedings of the National Academy of Sciences of the United States of America* **93**:3477-3481.

Hinterdorfer P and DufrÃªne YF (2006) Detection and localization of single molecular recognition events using atomic force microscopy. *Nat Meth Nature Methods* **3**:347-355.

Honda S, Kagoshima M, Wanaka A, Tohyama M, Matsumoto K and Nakamura T (1995) Localization and functional coupling of HGF and Met/HGF receptor in rat brain: implication as neurotrophic factor. *Brain research. Molecular brain research* **32**:197-210.

Ibanez CF (1998) Emerging themes in structural biology of neurotrophic factors. *Trends in Neurosciences* **21**.

Jiang WG, Hallett MB and Puntis MC (1993) Hepatocyte growth factor/scatter factor, liver regeneration and cancer metastasis. *The British journal of surgery* **80**:1368-1373.

Kawas LH, Yamamoto BJ, Wright JW and Harding JW (2011) Mimics of the dimerization domain of hepatocyte growth factor exhibit anti-met and anti-cancer activity. *JOURNAL OF PHARMACOLOGY AND EXPERIMENTAL THERAPEUTICS*.

Lee CU and Chrisey LA (1994) Direct measurement of the forces between complementary strands of DNA. *Science* **266**.

Lehenkari PP and Horton MA (1999) Single integrin molecule adhesion forces in intact cells measured by atomic force microscopy. *Biochemical and Biophysical Research Communications* **259**:645-650.

Lim CS and Walikonis RS (2008) Hepatocyte growth factor and Met promote dendritic maturation during hippocampal neuron differentiation via the Akt pathway. *Cell. Signal. Cellular Signalling* **20**:825-835.

Maina F and Klein R (1999) Hepatocyte growth factor, a versatile signal for developing neurons. *Nature Neuroscience* **2**:213-217.

Mart NF, Lozano JR, Herruzo ET, Garcia F, Richter C, Sulzbach T and Garcia R (2008) Bimodal atomic force microscopy imaging of isolated antibodies in air and liquids. *Nanotechnology* **19**.

Matsumoto K and Nakamura T (1997) Hepatocyte growth factor (HGF) as a tissue organizer for organogenesis and regeneration. *Biochemical and Biophysical Research Communications* **239**:639-644.

Miller M and Leonard EJ (1998) Mode of receptor binding and activation by plasminogen-related growth factors. *FEBS letters* **429**:1-3.

Miyazawa T, Matsumoto K, Ohmichi H, Katoh H, Yamashima T and Nakamura T (1998) Protection of hippocampal neurons from ischemia-induced delayed neuronal death by hepatocyte growth factor: a novel neurotrophic factor. *Journal of cerebral blood flow and metabolism : official journal of the International Society of Cerebral Blood Flow and Metabolism* **18**:345-348.

Naka D, Ishii T, Yoshiyama Y, Miyazawa K, Hara H, Hishida T and Kidamura N (1992) Activation of hepatocyte growth factor by proteolytic conversion of a single chain form to a heterodimer. *The Journal of biological chemistry* **267**:20114-20119.

Nakamura T, Nawa K and Ichihara A (1984) Partial purification and characterization of hepatocyte growth factor from serum of hepatectomized rats. *Biochemical and Biophysical Research Communications* **122**:1450-1459.

Nakamura T, Nishizawa T, Hagiya M, Seki T, Shimonishi M, Sugimura A, Tashiro K and Shimizu S (1989) Molecular cloning and expression of human hepatocyte growth factor. *Nature* **342**:440-443.

Naldini L, Tamagnone L, Vigna E, Sachs M, Hartmann G, Birchmeier W, Daikuhara Y, Tsubouchi H, Blasi F and Comoglio PM (1992) Extracellular proteolytic cleavage by urokinase is required for activation of hepatocyte growth factor/scatter factor. *The EMBO journal* **11**:4825-4833.

Naldini L, Vigna E, Narsimhan RP, Gaudino G, Zarnegar R, Michalopoulos GK and Comoglio PM (1991) Hepatocyte growth factor (HGF) stimulates the tyrosine kinase activity of the receptor encoded by the proto-oncogene Met. *Oncogene* **6**:501-504.

Osada T, Takezawa S, Itoh A, Arakawa H, Ichikawa M and Ikai A (1999) The distribution of sugar chains on the vomeronasal epithelium observed with an atomic force microscope. *Chemical senses* **24**:1-6.

Reddy CVG, Malinowska K, Menhart N and Wang R (2004) Identification of TrkA on living PC12 cells by atomic force microscopy. *BBA - Biomembranes* **1667**.

Rodrigues GA and Park M (1994) Autophosphorylation modulates the kinase activity and oncogenic potential of the Met receptor tyrosine kinase. *Oncogene* **9**:2019-2027.

Ros R, Schwesinger F, Anselmetti D, Kubon M, SchÃ¤fer R, PlÃ¼ckthun A and Tiefenauer L (1998) Antigen Binding Forces of Individually Addressed Single-Chain Fv Antibody Molecules. *Proceedings of the National Academy of Sciences of the United States of America* **95**:7402-7405.

San Paulo A and GarcÃ-a R (2000) High-resolution imaging of antibodies by tapping-mode atomic force microscopy: attractive and repulsive tip-sample interaction regimes. *Biophysical journal* **78**:1599-1605.

Tolbert WD, Daugherty J, Gao C, Xie Q, Miranti C, Gherardi E, Woude GV and Xu HE (2007) A mechanistic basis for converting a receptor tyrosine kinase agonist to an antagonist. *Proceedings of the National Academy of Sciences of the United States of America* **104**:14592-14597.

Tyndall SJ and Walikonis RS (2007) Signaling by hepatocyte growth factor in neurons is induced by pharmacological stimulation of synaptic activity. *Synapse (New York, N.Y.)* **61**:199-204.

Yamamoto BJ, Elias PD, Masino JA, Hudson BD, McCoy AT, Anderson ZJ, Varnum MD, Sardinia MF, Wright JW and Harding JW (2010) The Angiotensin IV Analog Nle-Tyr-Leu-ψ-(CH2-NH2)3-4-His-Pro-Phe (Norleual) Can Act as a Hepatocyte Growth Factor/Met Inhibitor. *The Journal of pharmacology and experimental therapeutics.* **333**:161.

CHAPTER FIVE

CONCLUSIONS

The studies presented in this dissertation focused on exploring the therapeutic potential of inhibiting the HGF/Met system and assessing the ability of Ang IV and Hinge derived compounds to alter the functions of the HGF/Met system. The work addressed three goals: (1) Identifying the molecular mechanism underlying the inhibition of the HGF/Met system by Norleual, an AngIV analog; (2) Developing more metabolically stable analogs (6AH family) that possess potent anti-HGF/Met activity; and (3) Establishing the sub-cellular distribution of Met on hippocampal neurons, which are critically involved with cognition.

Investigating the molecular mechanism of Norleual. Norleual is an AngIV analogue known to antagonize the biological effects of AngIV. Studies from our laboratory have indicated that the HGF/Met system is the likely target of AngIV and Norleual. Norleual was clearly shown to be a potent inhibitor of the HGF/Met system making it an attractive candidate for a wide array of diseases that are dependent on Met activity such as cancer, diabetic retinopathy, and malaria infection. Until the work described in this dissertation, the mechanism responsible for the biological activity of Norleual and other Ang IV analogs was unknown. A homologous sequence-conservation screen against all possible transcripts revealed a partial homology between AngIV and the hinge region of HGF. This realization triggered the hypothesis that these Ang IV analogs modify Met activity by interfering with HGF dimerization/multimerization and acting as dominant negative hinge region mimics. The data presented here validate this hypothesis by demonstrating that, as was expected, Norleual binds HGF with high affinity and blocks the dimerization process at concentrations sufficient to inhibit the HGF/Met system both *in vitro* and in *vivo*. These data spawned the corollary hypothesis that a peptide representing the

HGF dimerization domain, called the hinge region, will exhibit characteristics similar to Norleual. Data presented in Chapter two demonstrate that not only can a Hinge peptide block HGF dimerization and HGF-dependent cellular activity but it exhibit profound anti-cancer activity.

The design decisions that originally guided the synthesis of Norleual and most of our analogs were based on the structure of angiotensin and not HGF. The partial homology that these molecules exhibited with the Hinge region of HGF was pure serendipity. Thus, it is predicted that more effective HGF/ Met antagonists can be designed using the Hinge region peptide as the parent template. An effective antagonist should: 1) block HGF dimerization; 2) interfere with HGF/ Met-dependent signaling and cellular activity; 3) possess favorable pharmacokinetic (PK) characteristics; and 4) exhibit potent anti-cancer activity. Thus, the ultimate future goal will be to synthesize inexpensive orally-active analogs with potent anti-Met activity based, on the Hinge region structure.

Ongoing efforts and future studies will attempt to decipher the important structural features of both Norleual and Hinge, to identify the critical residues and to determine the optimum length and size of these molecules. The first step will be to identify the critical pharmacophore, contained with the Hinge peptide sequence that is essential for its inhibitory activity. Several synthetic approaches can be undertaken to identify the pharmacophore including the evaluation of the N- and C- terminal truncated peptides and mono-alanine substituted Hinge analogs. The goal of these types of studies is to establish the importance of each amino acid and side chain to the observed activity. **Figure 1** (Appendix A) shows results from a preliminary study of the effect of Alanine substitutions on the ability of Hinge to inhibit HGF-induced MDCK cell scattering.

Once the pharmacophore has been established the next step in this project this project is to produce drug candidates that have maximal activity and favorable pharmacokinetic (PK) characteristics. Two types of modifications are envisioned: those that alter the distance between key components of the side chain and the peptide backbone, and those that exaggerate the chemical properties of the side chain. The intent of these experiments will not be to try to introduce every possible amino acid substitution at every position within the hinge peptide sequence; but rather to determine and exploit those chemical features of required amino acids to impart maximum activity. Since we don't yet know which amino acids are essential for activity, we will use a hypothetical example to illustrate synthesis strategy. Let us assume that truncation and alanine substitution studies have clearly demonstrated that removal of tyrosine from position #3 eliminates the ability to block dimerization and HGF/Met activity. Examination of tyrosine indicates three properties that could be evaluated: 1) the distance between to the ring and the peptide backbone; 2) the aromaticity of the ring; and 3) the hydrogen bonding contribution of the hydroxyl group. The importance of the first property could be addressed by changing the length of the methylene chain linking the ring to the peptide backbone; for example, by substituting homotyrosine for tyrosine. The question of aromaticity could be probed by substituting an aromatic, double ring naphthalene for the benzene ring of tyrosine. The involvement of hydrogen bonding by the OH of tyrosine could be assessed by substituting other hydrogen-bonding amino acids like cysteine and homocysteine for tyrosine or non-hydrogen bonding amino acids like phenylalanine.

An implicit property of useful pharmaceuticals is that they are deliverable in such a way as to maintain therapeutic drug concentrations in the blood. Thus the second study would introduce N- and C-terminal modifications to the most active compounds, identified in the first

part of this investigation, to reduce susceptibility to exopepidase metabolism. C-terminal stability will be imparted by the addition of an amide. Several approaches will be employed to protect the N-terminal: 1) substitution with D- or non-α-amino acids; 2) acylation of the N-terminal amine; and 3) insertion of a non-peptide linkage between amino acids one and two. These peptides and peptidomimetics will be evaluated for biological activity but additionally monitored for stability in blood, liver microsomes, and in the circulation. Peptides are notoriously unstable both in blood and in the hepatic and renal vascular beds. Our experience dealing with peptide metabolism has taught us that N-terminal, and to a lesser extent C-terminal, protection is necessary to prevent rapid metabolism. The next step would be to apply modifications to both structures to improve stability characteristics, including the addition of D amino acids at the N-terminus to prevent metabolism by aminopeptidases, changes to the amino acid at the N or C terminal domains, in addition to the insertion of non-peptide linkages.

One additional area of future investigation will be to determine whether the design of therapeutics that targets the dimerization domain of growth factors is applicable beyond the HGF/Met system. In this regard we are currently examining the ability of putative dimerization domain mimics to modulate the activity of the macrophage stimulating protein (MSP)/RON (MSP receptor) system. This system is closely analogous from both structural and functional standpoints to the HGF/Met system. HGF and MSP exhibit extensive homology, as do Met and RON. Most relevant, however, is the observation that HGF and MSP have an equivalent domain structure that includes nearly identical hinge regions (Han et al., 1991). We predict that like, HGF, MSP must dimerize subsequent to RON activation and that hinge region mimics will block the dimerization process and thus RON activation. The significance of such a blockade is that hyper-activation of the MSP/RON system is a feature of several malignancies (Wagh et al.,

2008) where it is involved with exaggerated proliferation, migratory activity, and invasive potential. Current efforts are underway to develop anti-cancer agents targeted at the MSP/RON system (Guin et al., 2010).

Ongoing work continues to investigate the potential utility of Hinge, Norleual, or future second-generation molecules for other clinical indications. One particularly attractive application is the use of these molecules in hypervascular disease of the eye, such as macular degeneration and diabetic retinopathy. As such, we have begun to characterize the effect of these molecules on angiogenesis. **Figure 2** (Appendix A) shows data from a preliminary study demonstrating the ability of Hinge to block HGF-induced proto-vessels formed by human umbilical vein endothelial cells *in vitro*. Continued development of these compounds will examine their utility for other clinical indications, establish detailed dosing regimes, complete pharmacokinetic characterization, and perform non-GLP toxicological evaluations.

Development of more stable Angiotensin IV derivatives that are targeting the HGF/Met system: Despite Norleual's impressive anti-cancer profile, it is highly unstable making its transition to clinical use problematic. Thus another family of Ang IV-related peptidomimetics has been developed, which has been referred to as the 6AH family because of the 6-amino hexanoic amide substituted at the C-terminal position. This substitution, along with D-norleucine at the N-terminal, enhances the metabolic resistance of family members. From the pharmacokinetics characteristics described here, it is obvious that the 6AH family is a more metabolically stable when compared to Norleual. The lead compound in this family, 6AH (D-Nle-Tyr-Ile-6AH), as well as other members of the family, has shown a range of biological and therapeutic activities, as shown in the data presented within this dissertation. Upcoming studies should include a detailed structural activity relationship, as described above; with the aim of

identifying the important pharmacophore within the peptide sequences. Again optimization of analog structures would require detailed dosing studies, a complete pharmacokinetic characterization, and a non-GLP toxicological evaluation.

Investigations directed towards exploring the effect of these compounds on the numerous treatment possibilities that are dependent on Met activation, e.g., reversing fibrotic disease and macular degeneration, are again rich venues for therapeutics development. It is our long-term goal to bring these molecules to market to meet an ever-increasing demand for low-cost, effective treatments for Met-dependent pathologies.

Met differential distribution. HGF has been identified as a very potent synaptogenic and neurotrophic factor. The work presented here shows that Met is grossly localized to brain regions such as the hippocampus and prefrontal cortex (PFC), which are recognized as areas that undergo extensive synaptic remodeling. The sub-cellular localization of Met on hippocampal neurons indicates that most of the detected Met on the soma cell body is in the monomer/dimer form, while more of the active aggregated form of Met is concentrated at the dendrite, the site where active remodeling occurs. These findings fit nicely with the idea that the receptors of neurotrophic factors, in this case Met, are synthesized in the neuron soma where they are found in an inactive form, and then transferred to the dendritic site to incorporate the extra cellular membrane where they become activated.

HGF exerts its role as a determinant of synaptic connectivity by regulating the density and structure of dendritic spines, through direct binding and activation of its receptor, Met. Upon activation; Met tends to dimerize and/or multimerize. This means that in the non-activated hippocampal cultures, there is a basal level of active Met that is important for the development, maintenance, and protection of the neurons. The fact that active Met that was detected in our

studies in untreated cultures with HGF, means that either Met tends to spontaneously dimerize at the dendritic site or that the endogenous HGF that is present supports the formation of the activated form of Met. Future studies will aim to exclusively map activated Met, using a probe carrying an antibody for phospho-Met. Understanding the detailed localization of Met on hippocampal neurons from normal and ultimately diseased brains could provide a diagnostic comparison of remodeling and regenerative capacity in various neurodegenerative diseases such as Alzheimer's.

5.1 References

Guin, S., M. H. Wang, et al. (2010). "RON receptor tyrosine kinase as a target for delivery of chemodrugs by antibody directed pathway for cancer cell cytotoxicity." Mol. Pharm. Molecular Pharmaceutics **7**(2): 386-397.

Han, S., L. A. Stuart, et al. (1991). "Characterization of the DNF15S2 locus on human chromosome 3: identification of a gene coding for four kringle domains with homology to hepatocyte growth factor." Biochemistry **30**(40): 9768-9780.

Wagh, P. K., B. E. Peace, et al. (2008). "Met-Related Receptor Tyrosine Kinase Ron in Tumor Growth and Metastasis." Adv. Cancer Res. Advances in Cancer Research **100**: 1-33.

APPENDICES

A. Effect of HGF & Hinge on Proto-vessel Formation in HUVECs

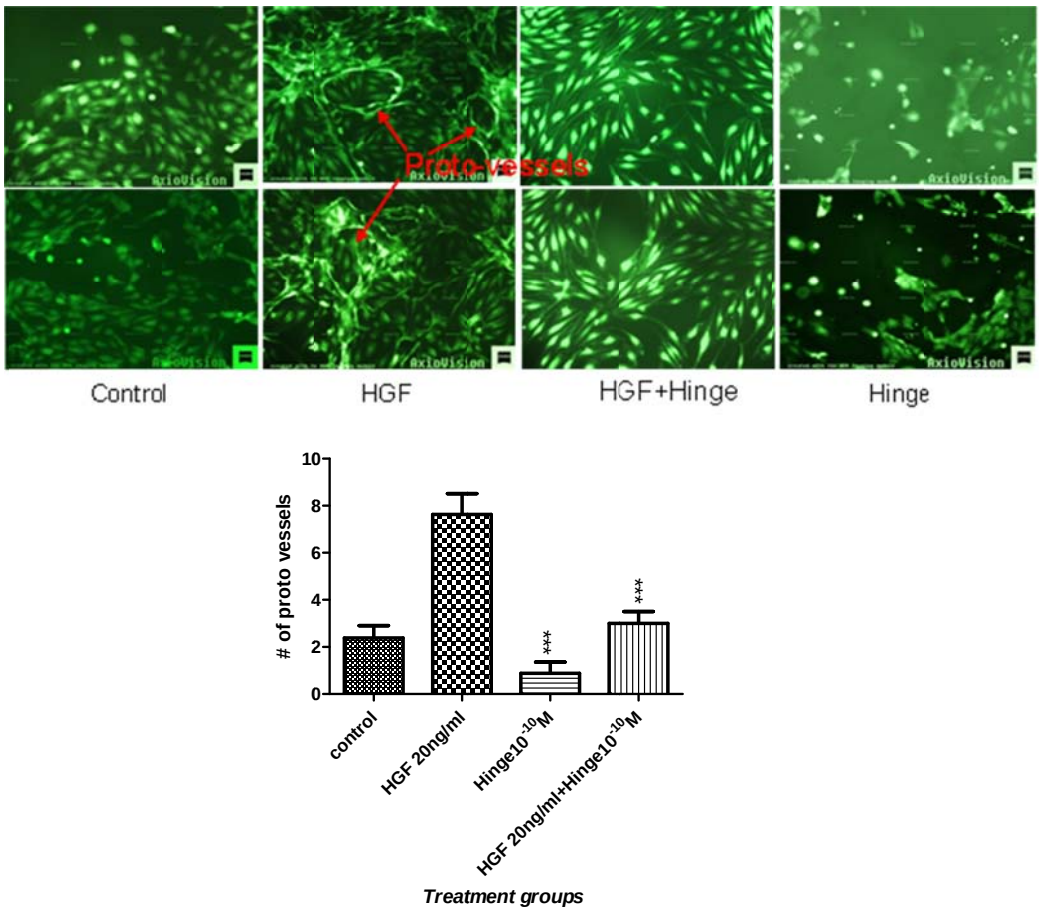

Figure 1.APPENDIX A: Effect of Hinge on in-Vitro proto-vessels formation. 96-well plate were coated with cell-based Extracellular Matrix Gel and allowed to solidify for 60 minutes. HUVECs single cell suspension that had either HGF 20ng/ml (+/-) Hinge 10-10M ,Hinge 10-10M alone, or the vehicle PBS for the controls were added to the top of each gel-coated well. Cells were incubated overnight in a 37°C cell culture incubator. At the end of the experiment cells were stained with calcein staining solution. (A) Picture of HUVECs proto-vessel formation on the extracellular matrix gel. (B) The effect of HGF and Hinge on proto-vessels formation were counted and quantified. ANOVA analysis shows that the Hinge treated groups were statistically different than the HGF alone group ($P<0.001$), but not different from one another or non-treated controls ($P>0.05$).

B. Mono- alanine substituted Hinge derivatives: Effect on MDCK cell scattering

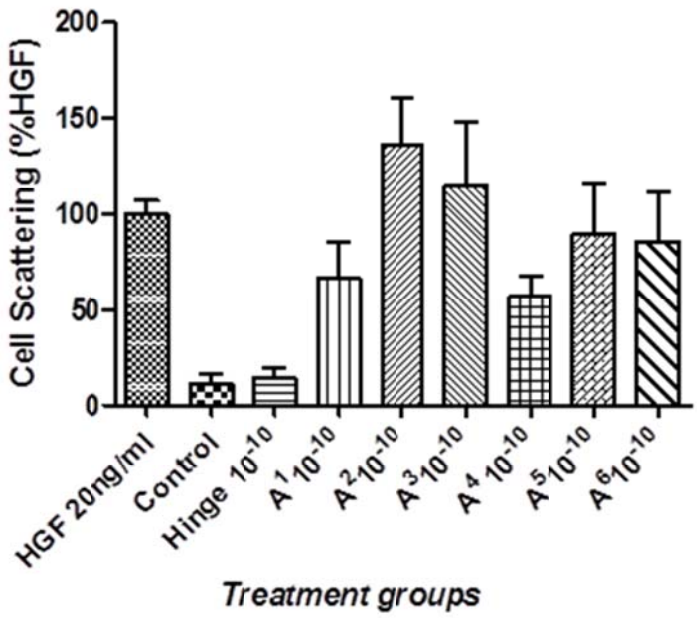

Figure 2. APPENDIX B: Effect of Mono- alanine substituted Hinge derivatives on MDCK cell scattering. Hinge derivatives with single alanine substitutions of the constituent amino acids [K(1)D(2)Y(3)I(4)R(5)N(6)] were evaluated for their ability to alter HGF-dependent scattering of MDCK cells. Cell scattering in which cells lose the cell-to-cell contacts and then migrate rapidly is the classic response to HGF. MDCK cells, the gold standard cellular model for studying the HGF/Met system, were grown to 100% confluence on coverslips and then placed in a clean plate. The cells were stimulated to scatter off of the coverslip by adding 20 ng/ml of HGF to the media alone or in combination with Hinge or an Ala-Hinge analog at 10^{-10}M. After 48 hours of scattering, the cells were fixed with methanol and stained with Diff-Quik. The effect of HGF on scattering was scored by a blinded evaluator using a five point scale. ANOVA analysis indicates that the Hinge group was significantly statistically different than the HGF treated group ($p<0.01$), but not different from non-treated controls ($p>0.05$). None of the Ala-Hinge analog were significantly different compared to the HGF group ($p>0.05$). Only A^2 and A^3 where statistically different from the control group ($p<0.05$). Mean +/-SEM, N=4.